In vitro evaluation of poloxamer 407-based formulations for topical antifungal administration of terbinafine HCl and assessment of keratin film from human hair as a nail plate model

Von der Fakultät für Lebenswissenschaften
der Technischen Universität Carolo-Wilhelmina
zu Braunschweig
zur Erlangung des Grades einer
Doktorin der Naturwissenschaften
(Dr. rer. nat.)
genehmigte
D i s s e r t a t i o n

von Frau Lusiana
aus Bandung / Indonesia

1. Referentin: Professorin Dr. Christel Müller-Goymann
2. Referent: Professor Dr. Dr. h. C. Reinhard Neubert
eingereicht am: 30.11.2011
mündliche Prüfung (Disputation) am: 20.02.2012

Druckjahr 2012

Gedruckt mit Unterstützung des Deutschen Akademischen Austauschdienstes

Vorveröffentlichungen der Dissertation

Teilergebnisse aus dieser Arbeit wurden mit Genehmigung der Fakultät für Lebenswissenschaften, vertreten durch die Mentorin der Arbeit, in folgenden Beiträgen vorab veröffentlicht:

Publikationen

Lusiana, Reichl S. & Müller-Goymann C.C. Keratin film made of human hair as a nail plate model for studying drug permeation. European Journal of Pharmaceutics and Biopharmaceutics 78: 432-440 (2011).

Lusiana & Müller-Goymann C.C. Preparation, characterization, and in vitro permeation study of terbinafine HCl in poloxamer 407-based thermogelling formulation for topical application. AAPS PharmSciTech 12: 496–506 (2011).

Tagungsbeiträge

Lusiana, Reichl, S. & Müller-Goymann, C.C.: Keratin film from human hair as a novel model in replacing human nail plate for studying drug permeation. (Poster) 2nd PharmSciFair, Nice (2009).

Lusiana, Reichl, S. & Müller-Goymann, C.C.: The influence of nail penetrant enhancers on novel nail model made of human hair keratin. (Poster) Jahrestagung der Deutschen Pharmazeutischen Gesselschaft, Jena (2009).

Lusiana & Müller-Goymann, C.C.: Permeation improvement of terbinafine HCl through human stratum corneum and bovine hooves. (Vortrag) Internationale DPhG-Doktorandentagung, Pichlarn-Aigen (2009).

Lusiana, Reichl, S. & Müller-Goymann, C.C.: Keratin films made of human hair keratin as a nail substitute for studying drug permeation. (Poster) 7th World Meeting on Pharmaceutics, Biophamaceutics and Pharmaceutical Technology, Valletta (2010).

Lusiana & Müller-Goymann, C.C.: Permeation study of terbinafine HCl from poloxamer 407-based thermogelling formulations across isolated human stratum corneum. (Vortrag) Jahrestagung der Deutschen Pharmazeutischen Gesselschaft, Braunschweig (2010).

Lusiana & Müller-Goymann, C.C.: Stability of terbinafine HCl in poloxamer 407-based thermogelling formulations for topical application during storage. (Poster) Skin Forum 12th Annual Meeting, Frankfurt am Main (2011).

Patentanmeldung

Lusiana & Müller-Goymann, C.C., Technische Universität Braunschweig: Arzneimittelformulierung zur Behandlung von Nagelerkrankungen. Deutsche Patentanmeldung 102009038512 (2009), Europäische Patentanmeldung EP10171387.3 (2010), US Patentanmeldung 12/846,536 (2010).

Acknowledgement

This thesis would not have been possible without all the support I received during all these years. It is thus my pleasure to thank those who made this possible.

First of all, my deepest gratitude to Frau Prof. Dr. Christel C. Müller-Goymann for assignment of the theme, the numerous discussions right from the initial to the final phase as well as for all the supports, opportunities and many precious experiences.

I would like to show my sincere gratitude to Herr Prof. Dr. Reinhard H. H. Neubert for the second opinion.

It is an honor for me to acknowledge Deutscher Akademischer Austauschdienst (DAAD) which opened numerous avenues for my research in Germany.

Also my sincere thanks to Dr. Stephan Reichl for his valuable suggestions and discussions in keratin film research area.

My sincere gratitude goes to Carlos van Hemelrijck for the introduction into the poloxamer system and the generous assistances in various occasions.

The various experiments involving keratin film and electrophoresis would not have been finished in such a good time without the kind assistance of Lucia Albrecht. My sincere gratitude goes also to Frau Schildt, Frau Jahn, Napi, Dagmar and Ulrike for the helpful assistances and a convenient work atmosphere during the practical work.

I would also like to thank Frau Carolin Rattunde for the time and assistances in conducting the microbiological assay. Also to not forget Prof. Dr. Ingo Rustenbeck who allowed me to conduct this assay in the Institut für Pharmakologie, Toxikologie und Klinische Pharmazie. My cordial thanks go also to Frau Petra Reich (Institut für Medizinische und Pharmazeutische Chemie) for the UV spectrophotometry measurements.

Croda GmbH, Dolorgiet and BASF are gratefully acknowledged for the supply of some materials for this study. My gratitude is also to Dr. med. Robert Schmidt (Wolfenbüttel) for the skin donation.

Last but not least is my sincere appreciation to all the colleagues who have given me their hands, minds and time during all these years.

Finally I would like to thank my parents and my little family for all the support, patience and spiritual motivation which keep me moving forward through all these years.

"Zwar weiß ich viel, doch möcht ich alles wissen."

Johann Wolfgang von Goethe

Faust I, Vers 601 / Wagner

Table of Contents

Glossary and Abbreviations

α	Thermodynamic activity
ε	Molar absorptivity
5-ALA	5-Aminolevulinic acid
ANOVA	Analysis of variance
BAN	British Approved Names
CE	Cornified envelope
DAB	Deutsches Arzneibuch (German Pharmacopoeia)
DAC	Deutscher Arzneimittel-Codex (German Drug Code)
DMIS	Dimethyl isosorbide
DSC	Differential scanning calorimetry
FD4	Fluorescein isothiocyanate-dextran MW 4000
FTIR	Fourier transform infrared spectroscopy
HPLC	High performance liquid chromatography
INCI	International Nomenclature of Cosmetic Ingredients
IPA	Isopropyl alcohol
KF	Keratin film
LLC	Lyotropic liquid crystal phases
MCT	Medium chain triglycerides, refers to Miglyol® 812N
MIG	Miglyol® 840
MIC	Minimum inhibitory concentration
MW	Molecular weight
NaOH	Sodium hydroxide
NMF	Natural moisturizing factor
P_{app}	Permeability coefficient

PB	Phosphate buffer pH 5.8
PBS	Phosphate buffer saline pH 7.4
PE	Penetration enhancer
Ph. Eur.	European Pharmacopoeia
POX	Poloxamer 407 (Pluronic® F127, Lutrol® F127)
R_F	Retardation factor
RB	Rhodamine B
RH	Relative humidity
SC	Stratum corneum
SF	Sodium fluorescein
SPR	Small proteins rich in the amino acid proline
TA	Thioglycolic acid
TBF	Terbinafine HCl
TEWL	Transepidermal water loss
TGases	Transglutaminase enzymes
TLC	Thin layer chromatography
TMTP	Refers to filter code of the Isopore™ membrane filters
UV	Ultraviolet

Chapter 1

Introduction

The treatment of infectious diseases caused by microorganisms has always been a particular interest in the medical world. Since penicillin was found by Alexander Flemming (1928), the exploration of new antimicrobial agents against various pathogenic microorganisms keeps growing. Finding a new active is however not the end goal of the battle; the innovation of an appropriate and effective vehicle to deliver the drug into the infected site has been the real challenge.

From all existing infectious diseases known, fungal infection is a long-standing hassle because of its long-term therapy and accordingly a low patient compliance. Moderate to severe infections demand oral administration since the infected site cannot be reached easily by the topical treatment, e.g., nail fungal infection. Onychomycosis, for example, needs an oral therapy for at least 6 weeks (for finger nail infection) or up to 12 months (for toenail infection) [1]. On the other hand, the peroral treatment with azole derivatives is overshadowed by either its high hepatotoxicity risk or systemic drug interactions with other medications. Considering all these issues, delivering the drug (trans)dermally may be a solution in reducing the length of the therapy and reducing the amount of unnecessary accumulated drug in the body.

Transdermal route has been the most favorite among other treatments, e.g., parenteral or oral, due to its non-invasive application and high patient's compliance. In accordance to this, a poloxamer 407-based vehicle, later referred to as thermogelling formulation was recently developed [2]. This formulation was successful in enhancing the permeation rate of 5-aminolevulinic acid (5-ALA) remarkably across human stratum corneum [2-4] compared to that from Basicreme DAC and water containing hydrophilic ointment, both described in German Drug Code (DAC) and German Pharmacopoeia (DAB). The permeation rates of 5-ALA were 7.5-fold and 19.5-fold higher compared to both standards, respectively [5]. 5-ALA, a very hydrophilic substance with log *P* of -1.51 cannot satisfactorily be delivered transdermally since stratum corneum, the lipophilic barrier of the skin, limits its diffusion into the deeper tissues.

In order to explore and expand the potential of this thermogelling vehicle for transdermal delivery purpose, a lipophilic antifungal drug terbinafine HCl with log *P* of 3.3 was chosen and incorporated. Terbinafine HCl (TBF), invented by Novartis AG, is available in the market now for oral and dermal administration (cream, gel, solution, spray) in superficial mycosis therapy under the brand name Lamisil® in Germany and several European countries. The thermogelling vehicle is composed of poloxamer 407, medium chain triglycerides, isopropyl alcohol, dimethyl isosorbide and water. This vehicle possesses some characteristics such as a reversible thermogelation [2] and an indication of the presence of liquid crystal structure of some formulations with ringing effect [6].

Still in line with the treatment of antifungal diseases, the limitation of human nail plate source has hampered the development of the therapy itself. Different from skin, nail plate consists of highly keratinized dead cells [7] and behaves as a hydrophilic gel membrane [8-10]. Animal hooves are up to now an accepted model to replace human nail for studying drug permeation but some significant differences have been reported [11]. The work group of Stephan Reichl in our institute has successfully extracted keratin alpha from human hair using the so-called Shindai method [12]. This keratin was previously intended as substrate for cell culture and tissue engineering purposes. Through further processes involving molding and oxidative procedures, a keratin film has been built. To test this film for its usefulness as a human nail plate model, physical characterization and serial permeation studies employing several markers were carried out to explore the properties of this film in comparison with bovine hoof, the accepted human nail model.

Based on previously elaborated results, the present study emphasizes as follows:

- Incorporation of antifungal drug TBF into the poloxamer 407 based thermogelling formulation intended for topical application
- Physicochemical characterization of the formulations
- TBF permeation from the formulations across human stratum corneum and bovine hooves
- Stability study of the formulations during storage at 20 °C for up to 6 months
- Microbiological assay of the formulations
- Testing the keratin film made of human hair keratin as a human nail plate model

Chapter 2

General Part

2.1 Human skin

Skin is the greatest human organ which carries not only the primary protection function but also other tasks such as regulation, immunity, sensory and many important synthesis functions [13]. As protector, skin constrains the body from environmental assaults as well as water loss [14,15]. To the skin, water confers flexibility and facilitates a proper desquamation [13]. A disrupted or perturbed skin barrier function is indicated from an increase in transepidermal water loss (TEWL) value up to 20-fold [13].

2.1.1 Anatomy of the skin

Human skin is stratified into layers and consists of epidermis and dermis. An anatomical view of human skin is displayed in Fig. 2.1. The epidermis is composed of keratinocytes that undergo differentiation originating from the stem cells in the basal layer. Besides keratinocytes, melanocytes, Langerhans cells and Merkel cells exist in the epidermis as well. Dermis contains mainly collagen and elastin which are responsible for skin tensile strength, besides other macromolecules with high water-retaining ability. Moreover, dermis is responsible for nutrients supply since this layer is rich in blood vessels [16]. Fat globules and part of the blood vessels lie in the subcutaneous tissue.

Keratinocytes make up about 95% of the total epidermis. Layers in epidermis can be distinguished as stratum basale/ stratum germinativum, stratum spinosum, stratum granulosum and in the uppermost, stratum corneum (SC) [16]. Keratinocytes move progressively from stratum basale towards the skin surface until they lose their nuclei; these dead cells without nuclei are called corneocytes. An area where keratinocytes still retain their nuclei is called stratum lucidum and these cells are referred to as *transitional cells* [16]. Interaction with the matrix protein fillagrin (filament-aggregating protein) transforms and aligns keratins into highly ordered and condensed arrays. Thereafter, fillagrin aggregates keratin filaments into tight bundles forming a flat shape of either hexagonal or pentagonal geometry [15,17].

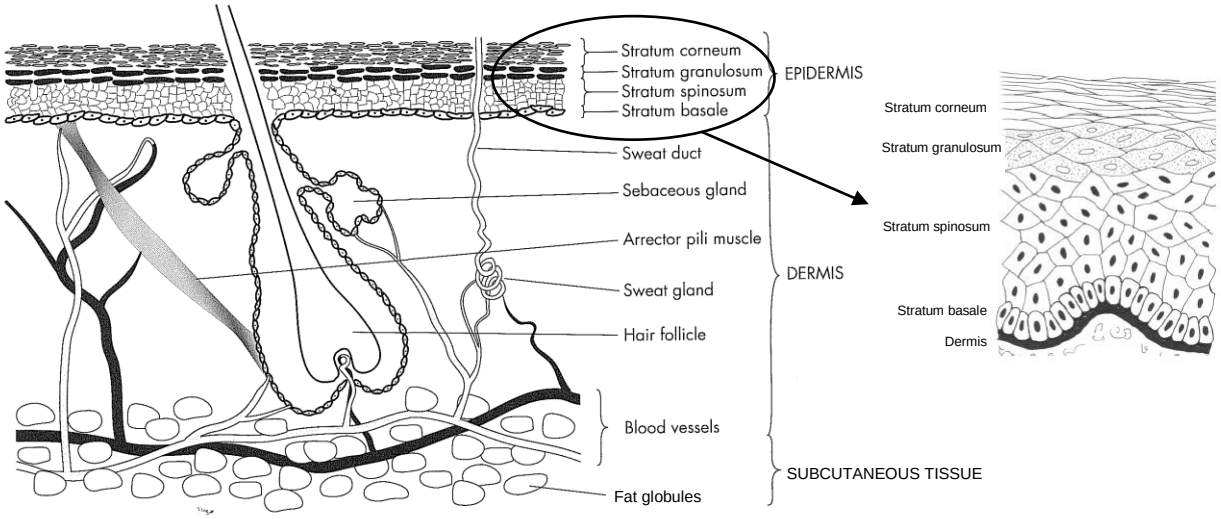

Fig. 2.1 Skin structure and layers of the human epidermis, taken from ref. [15,18]

SC consists of normally about 10 - 16 layers of corneocytes on most anatomical locations [19]. During the movement towards the skin surface, keratinocytes secrete phospholipids, sphingolipids and plasma membrane constituents which are subsequently enzymatically cleaved into free fatty acids and ceramides in SC. All these components blend together building continuous lamellar bilayers of SC [13].

Adjacent keratinocytes are connected through several junctions for the sake of mechanical, biochemical and signaling interactions. From all described junctions, desmosomes are probably the most important ones. Desmosomes display the major adhesive intercellular junction and bridge cells in epidermis together by affixing keratin intermediate filaments to the cell membrane [15,16]. Initializing desquamation, desmosomes are broken down by proteolytic, tryptic and chymotryptic enzymes; this is followed by shedding off the corneocytes after about 2 weeks [14,15,20]. Illustration on how desmosomes connect keratinocytes is shown in Fig. 2.2 (a). In a very dry skin, desmosomes cannot be shed completely and this causes shedding in large scales rather than as individual cells [15]. The entire turnover time of normal epidermis from basal layer to the outmost SC is a sum of three main important processes: proliferative phase (13 days), differentiation phase (10-14 days) and final transit of SC (14 days) [21]. There are variations in the reported epidermal turnover time and this was suggested to be due to the differences in methods, models and assumptions used for the calculation [22]. Yet, the epidermal turnover time can be shorter in pathological situations such as psoriasis [16].

Corneocytes are covered with a shell called cornified envelope (CE), mainly consisting of loricrin (80%) and involucrin (2-5%). CE is cross-linked by sulfhydryl oxidases and transglutaminase enzymes (TGases) synthesized in the stratum spinosum [16,23,24]. CE formation occurs during the late differentiation where the internal organelles of keratinocytes are being degraded and a thick band of protein is deposited on the inner aspect of the cell plasma membrane. TGases cross-link these protein bands via disulfide and isopeptide bonds, followed by the attachment of lipid at the outer surface, forming a cornified envelope [25]. A detailed CE assembly is displayed in Fig. 2.2 (b). CE consists of a protein and a lipid envelope conferring biomechanical strength and providing a Teflon-like coating to the cell, respectively [24]. CE is the most insoluble structure of the corneocyte due to its dense N^{ε}-(γ-glutamyl)lysine isopeptide cross-links and disulfide bonds formation as well [13,23,24].

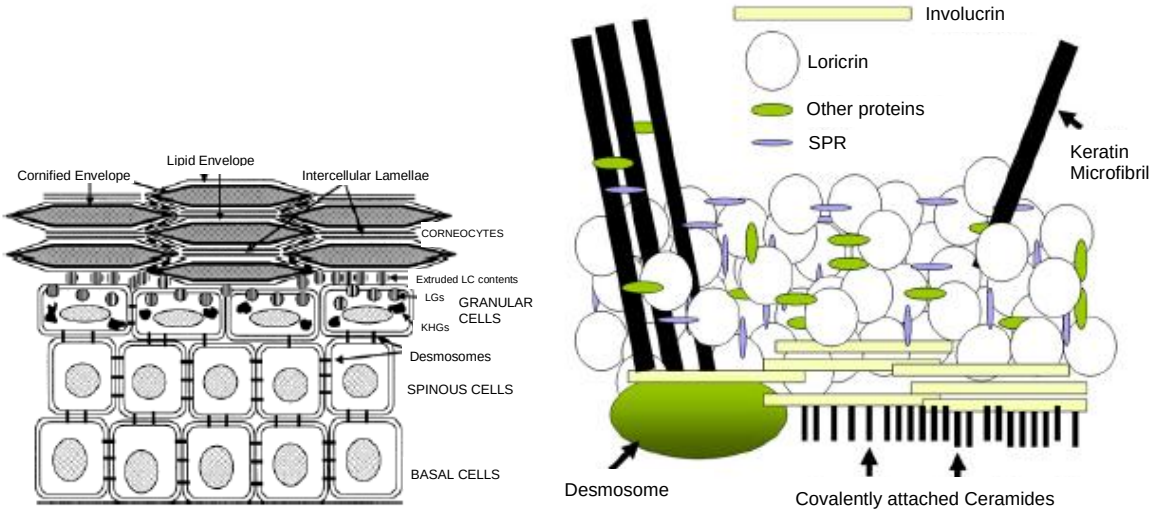

(a) (b)

Fig. 2.2 (a) Human epidermis, keratin filaments are omitted, from ref. [14], (b) Assembly of CE, previously proposed by Nemes and Steinert [24], modified by Wickett and Visscher [15]

Water is essential to secure a normal desquamation and all metabolic processes [13,15]. Natural moisturizing factor (NMF), which is the hydrolytic product of filaggrin, is produced to maintain SC hydration [13,14]. Hydrolysis of filaggrin to NMF will be initiated when water content in SC decreases. NMF consists of amino acid mixtures and their derivatives (pyrrolidone carboxylic acid, urocanic acid), lactic acid, urea and sugars which work as skin humectants [14]. Normal skin contains about 30% water in SC (by weight) whereas in a very dry SC the value can drop down to 10%. Water loss in SC is a vital signal for returning homeostatic condition. Once the barrier is altered or

perturbed, various signaling cascades will be initialized to return the skin back to normal function [13].

2.1.2 Stratum corneum (SC): bricks and mortar model

As skin most important barrier, SC is accompanied by the nucleated epidermis, cell-cell junctions and groups of cytoskeletal proteins. SC carries about more than 80% of the skin barrier function [26]. All other components such as lipids, acids, hydrolytic enzymes and macrophages build an immunological barrier for any environmental assault [17]. SC is now no longer described as a passive layer, but in reality is a dynamic layer with all its ongoing metabolic activities, particularly lipid synthesis, processing, and signaling cascades to the deeper layer as a response to any perturbation or stress [13,15].

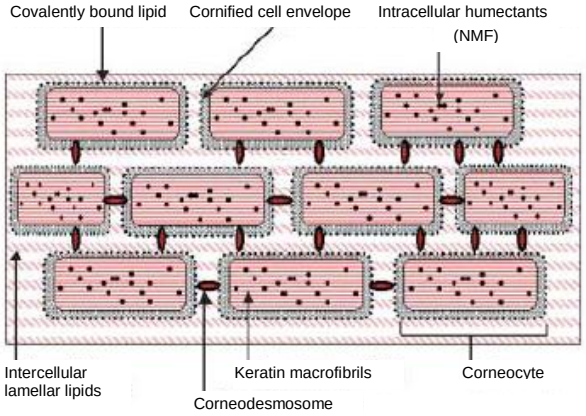

Fig. 2.3 Schematic model of "bricks and mortar", taken from ref. [13].

Corneocytes in the SC have been modeled as bricks embedded in a continuous lipid matrix (mortar). Corneocytes can be simply seen as piles of highly organized keratin macrofibrillar matrix and stabilized via interkeratin and intrakeratin filament disulfide bonds. The lipid matrix acts as “glue” sealing the corneocytes. It provides a water barrier and crucial protection against insults and injuries [26]. A schematic view of the former description “bricks and mortar” is shown in Fig. 2.3. The mortar has gained so much attention lately due to its uniqueness being composed of about 50% ceramides, 10-20% fatty acids, 25% cholesterol and other constituents, including small amounts of cholesterol esters and cholesterol sulfate. Among all, cholesterol esters, cholesterol sulfate and linoleic acid seem to play an important role for maintaining the skin barrier function [13,14]. The straight structure of ceramides enables a tight lateral packing of tight junctions and highly ordered gel phase membrane domains. Cholesterol on the other hand serves fluidity to the SC structure [14]. Deficiency in essential fatty acid

such as linoleic acid may lead to a poor water barrier function of the SC and increase in TEWL value [14,27]. The uniqueness of SC lipid content and structure makes this the most important barrier of the skin [25]. Lipid removal from the skin, e.g., by means of extraction with organic solvent, will increase its permeability.

2.1.3 SC microstructure

Barry [28] mentioned up to four endothermic transitions, referred as T1-T4, observed by means of differential scanning calorimetry (DSC), when SC is heated up to 120 °C. These transitions originate from the changes in SC lipid state, either liquefaction or packing rearrangement upon heating. T1 (~40 °C) is devoted to the lipid melting possibly from sebaceous lipids or cholesterol side-chain, T2 (~70 °C) is due to the lipid melting within the bilayer structure together with some non-polar material, T3 (~85 °C) describes the disruption of the association between lipid polar head groups and cholesterol-stiffened area (protein-lipid association) and T4 (~100 °C) is ascribed due to proteins (keratin) denaturation [28,29]. From all transitions, only T4 is irreversible due to protein denaturation. The T1-T4 transitions and the enthalpy involved can be identified and measured by means of DSC. As a prerequisite, SC water content must be sufficient since the transitions will not be visible when SC water content is below 15% [29]. Among all, T2 and T3 are the most reliable transitions since T1 and T4 were found to be strongly dependent on the skin source and its water content during measurement [28].

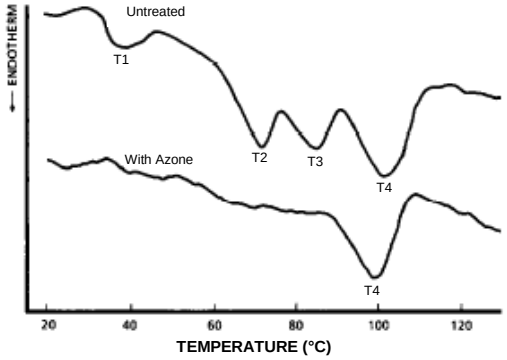

Fig. 2.4 DSC thermogram of SC untreated and treated with Azone, T1-T3 disappear upon treatment with Azone, taken from ref. [30]

Interaction of SC with penetration enhancers alters SC lipid's mobility and furthermore loosens its tight microstructure. This can be later observed as disappearances of one or more transitions from DSC thermogram as seen in Fig. 2.4. It shows SC thermogram before and after treatment with Azone, a potent transdermal penetration

enhancer. The mechanism thereof, how Azone disrupts SC lamellar packing and integrity, is illustrated by Barry in Fig. 2.5. The thermal transitions T1-T4 can be thus utilized as an indication for transdermal permeation enhancement.

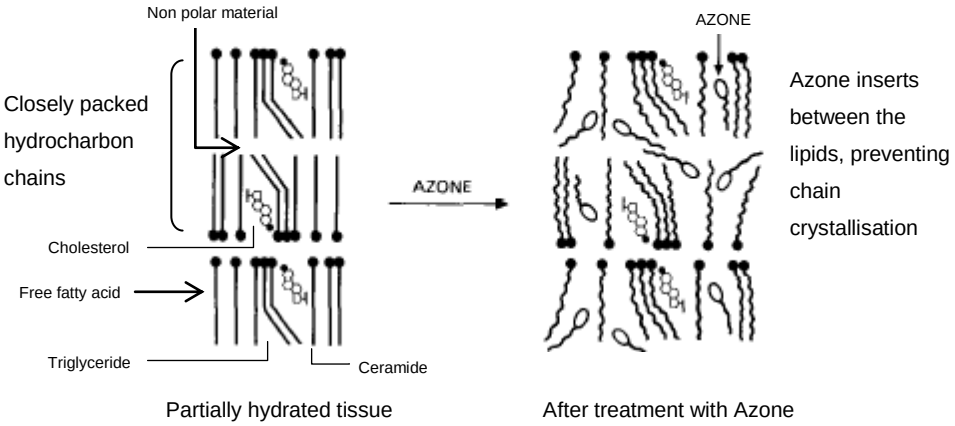

Fig. 2.5 Proposal on how Azone disrupts SC lipid structure, from ref. [28,30]

2.1.4 Drug permeation across skin

Considering the complex structure of the skin, one can imagine the tortuous pathway drugs have to penetrate or permeate upon topical administration. Skin offers three main entry routes for drugs: transcellular, intercellular and appendageal (primarily, follicular). It seems now that the intercellular pathway for most substances predominates over others routes [31]. Any perturbation to SC mortar such as fluidization or rearrangement of the lipid bilayer will thus reduce SC barrier function. The appendageal route has played hitherto insignificant role in human. In addition, the importance of the corneocytes membranes can be excluded as well [30].

Among all layers, SC as the outermost skin layer receives an important attention since this takes over the first skin barrier function and also provides the rate-limiting step in drug penetration process [32,33]. Considering its unique structure, Subedi et al. [33] emphasized that only drugs with log *P* between 1 and 3, MW less than 500 Da, melting point below 200 °C and required dose less than 10 mg/day have sufficiently high chance as candidates for transdermal administration.

As shown in Fig. 2.6, the transcellular pathway comprises routes through the protein-filled corneocytes and the multilamellar lipid matrix alternately meanwhile the intercellular pathway allows drugs to penetrate between the cells. Hydrophilic substances are likely to penetrate via the transcellular pathway alternately between the corneocytes and the lamellar lipid layers whereas the intercellular pathway could be more reasonable for the lipophilic drugs [32].

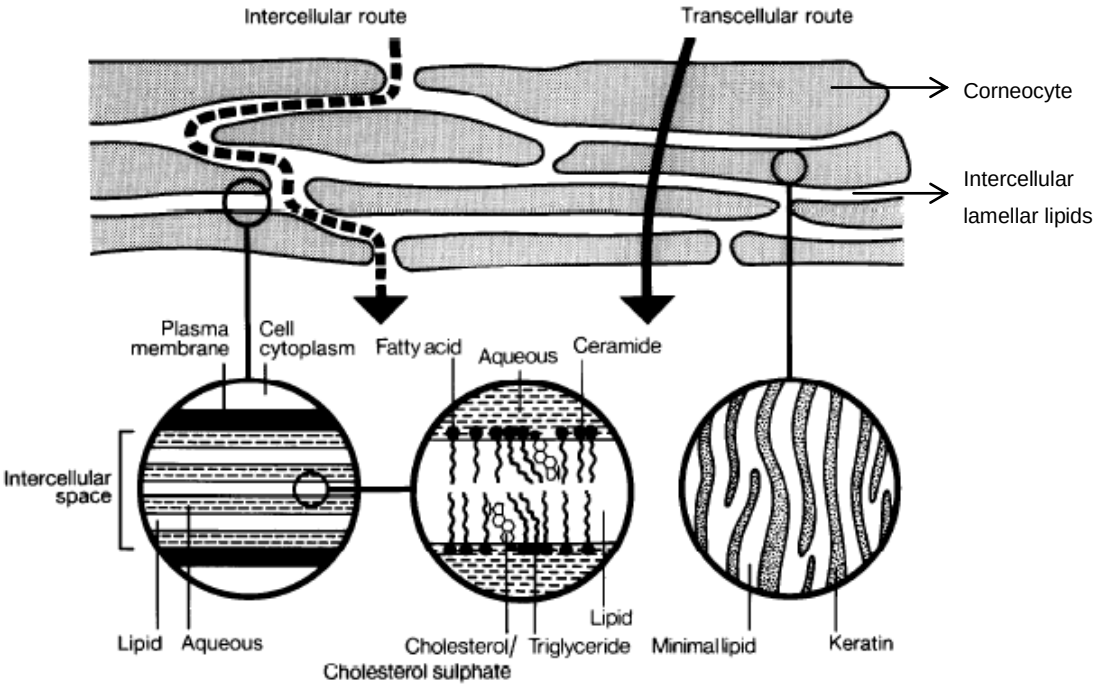

Fig. 2.6 Penetration pathways across SC: intercellular and transcellular, taken from ref. [30]

Neubert and Wepf [34] proposed a new insight into the structure of SC and realized this through the “hook like” structure of the corneocytes, the existence of the corneodesmosomes and the bilayer structure of the SC lipids. According to this new understanding, transcellular pathway is rather unlikely since the drug must penetrate or permeate through the hydrophilic and lipophilic layers of SC alternately. However, a penetration pathway through the corneodesmosomes is possible considering its large quantities per corneocyte. Therefore, this has been proposed as the possible route for the hydrophilic drugs replacing the previously transcellular pathway.

2.1.5 Quantitation of drug permeation across skin

Examining the possible pathways of drug permeation across the skin, SC has been the rate-limiting step for the most compounds. This led to the broad use of SC for analyzing most cases of transdermal drug delivery. Drug permeation across the skin is a diffusion-controlled process which can be quantified with the term flux (J), i.e., the amount of drug diffusing over time per unit area. At a steady-state condition, the diffusion process follows Fick’s 1st law which is expressed as [35]:

$$J = \frac{\mathrm{d}M}{\mathrm{d}t} = \frac{K_m \cdot D_S \cdot C_O}{\delta} \qquad \text{(Eq. 2.1)}$$

M = the amount of drug diffusing through a unit area of the skin in time t

C_o = drug concentration within the membrane surface/ in the vehicle

K_m = skin/ vehicle partition coefficient

D_s = (apparent) diffusion coefficient

δ = the diffusional path length

The applicability of this law is under assumptions that: (a) only a single drug is important in the formulation, (b) *D* must be constant in terms of time and position in the formulation layer, (c) only the drug is able to permeate out of the formulation; vehicle constituents cannot diffuse or evaporate and (d) the drug is rapidly removed as it reaches the receiver compartment (drug concentration ~0 at the receiver-formulation boundary for $t>0$) [36]. Concerning the last assumption, which is better known as *sink-condition*, has to be guaranteed that drug diffusion is ongoing since in the *in vivo* situation the permeated drug will be directly transported by the microvasculature, which lies beneath the epidermis at a depth of 150-200 µm from the skin surface [35]. In addition, Eq. 2.1 is acceptable when the amount of depleted drug from the donor is less than 10% from its saturated solubility in the receiver compartment during the diffusion process. For lipophilic drugs with limited aqueous solubility, the inclusion of solubilizing agents such as alcohol or surfactant in the receiver medium can help accomplishing the sink-condition besides maintaining a sufficient stirring rate within the receiver compartment [35]. Nevertheless, any of this treatment should not cause any significant alteration to the skin during the permeation.

The skin flux is determined from the slope of a plot of the permeated amounts [g/cm^2] vs. time [s], taken from the steady state part of the plot in accordance to Fick's 1st law. The lag time, t_L, can be determined by extrapolating the steady state line of the cumulative drug amount to the axis where drug release = 0 through Eq. 2.2:

$$t_L = \frac{\delta^2}{6D_s} \qquad \text{(Eq. 2.2)}$$

It is common to express K_mD_s/δ from Eq. 2.1 as permeability coefficient, *P*, so that the equation can be rewritten as in Eq. 2.3:

$$J = \frac{dM}{dt} = P \cdot C_O \qquad \text{(Eq. 2.3)}$$

Considering the influence of the viscosity of the formulation on the permeation process, this parameter is not the rate limiting step of the percutaneous absorption. However, it determines drug diffusion and drug release from the vehicle [37].

According to the Stokes-Einstein equation (Eq. 2.4), the solute diffusion coefficient (*D*) decreases when viscosity of the medium (η) increases. A low *D* will result in a low flux according to Fick's 1st law.

$$D = \frac{kT}{6\pi\eta R} \qquad \text{(Eq. 2.4)}$$

2.2 Human nail

The nail unit encompasses the nail plate, nail folds, nail matrix, nail bed and hyponychium [38]. Besides the protecting function, human nail supports the fine motor function and the daily activity, e.g., scratching and grooming [39]. The schematic illustration of human nail unit is displayed in Fig. 2.7.

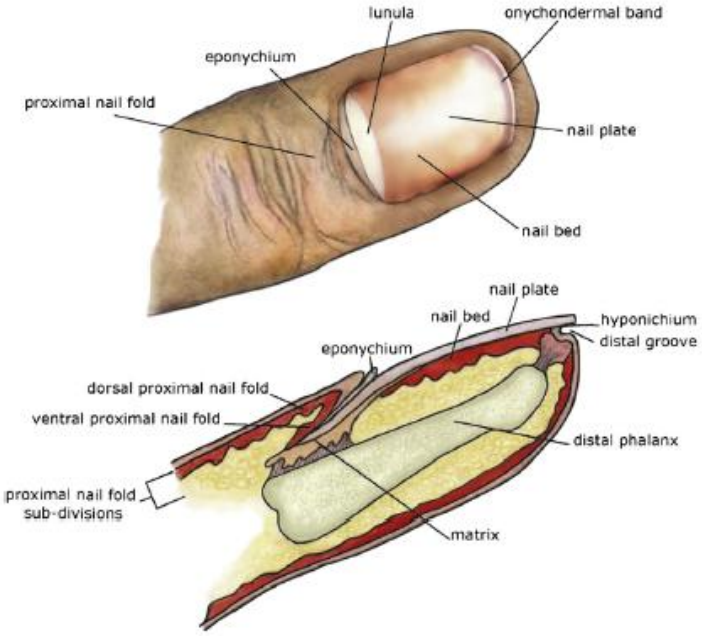

Fig. 2.7 Human nail unit, taken from Ref. [39]

2.2.1 Anatomy and function

Nail plate, the most demonstrative part of human nail, is the hardest part of the nail unit. It is composed of about 80-90 layers of dead, keratinized, flattened squamous cells which are tightly arranged to one another [38,39]. α-keratin makes up the nail with mainly hair-type keratins that are more dominant (>90%) than epidermal-type keratins [40]. Nail plate thickness varies according to different authors ranging from 0.25 to 1.0 mm [41]. Nail plate can be divided into three layers according to its matrix-origin: ventral, intermediate and dorsal [39,40]. Calcium is abundant in the nail plate (0.1%) but the sulfur proteins, and accordingly the disulfide crosslinks, are mainly

responsible for its strength [39,40]. In addition, nail plate contains 10-30% water and a small amount of lipid at 0.1-1% [38]. Nail bed consists of viable epidermis as in the skin except that nail bed is much thinner with less subcutaneous fat [39,42]. Similar to hair, nail has been shown to be more permeable than the stratum corneum to water. Water is important for nail since it confers elasticity and flexibility [40].

2.2.2 Keratin

Keratin is not a single substance. In fact, it is composed of a complex mixture of proteins with molecular mass between 40-70 kDa and variation in isoelectric point (pI) [43,44]. Two-dimensional electrophoresis is needed for resolving all keratin proteins, according to their molecular weights (MW) and thus isoelectric points. Human keratin proteins can be grouped as acidic/ type I with pI 4.9-5.4 and basic/ type II with pI 6.5-8.5. In bovines, pI values are slightly different being <5.6 for type I and >6.0 for type II. In addition, to enable the identification of a specific keratin protein after resolution according to MW, immunoblotting assay is needed. K13 is a good example; its size is 51 kDa in humans and 43 kDa in bovines [43].

2.2.3 Availability of human nail for studying drug permeation

Nail diseases, especially onychomycosis, which contributes to as much as 50% of nail disorders [45-47], should be efficiently treated to improve the patients' quality of life. Unlike skin diseases, for which medical treatments are continuously developed, treatments of nail diseases hitherto are not satisfying. The main obstacles are our limited knowledge of conquering the perfect barrier of the human nail and the limited source of human nails as the object of the study itself. Bovine hoof has been accepted until now as a substitute for human nail, but significant differences between bovine hoof and human nail have been reported [11]. The limitation of animal hoof as a study object is its great water uptake during hydration, which could lead to an overestimation of drug permeability, when this is translated to human nail. Khengar et al. [11] reported that the water uptake by human nail was 27 ± 3% whereas that of horse hoof was 40 ± 9%. Nail clippings have been used for permeation studies as well, but they are not the best model due to the limited nail bed [48] and the available contact surface with formulation.

Both human nail and animal hoof are composed of the same keratin type (i.e., α-keratin). The main difference includes the ratio of the amino acid components besides the inner structure, with the latter due to the specific differentiation pathways *in vivo*

[49]. However, both human nail and animal hoof possess α hair-type keratin which is well-known for its high sulfur protein content [50].

Mertin and Lippold [9] investigated the influence of drug lipophilicities and solubilities in water on their permeabilities across human nail and hooves. They found that drug permeability across both membranes was not dependent on its lipophilicity. Both materials were found to behave as a hydrophilic gel membrane rather than a lipophilic partition membrane, as in the case of human skin [8-10]. The mechanism of drug permeation across hoof resembled that in human nail plate, except that hoof retained more water. This was confirmed by a study with serial nicotinic acid esters that permeated across human nail and bovine hooves. Hoof permeabilities were found to be 10- to 30-fold greater than those across the human nail plate [9]. Nail hydration plays an important role in the ungual permeation by providing more space for the permeating substance. This has been observed by Walters et al. [10,51] as well, where the permeation of homologous alcohols was higher from aqueous solution than that from the neat liquids (undiluted).

2.2.4 The development of a human nail plate model made of human hair keratin

Human hair is abundant in nature, and its keratin type is present in human nail, too [43,49,52-54]. Baden et al. [53] studied human keratinized tissues (stratum corneum, hair and nail) and found that hair and nail showed many resemblances in their physical and chemical properties, despite their different morphological properties. The question was whether the extraction of keratin from hair with e.g., the Shindai method and its re-assembly into a film would enable its use as a nail plate model.

Keratin is insoluble in many common solvents, such as dilute acids, alkalines, water and organic solvents [43]. A common method to extract keratin involves the use of reducing agents because the native form is hard to extract due to its highly cross-linked state by disulfide bonds. Shindai method, which avoids a detergent, provides a sufficient amount of extracted proteins for analysis and can avoid protein hydrolysis [55]. Reducing agents such as dithiothreitol and 2-mercaptoethanol work by cleaving keratin’s disulfide bonds and thus increasing its solubility [43].

The Shindai method employs a mixture of Tris pH 8.5, urea, thiourea and 2-mercaptoethanol to extract hair [55]. A further process is needed to transform the hair extract into a film which is stable and water-resistant for permeation study. Reichl [12]

improved this method initially for producing substrate material for standard cell cultivation. After extraction, the hair extract was dialyzed against water to remove the excess of the reagents, producing keratin nanosuspension. Following centrifugation to eliminate coarse particles, the still turbid supernatant of this suspension is ready as a raw material for manufacturing a keratin film. The suitability of this keratin film as a human nail plate model still has to be tested in terms of its mechanical strength, water absorption ability and permeability to different markers with different physicochemical properties.

2.3 Superficial fungal infection (mycosis)

Fungal infections may be divided into two different types, i.e., a deep/ systemic infection and a superficial/ local infection. The former develops commonly into a life-threatening stage whereas the latter is considered to be mild. Superficial fungal infection occurs in the outermost layer of the body, such as stratum corneum, hair and nails. This kind of disease has not only been found in humans since many cases have also been developed in animals, for example in pet skin and animal hoof.

The microorganisms responsible for mycoses are mainly the dermatophytes. They feed on mammalian keratin as their essential nutrient source [56]. Keratin serves not only as nutrient, but functions also as the up-regulator for some putative virulence factors of the fungi. An example is the over-expression of G-protein subunit alpha in an *in vitro* condition which might play an important role in modulating the virulence factors [57].

Trichophyton rubrum accounts for more than 90% of the chronic dermatophytosis apart from other dermatophytes from the genera *Microsporum* and *Epidermophyton* [56,57]. Other non-dermatophytes have also been credited as the cause of onychomycosis or nail fungal infections such as *Scopulariopsis brevicaulis, Aspergillus versicolor, A. flavus, A. niger, A. fumigatus, Fusarium solani, F. oxysporum and Scytalidium spp* [58]. Although these non-dermatophyte fungi do not have sufficient keratinolytic activity, the external factors can still induce infection. A low hygiene level, local trauma, peripheral diseases, immunodeficiency stage and climate may elevate the risk factor of mycoses [58].

The absence of keratin in the deeper layer of the body is the main reason why mycosis remains superficial [56,58]. During occupation, dermatophytes produce not only keratinolytic enzymes such as keratinases which break down the keratin

structure, but also other pathogenic factors such as xanthomeganin (toxin), mannans (immunosuppresive agents), haemagglutinins, trigger factors for haemolytic reactions and antibiotics to bear the local bacterial colonization [56].

2.3.1 Host responses

There is a principal difference between antropophilic and zoophilic/ geophilic dermatophytes. The former type causes rather a chronic clinical manifestation meanwhile the latter produces a more acute reaction [59]. The invasion of dermatophytes into the tissue will trigger humoral and/or cellular immune responses as a host defense mechanism. This may prevent infections to get into the deeper tissues as well [56,60]. Dermatophytes possess two main antigens, i.e., glycopeptides and keratinases. The protein fragment from the former stimulates preferentially cell-mediated immune response whereas the polysaccharide fragment stimulates the humoral one. Keratinases, enzymes produced to invade the keratinous tissues, are able to induce a delayed-type hypersensitivity response in an *in vitro* experiment with animals [59,60].

During the fungal invasion multiple inflammatory cytokines, interferon and various interleukins (IL) such as TNF-alpha, IL-1 beta, IL-8 and IL-16 are released by keratinocytes and mononuclear cells [56]. This cell-mediated immune response is absent in the ‘dead’ SC and nail plate; this is an additional reason why the invasion cannot go into deeper viable tissues of the skin [59]. Nevertheless, people with lack of cell-mediated immune response do not develop a systemic dermatophyte infection. Complement, a series of plasma proteins that act as mediators of inflammation, defenses the body through the interaction of antibody with the microorganisms/ antigens (classical pathway) or interaction with certain microbial cell walls/ toxin (alternative pathway). The action of the complement will be followed by phagocytosis of the fungal cell by neutrophils or macrophages [61].

A severe infection is usually experienced by patients with an immune deficiency condition, especially AIDS, while in a normal circumstance this infection is not life-threatening. This fact shows the importance of human immune system in controlling the spreading and growth of dermatophytes in the environment [60].

2.3.2 Clinical manifestations

Lesions developing during the infection are known as tinea or ringworm [56]. The infection is distinguished according to the Latin term indicating the infected site, e.g.,

tinea capitis for infection of the scalp, tinea barbae in beard and mustache, tinea corporis in glabrous skin, tinea cruris in groin, tinea favosa in favus, tinea manuum in hand, tinea pedis/ Athlete's foot in feet, und tinea unguium in nail. In addition, several sites can be infected by a single fungal species and vice versa, different species may cause identical lesions [60,62].

The spreading of dermatophytes on the skin can be recognized from a marked erythema, scaling and palpable infiltration of the skin, sometimes accompanied by pustules. The inflamed sites often have an arched or circular shape (see Fig. 2.8 (a)); explaining the origin of term of ringworm [56]. Dermatophyte infections are often found in the skin, especially in the dead layer of stratum corneum, nails, hair follicles and hair [56]. Hair follicle has probably been the responsible site for relapses and recurrences since these sites are quite protected from topical and systemic therapies. Topical treatments usually do not penetrate deep into follicles meanwhile the systemic ones are delivered into the skin surface by sweat thus avoiding the follicular canal [59].

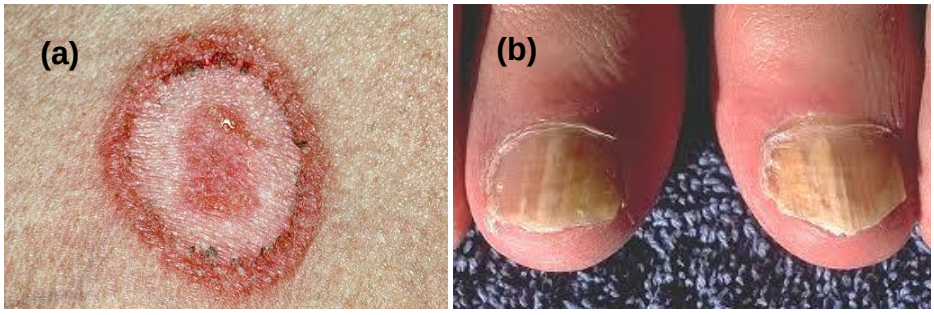

Fig. 2.8 Skin rashes (a) and infected nails (b) due to dermatophyte

Sources: (a) http://www.webmd.com/skin-problems-and-treatments/picture-of-ringworm-of-the-body-tinea-corporis; (b) http://dermatology.fromyourdoctor.com/

The visible lesions at the infected sites are due to the biological products of dermatophytes which are majorly able to digest keratin and induce inflammation at once. Inflammation occurs at the infected site since fungal hyphae are chemotactic to the host immune system. Different from skin, nail does not develop any inflammation at the infected site due to the absence of viable cells and immune cells (see Fig. 2.8 (b)). Furthermore, a slow growth rate of nails makes the fungal elimination more difficult and many cases develop into chronic infections [56].

2.3.3 Mycosis therapy and its drawbacks

Basically, the choice of the therapy is assessed from the malignancy of the infection. Meanwhile lesions at early stage can be treated with topical formulations, a more severe and widespread infection must be treated perorally [60]. Particularly, tinea unguium/ onychomycosis requires peroral therapy in most cases since topical treatments do not produce sufficient drug levels at the periphery. Steroid agents such as prednisone or betamethasone are often meaningful in the therapy to reduce the inflammation. In addition, an antibiotic is sometimes necessary to handle the arising secondary infection [1]. Various antifungal aägents have been described for dermatophytosis treatment [1,60] :

- the azole group: miconazole, clotrimazole, econazole, ketoconazole, oxiconazole, tioconazole, isoconazole, sulconazole, bifonazole, fenticonazole and sertaconazole
- allylamine group: butenafine, terbinafine and naftitine
- echinocandin group
- morpholine derivative: amorolfine
- ciclopirox olamine
- tolnaftate
- griseofulvin
- haloprogin

Topical medications are widely available for mycosis in the form of cream, gel, lotion and shampoo. They contain majorly the active from the azole, allylamine and morpholine derivatives. Five antifungal drugs are common for systemic therapy, i.e., terbinafine, itraconazole, fluconazole, griseofulvin and ketoconazole [1]. The current treatments available and approved for dermatophytosis are listed in Table 2.1.

Table 2.1 Available treatment of dermatophytosis

	Terbinafine	Itraconazole	Fluconazole	Ketoconazole	Griseofulvin
Tinea pedis/manuum	Cream[a]: twice daily, 1-4 weeks 1% solution[a]: twice daily, 1 week Oral: 250 mg/day, 2 weeks	Oral: 200 mg, twice daily for 1 week	Oral: 150 mg once weekly for 2-6 weeks	2% cream[a]: once daily for 6 weeks Oral[a]: 200-400 mg/day for more than 4 weeks	Oral : Microsize[a] 1g/day Ultramicrosize 660 or 750 mg/day for 4-8 weeks
Tinea corporis/ cruris	Cream[a]: twice daily, 1-4 weeks 1% solution[a]: twice daily for 1 week Oral: 250 mg/day for 2-4 weeks	Oral: 200 mg/day for 1 week	Oral: 150-300 mg once weekly for 2-4 weeks	2% cream[a]: once daily for 2 weeks Oral[a]: 200-400 mg/day for 4 weeks	Oral: Microsize[a] 500 mg/day Ultramicrosize 330-375 mg/day for 2-4 weeks
Tinea unguium/ Onychomycosis	Oral: 250 mg/day Toenail: 12-16 weeks Fingernail: 6 weeks	Oral: pulse therapy: 200 mg twice daily for 1 week followed by 3 itraconazole free weeks Toenail: 3 pulses Fingernail only: 2 pulses	Oral: 150 or 300 mg once weekly for 6-12 months Toenail approx. 9-15 months, fingernail approx. 4-9 months	Oral: 200-400 mg/day for 6 months (not recommended due to hepatotoxicity risk)	Microfine: 500 mg daily for 6-12 months Microsize[a] 1g/day Ultramicrosize[a] 660 or 750 mg/day for 4-12 months

[a] FDA approved; modified from Gupta, A.K and Cooper, E.A. [1]

The length of the treatment is depending on the malignancy of the infection and susceptibility of the fungus to the drug. Unfortunately, dermatophytosis treatment is not satisfying due to its low mycological cure rate, e.g., in the case of griseofulvin. In addition, other problems such as a high relapse rate subsequent to topical application and arising incidences of side effects, e.g., hepatotoxicity due to ketoconazole, have been reported [60]. Drug interaction with other medication has been reported as well, such as with antidiabetic agents, since these drugs share similar hepatic pathways for metabolism via the cytrochome P-450 system. Interference in metabolism can shift the plasma level of the counter drug to a higher or lower level thus followed by either intoxication or therapy failure, respectively. As a consequence, the use of itraconazole for example is prohibited for patients with ventricular dysfunction or with a history of congestive heart failure and the respective medications [1,63].

Special attention should be given to onychomycosis because its treatment is up to now still problematic due to the long treatment, thus a limited success because of non-compliance of the patients. Furthermore, the relapse incidence is high, 3-20 % after peroral administration with TBF [64,65]. To reduce relapse, onychomycosis treatment is still involving mechanical approaches through trimming, aggressive debridement (yet not for children), nail abrasion and nail avulsion (partial or full removal) [1]. Although not being convenient, mechanical interventions can reduce the fungal burden in the infected nail in most cases and thus accelerate the healing process [66].

The length of the treatment has been the major drawback of the therapy. Treatment risk is high for patients who receive other treatments which are metabolized through the hepatic pathway. Although the topical treatment is the most favorite among others, the cure rate is not satisfying even for mild to moderate infections. The cure rates were 33% for nail lacquer containing 8% ciclopirox (after 48 weeks) and 60-76% for nail lacquer containing 5% amorolfine (after 6-12 months of treatment) [1].

2.3.4 Therapy failures

There are many factors that lead to the failure of dermatophytosis therapy. Major factors are poor patient compliance, misdiagnosis, insufficient consideration of individual need/ condition of the patient, lack of patient counseling during the treatment and variation in host response [66]. Microscopic examination and culture of the causative fungi are the deciding factors to treat the infection properly. Unfortunately, the rate of false negative culture identification is high; this makes the

attempt to distinguish the occurrence of a new infection from relapse more difficult [1]. However, an improvement in identifying the fungi via biomolecular methods offers now better results, e.g., identification of fungal DNA [1,67].

The choice of the treatment is made solely by the physician. A lack of knowledge about the causative fungus, the severity stage of the infection and drug resistance issues may lead to an improper medication choice. Although topical formulations increase the compliance of patients, the cure rate is low. A prolonged oral therapy is the golden standard for dermatophytosis in many cases but still, a sufficient counseling must be altogether given to improve the compliance of the patients. Education about a good hygiene can avoid the spreading of the infection, e.g., to other family members. An individual need of each patient must be considered, especially for elderly, children, pregnant women and immunocompromised patients.

The possibility of a tailored therapy has been suggested to increase cure rates and to reduce relapses [1,66]. A combination of two antifungal agents with different mechanisms may give a synergistic effect, e.g., terbinafine with itraconazole. The combination is also possible for topical and oral therapy, e.g., amorolfine or ciclopirox nail lacquer with an oral antifungal drug. This suggestion needs however further clinical studies to assess the therapy improvement and is not yet currently approved [1].

2.3.5 Pharmacology and pharmacokinetics of terbinafine (TBF)

Terbinafine is a relative new synthetic antifungal agent from the allylamine group. Terbinafine works by inhibiting the transformation of squalene to squalene 2,3-epoxide via the fungal enzyme squalene epoxidase in the ergosterol pathway [68]. This inhibition leads to the accumulation of squalene and a decrease in metabolites such as ergosterol and lanosterol, the essential components of the fungal cell membrane [63,68-70]. Fuglseth et al. [68] suggested that the antifungal activity of TBF originated from its steric and electronic effects which are important for the squalene epoxidase inhibition. Furthermore, their results indicated that the nitrogen basicity of TBF is essential for the binding with this enzyme.

TBF acts fungicidal to dermatophytes and fungistatic to yeasts group of fungi such as *Candida spp*. The cidal action was associated with the high concentration of squalene within the fungal cell meanwhile the fungistatic action appears due to the deficiency in ergosterol [69]. Thus, the death of the dermatophyte cell is rather due to the

accumulation of squalene whereas in yeast cells, the growth inhibition runs parallel to the drop in ergosterol content [71]. The highly lipophilic squalene in a high amount within fungal cells acts as a lipid sponge, extracting the essential lipid components of the fungal cell membranes thus weakening its membrane integrity. Disintegration of the vacuolar membrane will then release lytic enzymes which is lethal to the cell [69]. The relation between TBF minimum inhibitory concentration (MIC) for complete suppression of the fungal growth and sterol biosynthesis can be seen in Table 2.2. In addition, the values shown in Table 2.2 reflect the different strengths of TBF to filamentous and yeast fungi. A low MIC value implies a great impairment to the sterol biosynthesis which is indicated as low IC_{50} and IC_{95} values, respectively.

Table 2.2 TBF: Relation between MIC [µg/ml] and sterol biosynthesis

Fungus	**MIC**	**Sterol biosynthesis**	
		IC_{50}	**IC_{95}**
Trichophyton rubrum	0.003	0.0005	0.02
T. mentagrophytes	0.003	0.002	0.04
Aspergillus fumigatus	0.8	0.07	1.2
Candida parapsilosis	0.4	0.006	0.3
C. albicans Δ124 (yeast)	3.1	0.008	0.2
C. albicans Δ126 (yeast)	12.5	0.014	0.63
C. albicans Δ126 (mycelial)	1.5	0.013	0.22
C. glabrata	100	0.04	0.9

IC_{50}, IC_{95} = drug concentration that produces 50% and 95% inhibition (n = 3); reproduced from ref. [69].

The allylamine group offers a higher selectivity compared to the azole group in terms of the work mechanism. Almost every step in the host steroid hormone synthesis can be affected by azoles but not by allylamines [70]. TBF does not impair the work of the human liver enzyme since its target, squalene epoxidase, does not belong to the cytochrome P-450 family [69]. Therefore, TBF acts only as a substrate for a fraction of cytochrome P-450 and it will be rapidly degraded to several less lipophilic metabolites. This action is different from the azole group which is involved in every step of the human cholesterol synthesis in the liver via a direct binding with the haem group of almost all cytochrome P-450 [70].

TBF shows a rapid absorption within two hours and is rapidly enzymatically metabolized in the liver. The hepatic cytochrome P-450 plays an important role for the metabolism of TBF. The metabolism process involves side chain oxidation at the *t*-

butyl group, dealkylation and aromatic oxidation. Despite its high selectivity, care must be taken for patients with liver impairments. Its lipophilic character drives a high distribution into tissues, especially adipose tissue and skin, thus the plasma level remains low. This unique distribution to the periphery is an advantage for the treatment [70].

2.3.6 Physicochemical properties of TBF

Terbinafine HCl ($C_{21}H_{25}N \cdot HCl$), the salt form of terbinafine with log *P* of 3.3 [72], is an allylamine/ benzylamine derivative together with other antifungal agents butenafine and naftitine. TBF structure is shown in Fig. 2.9. TBF salt is preferably used instead of its base form since the salt form gives a higher stability and aqueous solubility [73]. TBF melting point, after being recrystallized from 2-propanol, ranges from 204-208 °C [74,75]. TBF solubility in several pharmaceutical-related solvents is listed in Table 2.3. TBF has a rather limited aqueous solubility despite its salt form and its fairly high solubilities in alcohols.

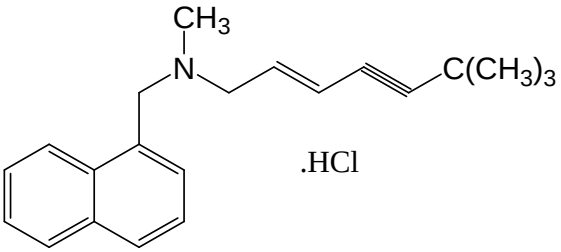

Fig. 2.9 Chemical structure of terbinafine HCl

2.3.7 TBF stability in bulk and in formulation

Several TBF degradation products may be found in formulations after several months of storage. They may also originate from impurities in the bulk material. 1-methylaminomethylnaphtalene (MAMN) is an impurity as well as a degradation product from the synthesis process. Further impurities from the synthesis are 4-methyl-terbinafine and β-terbinafine derived from β-MAMN as an impurity of the precursor MAMN. Z-terbinafine is proposed to be a potential degradation product of TBF [76]. The chemical structure from each compound is displayed in Fig. 2.10.

Ahmad et al. reported that no degradation products were found after storing TBF tablets and cream for 6 months in an accelerated condition at 40 °C and 75% RH [77]. Matysová et al. recommended the storage of TBF solution in acetonitrile at a low temperature of 4 °C. This solution was only stable up to 48 h, corresponding to

maximum of 1% TBF decrease (from the initial concentration). Furthermore, they found 0.253% MAMN, corresponding to the TBF amount, from a TBF cream after being stored for 6 months at 40 °C and 60% RH. In all cases, omitting light during the storage is recommended [76,78,79].

Table 2.3 TBF solubility in some pharmaceutical-related solvents

Solvent	Solubility [g/L]
Anhydrous ethanol[a]	freely soluble
Methanol	freely soluble
Isopropyl alcohol	120
Isobutyl alcohol	21
Water	8
Acetone	less than 0.5

[a] from ref. [78]

Solubility determination: ~0.5 g TBF was boiled with 5 ml solvent, kept for 24 h at room temperature and filtered, solubility was calculated from the difference of the filtrate and total weight; modified from ref. [75]

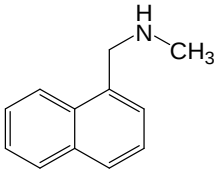

MAMN

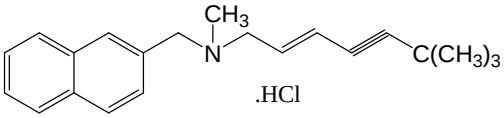

β-terbinafine

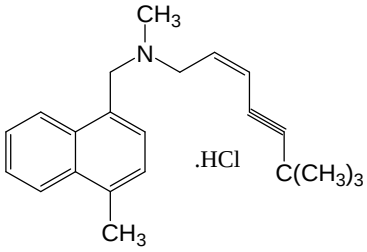

4-methyl-terbinafine

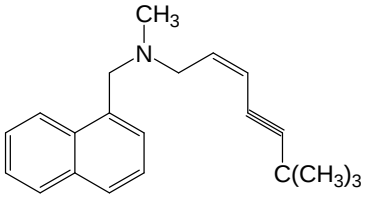

Z-terbinafine

Fig. 2.10 Impurities and possible degradation products of TBF

2.4 Development of formulation for topical administration

There are several approaches to enhance drug permeation rate across the skin. The most conventional one is the incorporation of chemical penetration enhancers, but the safety issues and irreversible damages caused by, limit their use. Other alternatives

such as modifying drug's thermodynamic activity and vehicles still remain to be explored.

2.4.1 Chemical penetration enhancers

The lipid-protein-partitioning theory suggested by Barry [30] proposes three main mechanisms of the chemical penetration enhancers, i.e., alteration of the intercellular lipid or the protein domains of SC, drug partition enhancement into the skin or the combination of both mechanisms. A new study utilizing an FTIR approach found that lipophilic penetration enhancers rather fluidize the arrangement of the ceramides so that the spaces between them increase. On the other side, hydrophilic enhancers decrease the strength of hydrogen bonds between the polar head groups of the ceramides [80]. Both types of enhancers perturb SC arrangement thus facilitating drug entry into the skin. Chemical penetration enhancers offer a broad choice in order to increase drug diffusion across the skin. Water, not to be neglected, is also a penetration enhancer working via an increase in hydration. Thus, the solute mobility is higher in the loosened SC lamellar arrangement [28]. Other groups from different chemical classes such as hydrocarbons, alkanols and alkenols, fatty acids, alkyl amino esters, amides, amines, sulfoxides, cyclic carbohydrates, terpenes and pyrrolidines have been acknowledged and reviewed extensively as transdermal penetration enhancers for various substances as well [33].

2.4.2 Drug's thermodynamic activity in the vehicle

The drug release rate from the formulation depends on drug's thermodynamic activity [81]. Thermodynamic activity has been described as the driving force of the drug to leave the vehicle and penetrate across SC [82,83]. A saturated drug concentration in the vehicle exhibits the highest thermodynamic activity, i.e., it reaches unity. Drug solution below its saturated concentration exhibits thermodynamic activity of less than unity and therefore its release rate is slower than that of the saturated drug concentration. A saturated drug concentration in different vehicles will exhibit similar release rates, accordingly similar penetration rates, since in this state the release rate will be independent of the vehicle [82,84]. The dependency of drug's penetration rate on its thermodynamic activity has been proposed by Higuchi in Eq. 2.5 as follow:

$$\frac{dq}{dt} = \frac{\alpha}{\gamma}\frac{D \cdot A}{L} \qquad \text{(Eq. 2.5)}$$

dq/dt = the steady state rate of penetration

α = thermodynamic activity of the drug in its vehicle

γ = effective activity coefficient of the agent in the skin barrier phase

D = the effective average diffusivity of the agent in the barrier phase

A = the effective cross section area

L = the effective thickness of the barrier phase

Following Higuchi, Ishii et al. [84], expanded Fick's 1st law and Nernst-Planck equation and resumed that under a constant temperature, steady-state flux of a drug (*J*) is a function of only drug's activity (A_v'). A suspension exhibits a unity-independent activity of different vehicles and thus the skin permeation rate is also independent of the vehicles. Vice versa, different vehicles with similar drug concentrations, yet different thermodynamic activity of the drug, can be expected to give different release rates. Following release from the vehicle, drug partition and permeation across SC is afterwards determined by the drug lipophilicity and melting point [81].

2.4.3 Liquid crystal phases as drug carrier

The current development in drug formulation and delivery seeks alternatives where the carrier/ vehicle is designed in such a way so that a drug can be delivered more readily across the skin. In some extent, the vehicle should even be able to modify the barrier function of SC or its integrity without causing any irreversible damage. For granting this need, liquid crystal as a carrier could enhance drug penetration across SC due to its low surface tension at oil/water interface; this can promote a higher drug partition into SC. Furthermore, this type of vehicle may enable higher drug loading compared to other conventional bases [85].

Different liquid crystal phases namely lamellar, hexagonal and cubic systems made of Pluronic® 105/ water mixtures have been reported to enhance permeations of some drugs across rabbit ear skin [85]. The enhancing effect was found to be specific for each drug, e.g., diclofenac sodium and paracetamol permeated faster from the hexagonal phase meanwhile propanolol and α-tocopherol were faster from the lamellar phase, all compared to other examined phases. A cubic phase, made of lauric acid, monolaurin and simulated endogenous intestinal fluid, was able to solubilize

cinnarizin, a lipophilic drug with log *P* of ~5.8 and aqueous solubility less than 1 µg/mL, to a $2 \cdot 10^5$-fold greater extent than its solubility in buffer pH 6.5 [86]. Brinon et al. [87] reported that the diffusion coefficient (*D*) of the hydrophilic sunscreen benzophenone-4 was the highest in the cubic phase, made of surfactant mixtures Brij® 30 and Brij® 35, whereas the lipophilic sunscreen octyl methoxycinnamate's *D* was the highest in the lamellar system containing similar ingredients. The corresponding liquid crystal bases without drug were used as diffusion receivers in those experiments; both being separated with a filter cellulose membrane as barrier. Unfortunately, the permeation enhancement across pig skin from these systems was not significantly higher than that from a control, hinting at the rate-limiting step of the skin for this process. Since entering of large aggregates of the liquid crystal into SC is rather unlikely, it has been hypothesized that the single constituent of the vehicle, e.g., surfactant monomer, is able to penetrate and thus improves drug penetration [87].

2.4.4 Thermogelling formulation

A novel vehicle for topical application based on poloxamer 407 had been developed which was denoted as thermogel. This formulation was composed of poloxamer 407 (Lutrol® F127), isopropyl alcohol, dimethyl isosorbide, Miglyol® 840 and water. In addition, this vehicle exhibited a reversible thermogelation property, it was semisolid at room temperature and liquid below 13 °C, e.g., in the refrigerator [4,5]. Thermogel containing 5-ALA, a hydrophilic drug with log *P* -1.51, showed a higher permeation rate across SC compared to other creams described in German Pharmacopoeia, i.e., 7.5-fold and 19.5-fold higher permeation rates than those from Basiscreme DAC and water containing hydrophilic ointment, respectively [5]. A synergistic work of all components was suggested to be responsible for this permeation enhancement since the absence of a single component decreased the permeation flux. In addition, DSC measurement displayed a stronger interaction between the vehicle and SC; this was evident from its highest endothermic shift transitions of T2 and T3, respectively, and its lowest enthalpy involved among other formulations [2,5].

The original thermogel vehicle was composed of 25% mixture of poloxamer 407/POX and Miglyol® 840/MIG (fixed at 4:1), 25 % mixture of isopropyl alcohol/IPA and dimethyl isosorbide/DMIS (fixed at 1:1) and 50 % of water. By varying the composition of the constituents, different appearances and physical properties were achieved. Interesting for dermal application would be the semisolid systems such as cream- and gel-like, located in the area with the composition of 20-60 % POX/MIG, 0-30 %

IPA/DMIS and 20-75 % water (all w/w) [4]. Outside this area the systems were not appropriate for topical application: they were paste-like, liquid or instable subsequent to the manufacture.

Thermogel featured a thermoreversible gelation upon heating and cooling. Gelation occurs upon heating via dehydration of the lipophilic blocks of propylene oxide groups, followed by dehydration of the hydrophilic blocks of the ethylene oxide groups. Thereafter, the transition from sol to gel occurs. The process is reversible and can be repeated by changing the heating/ cooling direction. Generally, gelation temperature increased with decreasing POX and IPA/DMIS contents [88].

Although the majority of the formulations were isotropic, few formulations were anisotropic, especially in the area rich in POX/MIG with water content less than 10%. The border between isotropic and anisotropic systems could be thus drawn at 10% water content. Only systems without water were anisotropic when POX/MIG<50%. From the measurement by means of wide angle X-ray diffraction, the birefringence of the systems originated from the incomplete solubilization of POX in the system; this was concluded from the appearances of POX crystalline reflections at about 2Θ of 19° and 23° [4].

Formulations located in the area with 25-70% POX/MIG, 0-30% IPA/DMIS and 20-75% water feature a so-called ringing effect upon knocking the jar to a hard surface. The manifestation of this phenomenon is suggested due to the existence of a cubic liquid crystal. Vice versa, in some cases ringing effect can be a hint for the presence of this structure [89,90]. Since the cubic structure is isotropic, an additional analysis by means of small angle x-ray diffraction (SAXD) is needed. This technique determines the spacing order of a highly ordered system such as a crystal or liquid crystal. The hint at a cubic liquid crystal was also supported by the high viscosity of the formulations. So far, three types of the cubic structure from this area have been identified, i.e., space groups of Fm3m, Pn3m and Im3m, respectively [6]. Referring back to the original composition of the thermogel, according to SAXD measurement, this composition possesses Pn3m cubic structure. Whether this cubic liquid crystal is also responsible for 5-ALA high permeation rate, further investigations are needed.

Subsequent to one year of storage in a climatized room at 20 °C, three kinds of instabilities had been observed for these thermogelling formulations. Microbiological growth was detected in formulations with low POX/MIG in absence of IPA/DMIS, liquefaction of gel-like formulations with POX/MIG less than 50% and inhomogeneity

in some liquid formulations. Furthermore, crystal growth was observed in anisotropic formulations [91]. Resuming these findings, IPA/DMIS plays an important role in preserving the formulation. Considering that the crystal growth originates from POX incomplete dissolution, anisotropic systems should then be no longer considered for dermal application. The same is also suggested for liquid systems which showed phase separation during storage.

2.4.5 Strategies in developing topical formulations containing TBF

The HCl salt of terbinafine offers a better stability and no doubt a higher aqueous solubility compared to the base form [73]. The existence of double and triple bonds in TBF rises however the concern of its vulnerable stability against possible chemical reaction such as oxidation. TBF base with a low melting point at around 43 °C and boiling point at 140 °C at 0.3 mbar receives a special attention compared to its salt form [73]. This consideration is also valid for the purification and manufacturing processes which involve heat. The HCl form and the base form are included in marketed formulations under the brand of Lamisil® Creme and Lamisil® DermGel, respectively.

So far, the HCl salt form is the only available raw material in the market. For the sake of mycosis treatment, a good drug delivery and a high drug deposit in the SC would be advantageous to enhance the cure rate. This would also reduce peroral administration, especially for moderate to severe infections. In accordance to mycosis therapy with TBF, a novel topical product should thus be able to:

- deliver TBF readily into SC
- enhance TBF deposit in SC

Various formulations containing TBF intended for topical application are available in the market as cream, gel, solution and spray under the brand name Lamisil® as well as the generic form. These topical dosage forms are recommended for mild infection only or as adjuvant for the oral therapy. The topical application is not a choice at all for nail infection. As alternative, iontophoresis has been introduced to improve TBF delivery into the skin. Sachdeva et al. [92] reported that TBF delivered into SC of hairless rat skin following iontophoresis from a glycerin-based solution was yet not significantly higher than that of passive diffusion. However, a significantly higher TBF amount beneath the skin after the application of anodal iontophoresis was evident over cathodal iontophoresis or passive diffusion [92].

Regarding the lipophilic nature of TBF, the main focus in developing a formulation for topical application may be an effective loading of the vehicle with drug. A hydrophilic vehicle offers a limited advantage due to its poor solubilization ability. A lipophilic vehicle has a high affinity to TBF, but may thus eventually hamper its release. A vehicle offering a high drug loading capacity and ability of enhancing TBF partition rate into SC would be advantageous.

Chapter 3

Materials and Methods

3.1 Materials

- **Terbinafine HCl** ($C_{21}H_{26}ClN$, MW 327.9) or (2*E*)-*N*,6,6-Trimethyl-*N*-(naphtalin-1-ylmethyl)hept-2-en-4-in-1-amine hydrochloride (BAN)) was purchased from Suzhou Leader Chemical Co., Ltd, China and was used as received. It is an odorless powder with a white to off-white appearance. The purity was determined to be 100-101% (potentiometry) according to the monograph in Ph. Eur. 6.0 [78]. The melting point was found to be at 211.9 °C measured with a differential scanning calorimetry (DSC 220C with disk station SSC 5200, Seiko Instrument, JP-Tokyo). In the following sections terbinafine HCl will be abbreviated as **TBF**.

- **Poloxamer 407** (Pluronic® F127, Lutrol® F127) is an ABA type block copolymer composed of a central, hydrophobic block of polypropylene oxide (PPO) flanked by two hydrophilic blocks of polyethylene oxide (PEO). The average molecular weight is 12,200 and the hydrophilic part contributes to about 73% of the molecular weight [93].

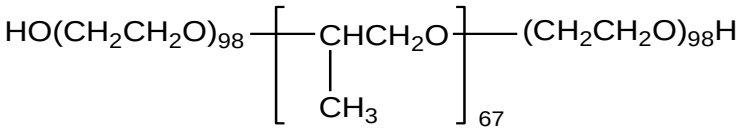

Fig. 3.1 Chemical structure of poloxamer 407, from Ref. [5]

The rich proportion in PEO makes poloxamer 407 readily soluble in water. The poloxamer 407 gel possesses a thermoreversible gelation property and exhibits a sol-gel transition upon heating and cooling. Poloxamer 407 has been used as a carrier for many routes of drug applications (oral, topical, intranasal, rectal, vaginal, ocular and parenteral) [94]. The substance was kindly donated by BASF (Ludwigshafen, Germany) and featured free-flowing prilled granules. In the further section poloxamer 407 will be abbreviated as **POX**.

- **Miglyol® 812N** (**MCT**), a medium chain triglyceride (caprylic/ capric triglyceride (INCI)), was purchased from Sasol GmbH (Witten, Germany). It is a neutral oil, clear, colorless with a neutral odor and taste. The oil is composed of saturated triglycerides of fatty acids C_8 and C_{10} with glycerol from fractionated plant oils

(coconut and palm kernel) [95]. MCT is used for many pharmaceutical purposes as carrier, solvent, dispersing agent, permeation enhancer in oral, topical and parenteral preparations [96].

- **Dimethyl isosorbide** (**DMIS**) was kindly donated by Dolorgiet (St. Agustin-Bonn, Germany). DMIS is a clear liquid with an odor and taste similar to isopropyl alcohol. It is hydrophilic and used as a solvent, drug solubilizer and penetration enhancer for topical preparations [96].

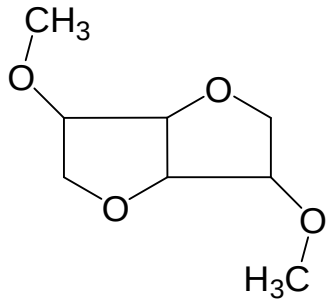

Fig. 3.2 Chemical structure of dimethyl isosorbide, from Ref. [5]

- **Isopropyl alcohol** (**IPA**) was purchased from VWR Int. (Leuven, Belgium). IPA has been used as a preservative and transdermal penetration enhancer.
- **Phosphate buffer pH 5.8** (**PB**) (Eur. Ph. 6.0, 4002100) was prepared from disodium hydrogen phosphate dihydrate and potassium dihydrogen phosphate according to Ph. Eur. 6.0 [78]. The pH value of the solution was verified before use and if necessary, adjusted. Both materials were purchased from Merck KGaA (Darmstadt, Germany).
- **Lamisil® Creme** and **Lamisil® DermGel** were purchased from a local pharmacy. Both are intended for topical therapy of skin fungal infections such as tinea pedis and tinea corporis. **Lamisil® Creme** is a semisolid formulation containing 1% terbinafine HCl, purified water, isopropyl myristate, polysorbate 60, stearyl alcohol, cetyl alcohol, cetyl palmitate, sorbitan stearate, benzyl alcohol and sodium hydroxide, meanwhile **Lamisil® DermGel** contains 1% terbinafine base, purified water, ethanol 96%, isopropyl myristate, polysorbate 20, carbomer, sorbitan laurate, benzyl alcohol, sodium hydroxide and butylhydroxytoluene.
- **Basiscreme DAC** was purchased from Caelo (Hilden, Germany). Basiscreme DAC is composed of glycerol monostearate 60 (4%), cetyl alcohol (6%), medium chain triglycerides (7.5%), white soft paraffin (25.5%), macrogol-20-glycerol monostearate (7%), propylene glycol (10%) and purified water (40%) [97].

- **For the manufacture of keratin film,** blond hairs were obtained from a local hairdresser. Bovine hooves were purchased from an online pet shop (Edingershops, Germany) and healthy nail clippings were donated from volunteers in the university surroundings. Shindai solution was prepared from urea, thiourea (Carl Roth GmbH, Karlsruhe, Germany), 2-mercaptoethanol and Tris base (Sigma, USA) according to a previous method [55]. A Spectra/Por membrane (MWCO: 6-8,000 Da Spectrum Laboratories, Inc. Rancho Dominiguez, Canada) was used as dialysis tubing. Sodium fluorescein (**SF**) was purchased from Fluka (Steinheim, Germany), rhodamine B (**RB**) from Fluka (Sweden), thioglycolic acid (**TA**) from Merck (Hohenbrunn, Germany), fluorescein isothiocyanate-dextran MW 4000 (**FD4**) and papain (from papaya latex) from Sigma-Aldrich (Steinheim, Germany). Chemical structures of the markers are shown in Fig. 3.3.

  Phosphate buffered saline pH 7.4 (**PBS**) was prepared according to Eur. Ph. 6.0. Disodium hydrogen phosphate anhydrous and sodium chloride were obtained from Merck (Darmstadt, Germany) and potassium dihydrogen phosphate was from Carl Roth GmbH (Karlsruhe, Germany). Sodium hydroxide (NaOH) was supplied from BASF (Darmstadt, Germany). Acrylamide (30% solution), N,N,N',N'- tetramethylethylenediamine and ammonium persulfate were obtained from Sigma-Aldrich, sodium dodecyl sulfate from Acros Organics (Geel, Belgium), glycine from ICN Biomedicals, Inc. (Aurora, Ohio, USA) and Serva Blue G (dye based on Coomassie® brilliant blue G-250) from Serva Electrophoresis GmbH (Heidelberg, Germany). Spectra™ multicolor broad range protein ladder #SM 1841 (10 – 260 kDa) from Fermentas GmbH (St. Leon, Rot, Germany) was used as the size marker for electrophoresis.

- Water was used in double distilled quality, except for HPLC analysis. For this purpose water was processed with an EASYpure™ LF from Barnstead (Dubuque, USA) to produce type I reagent-grade water with low organic content and high resistivity up to 18.3 MΩ-cm.

- Miscellaneous materials used for any specific method will be introduced and defined in the corresponding section.

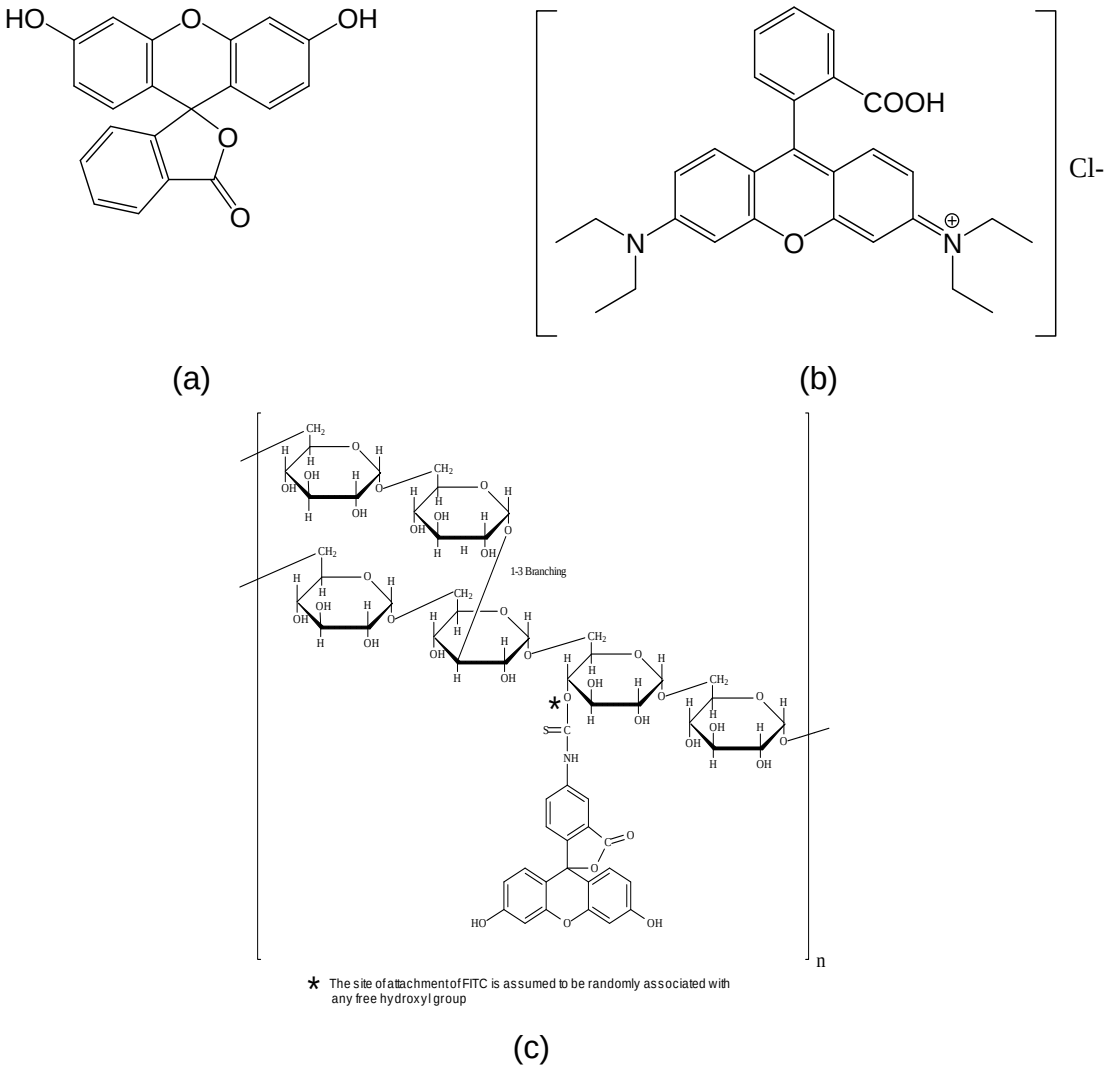

Fig. 3.3 Chemical structure of fluorescein (a), rhodamine B (b) and fluorescein isothiocyanate-dextran MW 4000 (c); source Ref. [98,99]

3.2 Methods

3.2.1 Manufacture of the POX-based formulations [100]

Formulations were given codes according to the drug content and the collective content of POX/MCT and IPA/DMIS in the vehicle alone. The ratios of POX/MCT and IPA/DMIS in all cases were fixed in accordance to Grüning and Müller-Goymann [5] at 4:1 and 1:1, respectively. For example, 1P5025 contained 1% TBF, while the vehicle itself was composed of 50% of POX/MCT, 25% of IPA/DMIS and 25% of water (all w/w). An example is given in Table 3.1. Formulations were produced according to the pseudoternary phase diagram presented in Fig. 4.1. All materials, including TBF for formulations containing drug, were weighed in a special jar designed for Cito Unguator 2000 Konietzko GmbH (Bamberg, Germany) and were mixed at 1450 rpm for 1.5 min. The composition of the vehicle constituents was varied depending on the

characterization requirement. TBF, POX/MCT and IPA/DMIS ranged from 0 – 4%, 25 – 75% and 10 – 70% (all w/w), respectively.

Table 3.1 Composition of 1P5025 as example

Components	Amount [g/ 100 g]
Poloxamer 407	39.6
Isopropyl alcohol	12.38
Dimethyl isosorbide	12.38
Medium chain triglycerides	9.9
Terbinafine HCl (TBF)	1.0
Water	24.75

3.2.2 Physicochemical characterization of POX-based formulations [100]

Physicochemical characterization was carried out after 24 h to allow for sufficient equilibration of the microstructure. The characterization was performed visually in terms of appearance and ringing effect, as well as microscopically in terms of isotropy and TBF concentration at saturation. The ringing effect was examined by knocking the jar to a hard surface. A “ringing” gel responded to agitation with a particular back-resonance. Isotropy and TBF concentration at saturation were examined under a polarizing microscope Leica LMDM equipped with camera Olympus DP12 (Hamburg, Germany). The lowest TBF concentration representing detectable crystals was defined as the saturation/ solubility concentration.

3.2.2.1 Rheometrical measurement [100]

Rheometrical measurements were performed in an oscillation mode using a controlled stress rheometer CVO 50 from Bohlin (Bamberg, Germany) with a conical disk plate of an angle of 1° (Ø 20 mm). Gelation temperatures and complex viscosities were measured within the linear viscoelastic regions of the formulations, which were previously determined with an amplitude sweep at a fixed frequency of 0.5 Hz according to Ref. [5]. This low frequency was chosen to prohibit any major change in the microstructure during the subsequent measurements, especially during gelation point detection [101]. Complex viscosities (η*) were measured at 32 °C to make sure that the formulation was in its viscoelastic state, i.e. storage modulus G’>loss modulus G”. Gelation temperatures were determined within the temperature range of 5 to 30 °C using a temperature gradient program with a rate of 2 °C/min. Samples of approximately 1 g were applied and renewed prior to the proximate measurement.

The cone/ plate rheometer including the sample were placed under a protecting cover during the measurements to prevent any excessive evaporation of volatile ingredients. The gelation temperature was considered to be the temperature, where G' and G" crossed over (G'=G") [101] or when the phase angle δ = 45° or tan δ = G"/G' =1 [102].

3.2.2.2 Small angle X-ray diffraction (SAXD)

Small angle X-ray measurements were carried out using a compact Kratky camera (Hecus Braun X-ray systems, Graz, Austria) connected to a Roentgen generator Iso-Debyeflex 3003 60 kV (Seifert-FPM, Freiberg, Germany). Samples were measured at room temperature for 600 s and detected with a position sensitive detector PSD-50M (M. Braun, Garching, Germany). Distance to sample was 27.7 cm meanwhile the length of the channel was 54 µm. Sample was placed in a paste carrier from Hecus Braun X-ray systems (Graz, Austria). The measured curves were desmeared and smoothed to obtain the final diffractograms.

Table 3.2 Bragg reflection ratios and Miller indices for cubic lattice structures

Cubic lattice	Bragg reflection ratio	Miller index {hkl}
lm3m (primitive cubic, bcc)	$\sqrt{2}, \sqrt{4}, \sqrt{6}, \sqrt{8}, \sqrt{10}$	{110}, {111}, {200}, {211}, {220}, {221} and {310}
Pn3m (double diamond)	$\sqrt{2}, \sqrt{3}, \sqrt{4}, \sqrt{6}, \sqrt{8}, \sqrt{9}, \sqrt{10}$	{110}, {200}, {211}, {220} and {310}
la3d (gyroid cubic)	$\sqrt{6}, \sqrt{8}, \sqrt{14}, \sqrt{16}, \sqrt{20}$	{211}, {220}, {321}, {400} and {420}

Since the examined formulation P2525, P4020 and P5015 displayed ringing effects and were not birefringent, a cubic lattice structure was expected. The influence of TBF (0-3%) and heating (20 and 40 °C) on P2525 structure were investigated. The scattering pattern of a system possessing a cubic structure will follow any of the Bragg reflection ratios. Some possible Bragg ratios are listed in Table 3.2. These reflections can also be indexed into diffraction planes according to Miller indices.

3.2.3 Stability of terbinafine HCl

3.2.3.1 TBF stability in aqueous media

TBF was dissolved in water, PB and phosphate buffer saline pH 7.4 (**PBS**), respectively. Each sample containing 10 mL solution was stored in a sealed, air tight

glass and was protected from light during storage. Sampling at every determined point of time was performed using a syringe to reduce the contact with the environment.

3.2.3.2 Influence of pH on TBF stability in aqueous media

UV spectra of 0.1% TBF solutions in PB and PBS were recorded at 0, 2, 5, 24, 48 and 144 h by means of Spectrophotometer UV Specord® 200 from Analytik Jena AG (Jena, Germany) equipped with the software WinASPECT® PLUS. Measurements were carried out within the wavelength range of 200-400 nm at ambient temperature. This measurement was aimed to investigate the influence of two different pH values on TBF stability.

3.2.3.3 Influence of temperature on TBF stability in aqueous media

TBF solutions of 50 µg/mL in water, PB and PBS were stored at different temperatures: 20 °C and 32 °C for 72 h. Changes in TBF concentration during storage were monitored by means of HPLC measurements.

3.2.4 TBF stability in formulations during storage at 20 °C

3.2.4.1 Macroscopical examination

Samples were manufactured according to the pseudoternary phase diagram in Fig. 3.4 and stored in a climatized room at 20 °C for up to six months. Samples were placed in their original jar (Unguator Kruke) to simulate the real storage condition. Examinations were carried out after 1, 3 and 6 months. Examinations included physical appearance, color change and phase alteration.

3.2.4.2 Changes in TBF concentration

Formulations from Fig. 3.4 were manufactured, divided and placed in several airtight glass vials. They were sealed and stored in a climatized room at 20 °C for up to three months. Samples were taken at 0, 1 and 3 months. TBF was extracted from the formulation and its concentration was determined by means of HPLC.

3.2.4.3 TBF extraction from the formulation

An amount of ~50 mg formulation was weighed in a volumetric flask of 10 mL volume and was given up to 10 mL methanol. Following shaking, the formulation was completely soluble in methanol. 40 µL of this mixture was injected into the column and

analyzed using the HPLC system as in section 3.2.6.6. The extraction was done in triplicate for each formulation. Calibration curves were performed in methanol within the range of 0.1-50 µg/mL (r^2>0.9999) with LOD and LOQ at 0.014 and 1.654 µg/mL, respectively. The recovery of this extraction process was found to be more than 99 %. The obtained TBF concentrations were recalculated based on the recovery result from each formulation.

3.2.5 Instability of TBF in the formulation

3.2.5.1 Finding the instability trigger

After one month of storage in the climatized room (section 3.2.4.1), some formulations containing TBF turned yellow. This color change initially occurred in formulations with IPA/DMIS contents of more than 40%. Upon storage the color change gradually continued with other formulations which contained less IPA/DMIS. In order to find the trigger of this phenomenon, several binary and multiple mixtures were prepared according to the composition of 2P2570. They were stored for one month in airtight glass vials in similar condition as for the stability study.

3.2.5.2 Thin layer chromatography (TLC)

TLC is a fast and reliable method to detect and separate degradation products from the parent compound. As the stationary phase, an HPTLC plate Kieselgel 60F (20 cm x 10 cm) with UV fluorescence at 254 nm from Merck (Darmstadt, Germany) was used. The mobile phase was composed of chloroform, methanol and 25% aqueous ammonia solution (12: 0.1: 0.1) [79]. The chamber was previously saturated for two hours with the mobile phase before running the sample.

Several samples which had turned yellow after one month of storage were examined, i.e., 1P2570, 2P2570, 1P2560, 1P3050, 1P3060 and 1P4050. One-month-old formulations without TBF were analyzed as well, i.e., P2530, P2550, P2560 and P2570. A freshly prepared 1% TBF solution in methanol was used as reference. Prior to TLC, all formulations were diluted 1:1 with methanol. 10µL of the solution (including the reference) was then applied on the plate using an Eppendorf pipette with distances between point-shaped samples of 1.5 cm. Samples were dried (~30 min under a fume hood) and developed in a TLC chamber at ambient temperature (20 ± 2 °C). Afterwards, the plate was dried under a fume hood and finally examined under a UV lamp at λ 254 nm to observe the spots.

The retardation factor (R_F) from each visible spot can be calculated as follows [103]:

$$R_F = \frac{\text{distance travelled by the center of the spot}}{\text{distance simultaneously travelled by the mobile phase}} \quad \text{(Eq. 3.1)}$$

3.2.6 Permeation of TBF across human stratum corneum (SC) and bovine hooves

3.2.6.1 Isolation of human SC [100]

Isolated human SC was used for the permeation studies. Skin was donated from plastic surgery of the abdominal region of 38- and 55-year-old women with consent of the patients and ethical approval according to the Declaration of Helsinki of the World Medical Association. After removing the fat tissue, the skin was immediately frozen with liquid nitrogen and stored at – 20 °C. The isolation of the SC was performed using the trypsination method described by Kligman and Christophers [104]. Briefly, the vital layers of the skin are removed manually using a scalpel. After 48h of incubation with 0.5 mg/mL trypsin solution (Trypsin 2500 USP Unit/mg from Carl Roth GmbH, Karlsruhe, Germany) at 37 °C, SC can be separated from the rest of the skin layers. The SC is further introduced to 0.4 mg/mL trypsin inhibitor solution (Type II-O: chicken egg white from Sigma-Aldrich Chemie, Steinheim, Germany) to stop the enzymatic process. Finally it is rinsed twice with excessive water. This ready-to-use SC was put on a Teflon sieve and kept in a desiccator prior to use to protect it from humidity. The isolated SC was used within two months to avoid any skin lipid degradation. Stability has been reported in the literature for up to four months [105,106].

3.2.6.2 Bovine hooves preparation

Only the sole part of the bovine hooves was used for this study. Soles were first cut in squares (2 cm x 2 cm) and submerged overnight in water before being sliced with a rotational microtome MICROM HM 355S (Walldorf, Germany) to a thickness of 100 µm. For the permeation study, these membranes were then punched out (15 mm diameter).

3.2.6.3 Examined formulations

1P2525 vs. other semisolid vehicles containing 1% TBF

A concentration of 1% TBF was chosen to be incorporated in P2525, the original thermogelling formulation from a previous publication [5] since the marketed product

Lamisil® Creme contains a similar drug concentration. Other formulations such as 1P3030, 1P4030 and Basiscreme DAC containing 1% TBF were prepared as well.

Considering that onychomycosis may occur in nail, it is valuable to measure the permeation rate of TBF across bovine hoof, an accepted human nail model. Furthermore, semisolid formulations obtained from variation of the composition of the thermogelling vehicle enable a good applicability and a sufficient adhesive property for the treatment of nail infection. Lamisil® DermGel, a marketed product, was chosen as a standard of comparison for the permeation across hooves regarding the vehicle's rather hydrophilic properties.

Variation of the thermogelling formulations

Several formulations from the semisolid area of the pseudoternary phase diagram were chosen for permeation experiments across human SC and hooves. For only examining the influence of a single "component" on the permeation, two other "components" were kept constant at 1:1. An overview to the examined formulations is shown in Fig. 3.4. As example, in order to examine the influence of POX/MCT on TBF permeation rate, the ratio of IPA/DMIS to water was kept constant at 1:1. This is depicted as the line with empty triangles from 1P2836 up to 1P5025. Each line comprises four formulations with 1P3333 as the intersection point. A detailed composition of each formulation can be further seen in Table 3.3.

Thermogelling formulations containing more than 1% TBF

The influence of TBF content on the permeation rate across SC was assessed by including 2P2525, 2P3030 and 4P4030 in this study. All prepared formulations were given 24 h equilibration time after manufacture. An examination by means of polarizing microscope showed that TBF was soluble in all tested formulations for the permeation study. Considering the permeation from formulations with more than 1% TBF, an enhancement factor from each formulation could be calculated as follows:

$$\text{Enhancement factor} = \frac{\text{flux from the formulation containing more than 1\% drug}}{\text{flux from the formulation containing 1\% drug}} \qquad \text{(Eq. 3.2)}$$

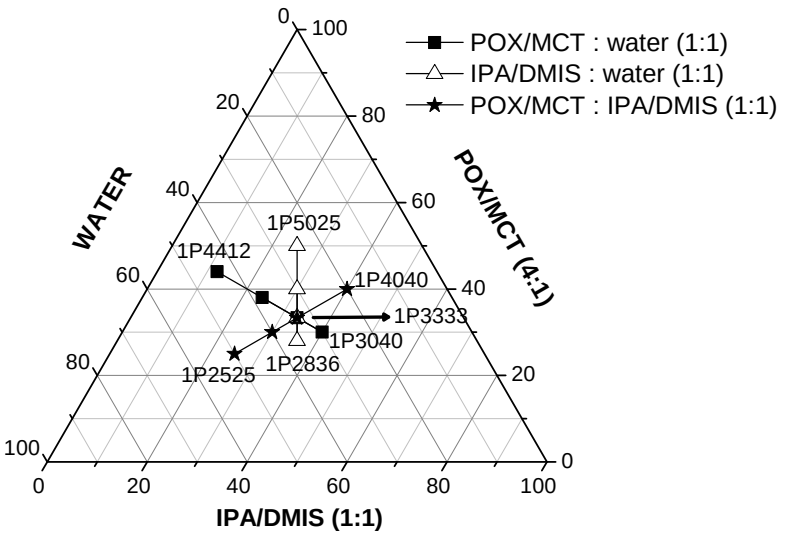

Fig. 3.4 Position of all examined formulations in the pseudoternary phase diagram for the permeation study

Table 3.3 Composition of the examined formulations for the permeation study

Group of formulations	% POX/MCT	% IPA/DMIS	% water	% TBF
POX/MCT: water (1:1)				
1P3040	29.70	39.60	29.70	1
1P3333[a]	32.97	32.97	32.97	1
1P3824	37.62	23.76	37.62	1
1P4412	43.56	11.88	43.56	1
IPA/DMIS : water (1:1)				
1P2836	27.72	35.64	35.64	1
1P4030	39.60	29.70	29.70	1
1P5025	49.50	24.75	24.75	1
POX/MCT: IPA/DMIS (1:1)				
1P2525	24.75	24.75	49.50	1
1P3030	29.70	29.70	39.60	1
1P4040	39.60	39.60	19.80	1

[a] 1P3333 was the intersection point of the three examined lines

3.2.6.4 TBF solubility in the receiver solution

According to the literature, PB was chosen as a receiver solution in permeation experiments. TBF solubility in PB and water (as a comparison) was determined as follows. An excess of TBF was given into 5 mL of each examined solvent. The mixtures were placed and sealed in air-tight glass vials and then stirred at 300 rpm, 32 °C for 24 h to mimic the *in vitro* permeation condition. The insoluble drug was removed by filtration using a cellulose acetate filter with pore size of 0.2 µm from Sartorius AG

(Göttingen, Germany). The filtrate was analyzed with HPLC. The samples were diluted 100-fold with the corresponding solvent prior to analysis. The standard solutions for the HPLC analysis were prepared in the corresponding solvents, i.e., water or PB, respectively. TBF solubility in water and PB at 32 °C was 0.698% and 1.360%, respectively. The solubility in PB was sufficient to maintain the sink condition during the permeation experiment.

3.2.6.5 Permeation study [100]

Both rims of the diffusion cell compartments were given a thin layer of silicone paste (Baysilone-paste medium viscous, Bayer AG, Bad Berleburg-Raumland, Germany) to aid adhesion. After a fully hydration of SC in water, it was mounted on a TMTP (pore size 5 µm) polycarbonate filter Isopore^{TM} Millipore (Ireland) to support its mechanical stability and clamped between donor and receiver compartments. This filter did not represent any diffusion barrier. Since the intersubject skin variability of permeation studies was found to be larger than the intrasubject variability [107], the results of the permeation studies were always compared to those from the same donor. Bovine hooves were equilibrated in the buffer for 1 h before being mounted between both compartments.

Prior to permeation, the intactness of the membrane was checked by its trans epithelial electric resistance/ TEER using an EVOM instrument (World Precision Instruments, US-Sarasota) with a measurement range up to 20 kΩ. This method was developed by Fokuhl and Müller-Goymann [108]. An intact membrane shows a high resistance represented by a TEER value of >20 kΩ (the maximum measurable value of the instrument). A damaged membrane shows a TEER value less than 20 kΩ.

Modified Franz diffusion cells with membrane areas between 0.418 and 0.534 cm^2 were used for the permeation studies. The volumes of the receiver compartments varied between 5.18 and 6.37 mL and were filled with phosphate buffer pH 5.8 (**PB**). The pH value of 5.8 was chosen in accordance to previous TBF stability reports from Lebo et al., Özcan et al. and Sachdeva et al. [92,109,110]. This buffer was also sufficient to maintain the sink condition for TBF partitioning, i.e., TBF concentration in the receiver compartment during permeation study did not exceed 10% of the initial concentration in the donor compartment. TBF solubility in PB was determined in the section 3.2.6.4 to confirm this. Approximately 2 g of the formulation was filled into the donor compartment.

The diffusion cells were thermostated at 32 °C and the receiver compartments were stirred at 300 rpm. Receiver solutions from SC permeation were probed (250 µL) for over 40 h and replaced by the same amount of fresh buffer. The samples were taken in the beginning after 4 h and 10 h followed by an interval of 3-4 h (night break: 11 h) up to 48 h. This sampling time was extended for some formulations up to 72 h. Receiver solutions from hooves permeation were probed at the 2^{nd}, 4^{th}, 6^{th}, 9^{th} and 12^{th} h.

The samples were kept in a refrigerator (6-8 °C) and analyzed within 48 h without any additional dilution. The flux value of TBF was obtained from the slope of a plot of the permeated amount [g/cm^2] vs. time [s]. The slope was taken from the steady state part of the plot in accordance to Fick's 1^{st} law [111].

3.2.6.6 Analytical measurement by means of high performance liquid chromatography (HPLC) [100]

Samples from permeation experiments were analyzed with an HPLC which consisted of a pump 515, autosampler 717 plus and a UV tunable absorbance detector 486 from Waters (Milford, USA). Mobile phase was modified from Cardoso and Schapoval [112] being composed of methanol : water (95:5) with an addition of 10 mM triethylamine (694 µL for 1 L mixture). Flow rate was set at 1.5 mL/min with detection at wavelength of 254 nm. Samples were eluted through a column Zorbax SB-C18 (Agilent, USA) with particle size of 5 µm and dimension 4.6 x 250 mm for 5 min with retention time at 4.1 min. Peaks were integrated and evaluated using software Clarity V. 2.6.3.313. Sample injection volume was 40 µL. Calibration was performed in PB from 0.1-50 µg/mL with r^2 of more than 0.999. Limit of detection (LOD) and limit of quantification (LOQ) were determined according to the ICH Guideline [113] and the values were 0.122 and 3.446 µg/mL, respectively.

3.2.6.7 Quantification of TBF retained in SC and hooves [100]

SC and hooves were isolated directly after terminating the permeation at 48^{th} and 12^{th} hours, respectively. Excess formulation was cleaned by wiping off the surfaces with cotton swabs followed by tissue paper. This was done to assure that there would be no rest of the formulation left on the surface. The residual humidity was absorbed once more with tissue paper and the membranes were finally placed in reaction vessels of 1.5 mL volume (Roth, Karlsruhe-Germany). These vessels were stored without lids in a refrigerator (6-8 °C) for 48 h. The dried membranes were afterwards

transferred into fresh vessels, extracted with 1 mL methanol and agitated with an orbital shaker (IKA Vibrax-VXR) at 150 rpm for 24 h. The amount of TBF extracted was determined by injecting the extract into HPLC with the same parameter as in earlier section. Calibration curves were performed in methanol within the range of 0.1-50 µg/mL (r^2>0.9999) with LOD and LOQ at 0.014 and 1.654 µg/mL, respectively.

3.2.6.8 Recovery of the extraction process [100]

SC and hooves with the size of 1 cm x 1 cm (n = 6) were given about 10 µL drop of a defined concentration of TBF solution in methanol and then weighed. The solution concentrations ($c_{standard}$) for SC were 4.88 and 0.488 mg/mL. Blank was dropped with methanol only. Drying and extraction process were carried out in the same manner as in section 3.2.6.7. Neither cleaning nor wiping process was necessary to clean the surface for the extraction process since TBF is freely soluble in methanol. The recovery of the extraction process was calculated as follows:

$$\%\,\text{recovery} = \frac{\text{detected concentration}\,[\mu g/mL]}{\text{actual concentration}\,[\mu g/mL]} \cdot 100\% \qquad \text{(Eq. 3.3)}$$

The detected concentration was obtained by HPLC measurement, meanwhile the actual concentration was calculated as follows:

$$\text{actual conc.}\,[\mu g/mL] = \frac{\text{weight of the solution}\,[g] \cdot c_{standard}\,[g/mL] \cdot 10^6}{\text{density of the solution}\,[g/mL] \cdot 1[mL]} \qquad \text{(Eq. 3.4)}$$

3.2.7 SC measurement by means of differential scanning calorimetry (DSC) [100]

Any changes in the SC due to its interaction with the formulation component can be well recorded by means of DSC, which enables the detection of heat transitions and even measures the amount of enthalpy involved quantitatively. SC was first hydrated to gain water content of 20% in a desiccator filled with saturated sodium chloride solution in water for at least 48 h at ambient temperature. A size of 1.5 cm x 1.5 cm was eligible for each measurement. The formulation to be tested was equilibrated at 37 °C before the SC was inserted for incubation at 37 °C for 30 min. After incubation, an excess of the formulation was wiped off by means of tissue paper and weighed in a hermetically closed aluminum crucible of 40 µL volume (ME-27331, Mettler Toledo).

Sample was directly measured from 20 to 120 °C with a heat rate of 5 K/min using DSC 1 Star^e System (Mettler Toledo, Schwerzenbach, Switzerland). An empty aluminum crucible was used as reference. Care was taken to assure a uniform contact time between SC and formulation and to perform the DSC measurement immediately after incubation. Up to four endothermic thermal transitions could be recorded, denoted as T1 – T4, but only the middle transitions (T2 and T3) were reliable for further interpretation. The transition temperatures were determined and evaluated using software STARe DB V9.20.

3.2.8 Development of human nail plate model made of human hair keratin [114]

Keratin film made of human hair keratin was produced and its suitability was tested for the permeation study purpose. The permeability of the keratin film was investigated using three markers with different properties as well as several ungual penetration enhancers with different mechanism of action. In addition, water absorption of the keratin film as well as its SDS-PAGE profile were compared to bovine hoof and human nail.

3.2.8.1 Keratin film (KF) manufacture

Keratin from hair was extracted under reducing conditions with the so-called Shindai method [12,55]. The hair was pulverized using a ball mill MM301 Retsch (Haan, Germany) at 29 Hz for 10 min. An amount of 25 g of hair powder was mixed with 500 mL Shindai solution containing 25 mM Tris pH 8.5, 2.6 M thiourea, 5 M urea and 5% (v/v) 2-mercaptoethanol and was extracted at 50 °C for 72 h. The mixture was filtered with medical gauze and further with filter paper with a 2.5 µm pore size to remove the insoluble hair. The extract was centrifuged at 4,500 x *g* for 15 min; the supernatant could be stored at -20 °C and thawed, if required. Dialysis against demineralized water was conducted to remove the rest of the Shindai components using Spectrapore® tubing, MWCO 6,000 – 8,000 Da, for 48 h at ambient temperature. The dialysate was further centrifuged at 10,000 x *g* for 30 min to remove coarse aggregates and immediately used for KF manufacture. The dialysate's protein content was determined using the Bradford colorimetric method [115] using bovine serum albumin as standard. Prior to film manufacturing, 1% (w/w) glycerol was added to the dialysate as film plasticizer. A volume of 2 mL of this mixture was optimum to produce about 100 µm thick KFs. This volume was added stepwise (2 x 1 mL within 4 h) into molding rings,

which were made of polytetrafluoroethylene (PTFE/Teflon) with 2 cm inner diameter in our studio, and dried at 40 °C for 24 h. A siliconized polyethylene terepthalate (PET) foil from LTS Lohmann (Andernach, Germany) was used as base. The produced soft films were punched out (diameter 1.5 cm) before curing. Curing at 110 °C for 3 h was essential to oxidize the disulfide bridges between keratin molecules, producing stable, water-insoluble films. The thicknesses of the prepared KF and hoof membrane were measured with a micrometer screw gauge after a complete hydration in PBS for 1 h.

3.2.8.2 Water absorption profile of keratinous material under study

All the studied keratinous materials, i.e., hoof membranes, KFs and human nail clippings were submerged in double distilled water and repeatedly weighed until a constant weight was obtained. Prior to weighing, the water on the surface was wiped off with tissue paper. The amount of water absorbed was compared to the dry weight.

3.2.8.3 SDS-polyacrylamide gel electrophoresis (SDS-PAGE)

SDS-PAGE was performed according to Laemmli [116] to separate the protein components of the keratinous materials under study according to their molecular weights. The aqueous dialysate and the hair extract in the Shindai solution were previously diluted 5-fold with water. The other keratinous samples were previously extracted with the Shindai solution. Nail clippings (2.5% (w/w)) were extracted and agitated overnight, whereas KF and hoof (5% and 2.5% (w/w), respectively) were extracted for 72 h at 50 °C. All the samples were finally diluted 2-fold with Laemmli buffer (Sigma, Deisenhofen, Germany) and boiled for 5 min before running SDS-PAGE. The sample volume for the separation was 5 µl, except for hoof extract and marker, which was 7.5 and 10 µl, respectively. A vertical slab gel electrophoretic system (EC 120, 80 x 100 mm, EC Apparatus Corp., Holbrook, US) with a 4% stacking gel and 12% separation gel was used. The system was run at 180 V, 80 mA and 25 W. After running, the gel was stained with 0.1% (w/v) coomassie brilliant blue in a mixture of methanol: acetic acid: water (4:1:10) and further destained with this acidic methanol mixture for 30 min.

3.2.8.4 Permeability of the keratin film: finding the thickness analogue

The permeability of KF was examined by using several markers and ungual penetration enhancers. Because of similarities between bovine hoof and human nail,

bovine hoof was chosen for comparison. Moreover, bovine hoof is available in the market and can be obtained for screening purposes in great quantities whereas the availability of human nail is limited and costly. Three markers were chosen to represent drugs with different physicochemical properties. Sodium fluorescein (MW 376, log *P* -1.52), rhodamine B (MW 443, log *P* 2.38) [117] and fluorescein isothiocyanate-dextran (MW 4400, log *P* -2.0) [118] were chosen as water soluble, lipid soluble and large molecule model drugs, respectively. The slight differences in size between sodium fluorescein and rhodamine B were not taken as considerable.

The thickness analogue of KF, in terms of permeability and marker retaining ability, was compared with 100 µm thick bovine hoof. KFs with thicknesses of 110, 120 and 130 µm were examined. Permeation experiments were carried out using modified Franz diffusion cells [119] at 32 °C. The cell opening areas were between 0.418 and 0.534 cm^2 and the volumes of the receiver compartments varied between 5.18 and 6.37 mL. Bovine hoof membranes and KF were equilibrated for 1 h with PBS and were then mounted between donor and receiver compartments. The receiver compartments were filled with PBS, whereas the donor compartments were filled with marker solutions in PBS with the concentration of **500 µg/mL** for SF, **250 µg/mL** for RB and **1000 µg/mL** for FD4 (all w/v). Samples of 100 µl were taken from the receiver for 40 h and replaced by the same amount of fresh buffer. The first sample was taken at 10 h; afterwards, 3- to 4-h intervals were employed over the remaining time. The samples were placed in a 96-well plate from Corning (Roskilde, Denmark) and the fluorescence intensities were directly measured after terminating the permeation using a fluorescence plate reader, Tecan Genios (Switzerland), with λ excitation at 485 nm, λ emission at 535 nm (filters) for SF and FD4, and λ excitation at 535 nm, λ emission at 590 nm for RB. Calibrations for the markers were performed in PBS within the range of 0.1-5 µg/mL for SF and RB, and 1-10 µg/mL for FD4 with r^2 more than 0.999.

3.2.8.5 The application of ungual penetration enhancer (PE)

Three acknowledged nail penetration enhancers with different mechanism of action were chosen, i.e., urea, thioglycolic acid and papain from papaya latex to provide more information about the usefulness of keratin film made of human hair as a human nail plate substitute. Urea works by increasing nail hydration [120], thioglycolic acid by cleaving the disulfide bonds between keratin molecules [72,121], and papain, an endopeptidase enzyme that contains a highly reactive sulfhydryl group, by hydrolyzing

peptide bonds, thus promoting the formation of pores between nail corneocytes [122,123].

PEs were not mixed into the marker solutions to avoid any interaction between the PE and the marker. After assembling the diffusion cells, the receivers and the donors were filled with PBS and PE solution, respectively. All PEs were dissolved in water, except for papain which was dissolved in PBS (pH 7.4 is the optimum papain pH), with the concentration of 40% for urea, 5% for TA and 2% for papain (all w/w). The pH values of the aqueous PE solutions were 9.23, 1.63 and 2.93 for urea, TA and TA-urea combination, respectively. The treatment lengths were 3 days for urea and 15 h for TA and papain. Combinations (15 h) and serial treatments (3 days urea + 15 h TA) were examined as well. The treated KF or hoof was kept at ambient temperature during treatment, except for papain, which was equilibrated in a water bath at 32 °C. Afterwards, both compartments were rinsed twice with double distilled water (donor) or PBS (receiver) after the treatment. After the treatment with papain, both compartments were rinsed twice with PBS. The receivers were ultimately filled with fresh PBS and the donor with the marker solution. Samples of 100 µl were taken from the receiver for 7-40 h (depending on the treatment) and replaced by the same volume of fresh buffer. Sampling time was adjusted for every PE. The use of TA, its mixture and serial application allowed for a sampling time of only up to 7 h before the KF was damaged. Therefore the sampling was performed hourly for all markers in the presence of TA. This was also the case for papain and urea (7h), except for FD4 the sampling interval was employed as in section 3.2.8.4 (40h). The fluorescence intensities of the samples were measured using a fluorescence plate reader with the same parameters as in section 3.2.8.4.

3.2.8.6 Marker extraction from membranes

Hooves and KFs (without PEs) were isolated directly after terminating the permeation. The membranes were rinsed with double distilled water twice to remove the rest of the donor solution. The residual humidity was absorbed with tissue paper and the membranes were finally placed in reaction vessels of 1.5 mL volume (Roth, Karlsruhe, Germany). These vessels were stored without lids in a desiccator for 48 h. The dried membranes were extracted using 1 mL aqueous solution of 2% (w/v) NaOH. These membranes were agitated overnight (3 days for RB) with an orbital shaker IKA Vibrax-VXR (Staufen, Germany) at 150 rpm. The fluorescence intensities were measured

afterwards, as in section 3.2.8.4. Calibration curves were performed in 2% NaOH aqueous solution within the same concentration ranges as in the permeation study with r^2 values greater than 0.999.

3.2.8.7 Determination of the extraction recovery in hoof and KF

Hoof of 100 µm thickness and KF of 120 µm thickness (each n = 6) were given about 10 µl drop of a defined concentration of marker solution ($c_{standard}$) in PBS and then weighed. The marker concentration was similar as in section 3.2.8.4. Blanks for both membranes were dropped with PBS only. Afterwards, drying and extraction process were carried out as in section 3.2.8.6. The recovery of the extraction process was calculated using Eq. 3.2. The detected concentration was obtained through the fluorescence measurement; the actual concentration was calculated using Eq. 3.3. The amount of the accumulated marker in the membrane from section 3.2.8.6 was adjusted according to the recovery result of the individual marker.

3.2.9 Microbiological assay

The thermogelling formulation was tested in terms of its efficacy against dermatophyte *Trichophyton rubrum*, the main cause of human tinea. TBF needs to diffuse from the formulation across hooves and keratin film (both as permeation barriers) to inhibit the growth of *T. rubrum*. The efficacy of the formulation is a function of the zone of inhibition width. An effective formulation will show a wide zone of inhibition and vice versa. Since hooves and keratin film were used as human nail plate models, this assay simulated an infected nail bed, one clinical manifestation of onychomycosis.

3.2.9.1 Fungi strain and medium

T. rubrum strain DSM 19959 was obtained from DSMZ (Deutsche Sammlung von Mikroorganismen und Zellkulturen GmbH Braunschweig, Germany) as an active culture. The culture was delivered and rejuvenated on an agar slant with a malt extract-charcoal medium at 30 °C. The medium was composed of 3% malt extract (Fluka Analytical, Steinheim-Germany), 0.3% medical charcoal (Caelo, Hilden-Germany), 1.65% agar (agar-agar, Danish) from Carl Roth GmbH (Karlsruhe, Germany) and distilled water up to 1000 mL. Prior to use, the medium was autoclaved at 121 °C for 10 min. Rejuvenation of the fungal culture was done on the agar slant for 9 days. For the assay, the medium was placed on disposable Petri dishes (92 x 16)

with cams (Sarstedt AG, Nümbrecht-Germany). The culture tube for the agar slant and the Petri dish for the assay were filled with 12 mL and 20 mL medium, respectively.

3.2.9.2 Efficacy test of the formulation

Preparation of the membranes

Hooves and keratin films were prepared as for the permeation study. The thickness of the membranes for this assay was uniformly 100 µm. These membranes were autoclaved in a chemical flask filled with PB at 121 °C for 10 min. The sterile membranes were used within 24 h to assure a uniform hydration.

Membrane treatment with the formulation

Prior to use, all the equipment needed to be sterilized either in an autoclave (121 °C, 10 min) or with a dry heat method in an oven at 170 °C for 1 h. First of all, membrane surfaces were wiped with tissue paper to remove the residual humidity. The rim of the donor part of the modified Franz diffusion cell was given a sufficient amount of silicone paste to assure close contact between the donor compartment and the membrane. This donor part was then filled with the sample. The underlying side of the membrane was backed with filter paper to avoid a direct contact with the interior of the incubation chamber. This assembly was then transported into a sterile box serving as an incubation chamber and incubated at 32 °C up to the determined time points. The procedure of this assay is illustrated in Fig. 3.5 (1). For a preliminary orientation, the membrane was treated with 1P3030 for 1, 5, 15 and 24 h (n = 3 for each hoof or KF). 1P2525 and 1P4412 were also involved for 24 h incubation on both membranes (n = 3).

Transfer of the membrane onto the inoculated plate

Agar plates were inoculated with a 2-weeks-old *T. rubrum* culture using a sterile cotton swab (Carl Roth, Karlsruhe-Germany). A sterile cotton swab was dipped onto the slant agar culture and afterwards the Petri dish containing medium was streaked evenly over the entire surface in three directions. The plate was allowed to dry for 15 min before being used in the assay.

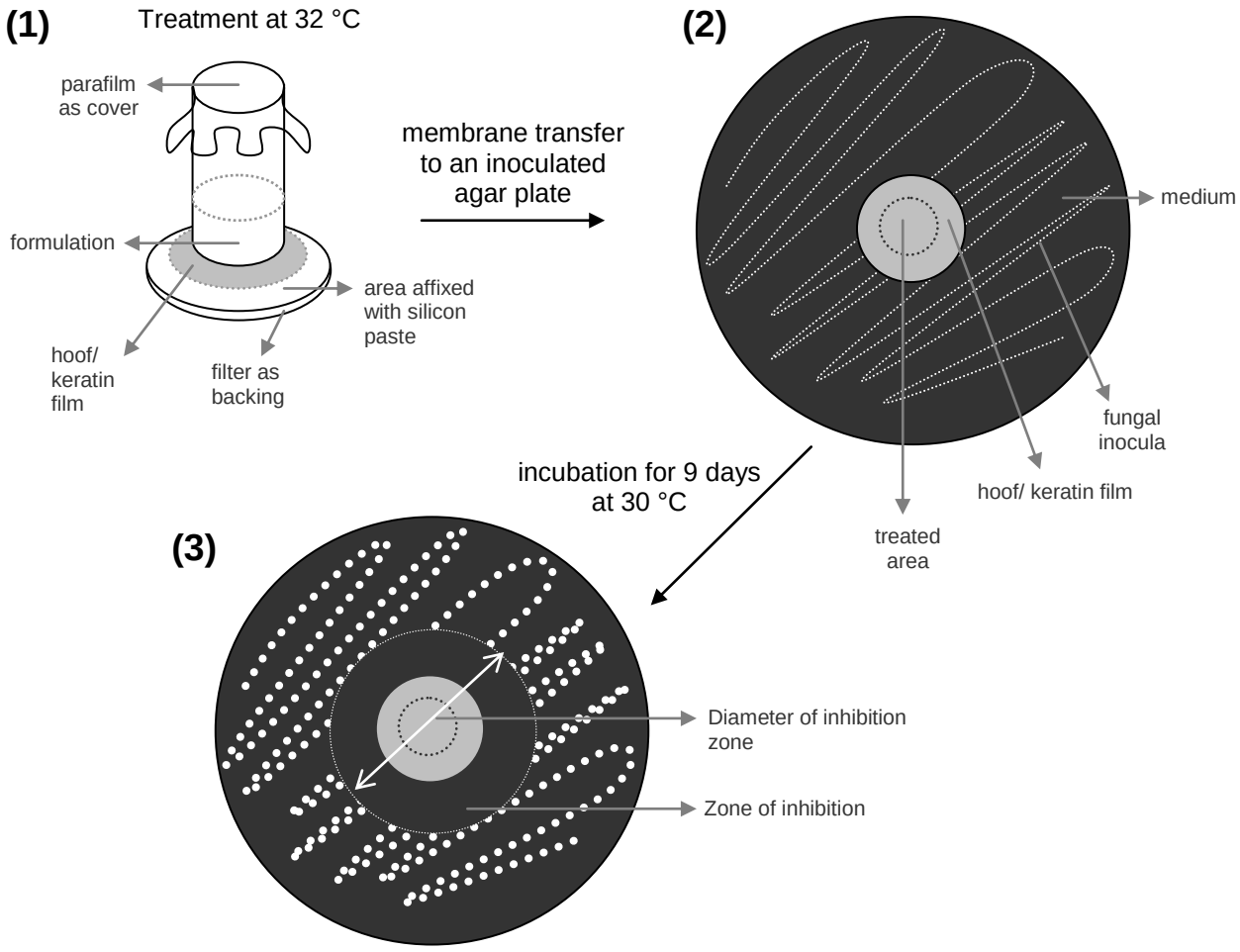

Fig. 3.5 Microbiological assay procedure for testing the efficacy of the formulation

The previously treated membrane was isolated from the donor of the diffusion cell and the remainings from the formulation were wiped off with sterile cotton swabs. The cleaning process is a crucial step to avoid the spreading of the formulation residues over the membrane during the subsequent incubation. A spread formulation would cause a wider zone of inhibition due to a higher TBF amount. An untreated and sterile membrane was used as the positive control for this assay.

The membrane was transferred in such a way that the upper side which was previously in contact with the formulation stayed on top (see Fig. 3.5 (2)). In other words, TBF needed to permeate across the membrane to inhibit the growth of *T. rubrum*. The permeation rate was expected to be different from each formulation depending on its composition. The Petri dishes containing these assemblies were subsequently incubated at 30 °C for 9 days. After 9 days, the diameter of inhibition was measured which is defined as the diameter where no fungal growth could be observed.

3.2.10 Statistical analysis

3.2.10.1 Statistical analysis for the permeation study

All data were presented as means ± standard deviations. Statistical analysis was performed with the software program PASW Statistics 18. The Kolmogorov-Smirnov or the Shapiro-Wilk test was applied to assess the normality of the data. When the data were normally distributed, F-test was performed to examine the variances between the groups, continued with the Student's t-test (two tails, $\alpha = 0.05$) for testing the significance of the differences between the means. *p* values of <0.05 and <0.01 are considered as significant and highly statistically significant, respectively. ANOVA can also be applied to test the differences of the means between groups (more than two groups).

When the variances of the samples were unequal, Welch's test or Brown-Forsythe's test was used to test the difference of the means. A post-hoc test can also be applied to track the group which gives the significant difference to the result. As example, Games-Howell's post-hoc test is used when the variances of the sample as well as the number of the samples are not equal.

3.2.10.2 Statistical analysis for the stability test of TBF

Means of the concentrations from each group of the stability test data were compared with one way ANOVA test at 0.05 level followed by a post-hoc Gabriel test. Gabriel test was performed since the samples of the stability test were not equal (ranging from 3 to 5).

Chapter 4

Results and Discussion

4.1 Physicochemical characterization of the formulations

The formulations were characterized macroscopically and microscopically. Complex viscosity and gelation temperature were determined for some selected formulations. Small angle X-ray diffraction was employed as well to detect the presence of a liquid crystal structure.

4.1.1 Appearance and consistency of the formulation [100]

The produced 5-component-systems resulted in a broad range of consistencies and appearances, from liquid to paste-like consistencies. The semisolid area of the pseudoternary phase diagram could be distinguished as cream-, gel- and paste-like, meanwhile the liquid area included milky/white and transparent appearances. The liquid formulations could be further characterized as homogeneous and inhomogeneous.

As can be seen from Fig. 4.1 (a) the border between the liquid and semisolid area was mainly determined by IPA/DMIS content. More than 35% of IPA/DMIS resulted in liquid formulations; except for low POX/MCT, a liquid formulation was already achieved with 30% IPA/DMIS. Some liquids with POX/MCT<35% were inhomogeneous. An area of transparent mixtures, possibly microemulsions, could be found within these liquids as well. Semisolid formulations existed in a region with low content of IPA/DMIS (<40%), while appearances and consistencies varied. The consistency rather increased with increasing amount of POX/MCT whereas the appearance changed from cream-like (25-50% POX/MCT) to highly viscous gel-like (50-70% POX/MCT) and then paste-like (≥70%). The addition of 2% TBF into these bases extended the liquid area and transformed the appearances of some formulations, e.g. from transparent to milky-inhomogeneous as shown in Fig. 4.1 (b).

From the pseudoternary phase diagram in Fig. 4.1, it can be seen that water and IPA/DMIS play an important role in terms of consistencies and appearances of the formulations. Appearances and consistencies depend on the degree of POX swelling especially by water, considering that POX swells better with water than with organic solvents. A lack of water and an excessive amount of IPA/DMIS lead to

inhomogeneous systems. On the other hand, IPA/DMIS enables a complete solubilization of POX and the oily component (MCT); this was evident from the liquid area with transparent appearance. An optimum composition of all components resulted in stable formulations, e.g. cream-like or milky-white (macro)emulsions.

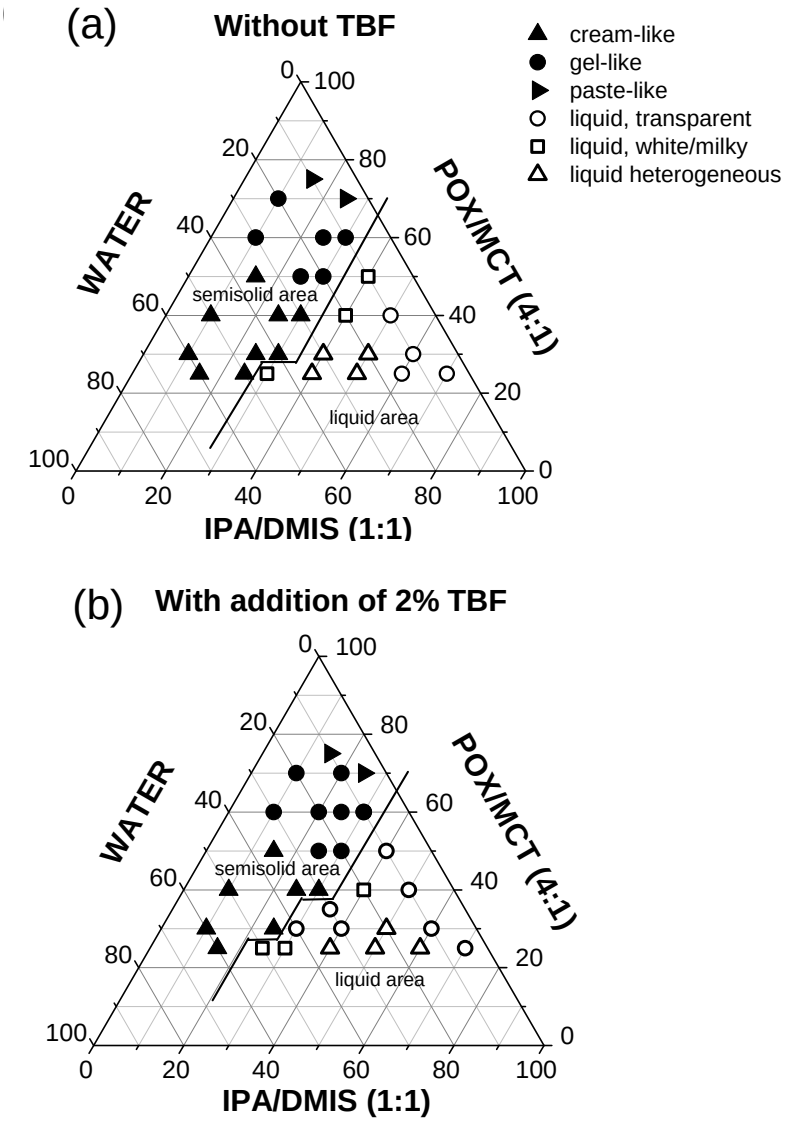

Fig. 4.1 (a) Appearances in pseudo ternary phase diagram without and (b) with 2% TBF; the line in the middle separates liquid from semisolid systems [100]

The enlargement of the liquid area upon addition of 2% TBF hints at the participation of TBF in POX micellization. TBF, a lipophilic drug with log *P* of 3.3, would preferably reside close to POX hydrophobic part/ PPO; any interaction with this block will hamper the dehydration process, the origin of the gelation process [124]. As a consequence, the liquid area was larger compared to that without TBF. The observed appearances

and consistencies were the same as in the case when Miglyol® 840 was used [3]. This indicated that the oil substitution did not affect the resulting appearances.

4.1.2 Ringing effect and isotropy [100]

A special feature of semisolid drug-free systems with creamy appearance was the existence of a so called “ringing effect”, which was noticeable upon slight mechanical agitation. This phenomenon is however not specific for POX containing formulations, but mostly occurs in systems of liquid crystalline cubic phases [89,125] which are highly elastic with shear modulus between 10^4-10^6 Pa [126]. Formulations with ringing effect were located in a particular area with 30-60% water, 25-50% POX/MCT and 10-30% IPA/DMIS (Fig. 4.2). The addition of 2% TBF shifted this area slightly to the upper level of the phase diagram, now ranging from 30%-60% POX/MCT. The addition of 2% TBF to the formulations moved the area to the upper part only, whilst the area broadness was kept. Compared to formulations containing Miglyol® 840, Miglyol® 812N did not change the location of the systems with ringing effect at all, but the anisotropic area became somewhat narrower [3].

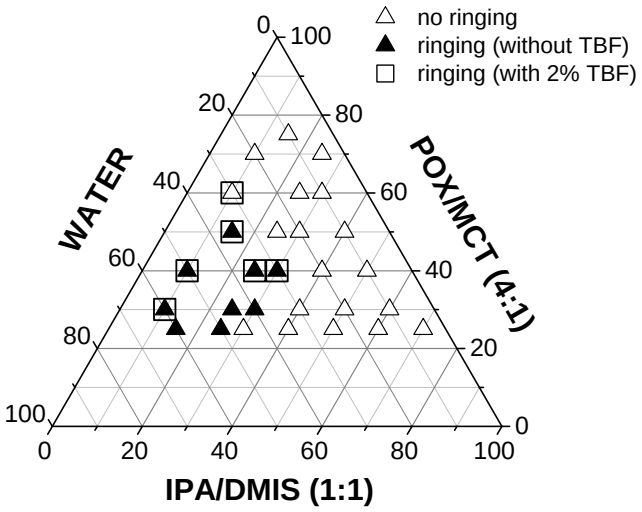

Fig. 4.2 Ringing effect of formulations with and without 2% TBF [100]

The anisotropic formulations could only be found in the area with high content of POX/ MCT. The addition of 2% TBF also enlarged the anisotropic area as shown in Fig. 4.3 from ≥70% POX/MCT to ≥60% POX/MCT. The anisotropic formulations resulted from a POX solubility decrease within the systems. The crystalline characteristics of POX were confirmed by the appearance of a characteristic POX reflection in the wide-angle X-ray diffractograms [3]. In this present study, TBF extended the anisotropic area and

this can be explained through the water competition between POX and TBF, regarding that TBF is also partially soluble in water. Thereafter, POX crystallizes out easier, which is birefringent under the polarizing microscope.

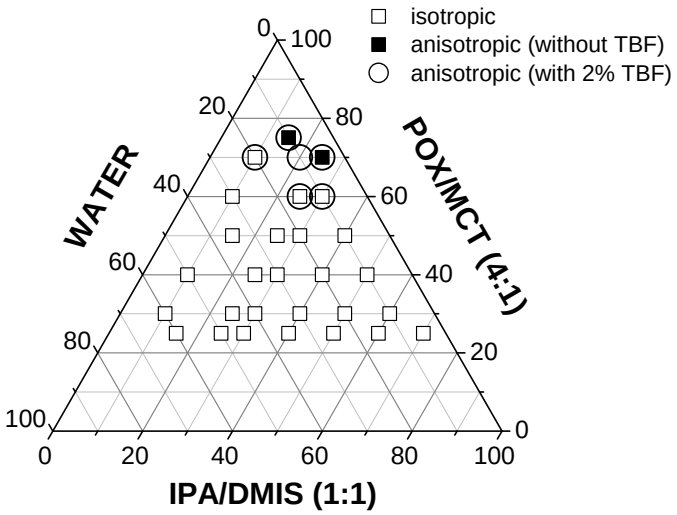

Fig. 4.3 Isotropy of formulations with and without 2% TBF [100]

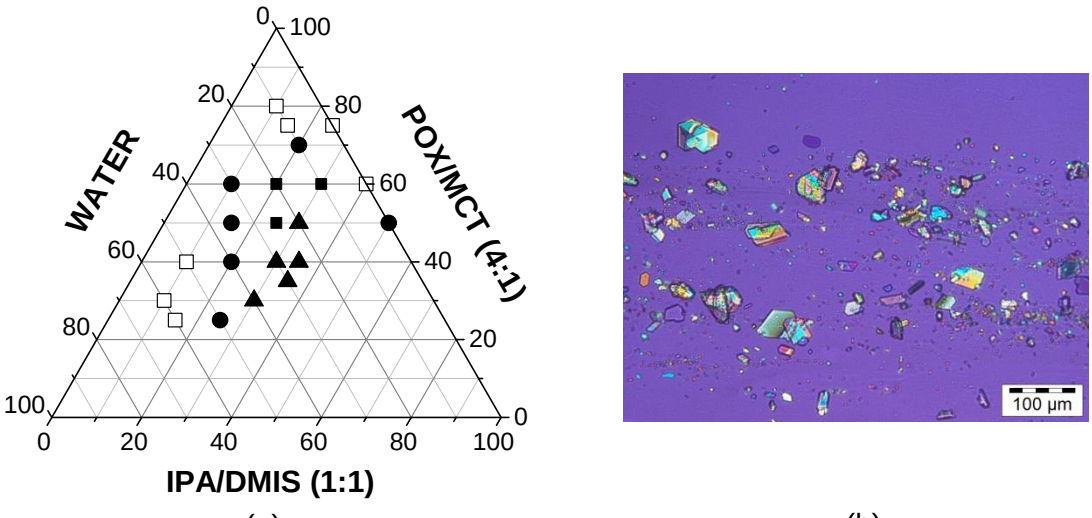

Fig. 4.4 TBF concentrations at saturation (a) and an example of TBF crystals under polarizing microscope (b); □ < 2%, ● 2%, ■ 3%, ▲ 4% [100]

4.1.3 TBF solubility in the formulation [100]

TBF solubility up to 4% was achieved for several formulations and these formulations resided just next to the border between semisolid and liquid area (Fig. 4.4 (a)). An example of insoluble TBF in the formulation examined under polarizing microscope is shown in Fig. 4.4 (b). Since TBF solubility up to 4% has already been achieved with the semisolid formulations, the liquid area (where POX/MCT<25% and

IPA/DMIS>40%) was no longer taken into account for topical application in this study. On the other hand, only up to 1% TBF was soluble in the Basiscreme DAC and an attempt to incorporate more TBF in Lamisil® Creme up to 1.5% was not successful either. These results could be used as an orientation to assess TBF's thermodynamic activity in the formulations. For comparative purposes a POX hydrogel containing 20% POX and 80% water was also prepared and supplemented with 1% TBF. This formulation resulted in a transparent, semisolid (at 20 °C) and not ringing formulation. TBF was completely dissolved in the system.

4.1.4 Rheometrical measurement: complex viscosity and gelation temperature [100]

Several formulations containing TBF from the semisolid area of the pseudoternary phase diagram were rheometrically characterized, in terms of their complex viscosities and gelation points. As depicted in Fig. 4.5 and Fig. 4.6, TBF had a stronger influence on gelation points than on complex viscosities. The incorporation of TBF up to 2% resulted in only slight changes in complex viscosities. The mean values oscillated with an upwards trend towards higher POX/MCT contents. A drop in complex viscosity was observed initially at 3% TBF for the formulation with low content of POX/MCT, e.g. P2525 (see Fig. 4.5). In contrast, gelation points increased remarkably upon TBF addition. Changes were dramatic with increases in POX/MCT. TBF addition from 2% to 3% increased gelation point temperatures from below 5 °C (lower temperature limit applied) to 25 °C for P3535, whereas P3030 changed its gelation point only from 8 to 15 °C for equal TBF concentrations. A linear correlation between TBF content and gelation point increase could be drawn for P3030, but this was not the case for other formulations.

Formulations with higher POX content needed apparently more stress to enable the gelation point detection. All examined formulations could be tested rheometrically at shearing stress of 100 Pa, except for the gelation point detection of P3535. Its gelation point could only be measured at TBF contents of 3% and 4% under a shearing stress of 200 Pa. Further formulations with even higher POX/MCT contents (≥35%) were no longer measurable, with respect to gelation points, even with increasing shearing stress up to 400 Pa. Since gelation points of 1P3030, 1P3535 and 2P3535 could not be detected by rheometer within the temperature range applied (30 °C – 5 °C), they were not plotted on the graph (Fig. 4.6).

TBF showed a stronger influence on the gelation process than on the complex viscosities of the formulations (at least up to 2% TBF addition). The measurement of the complex viscosity had to be done at 32 °C which guaranteed for the viscoelastic state needed. However, this temperature was apparently not appropriate to detect any influence of TBF on the complex viscosity. Furthermore, all the formulations examined showed gelation temperatures below 32 °C; above the gelation temperature, no sharp change in viscosity can be observed.

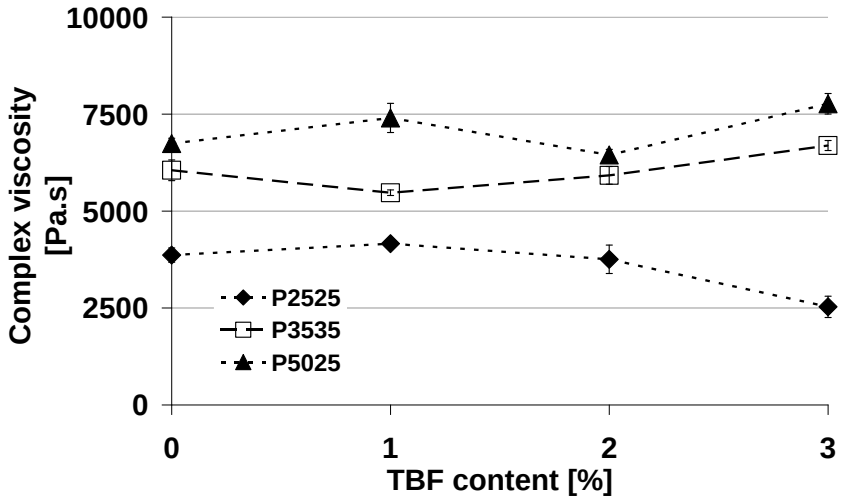

Fig. 4.5 Complex viscosity of several semisolid formulations (n = 3) [100]

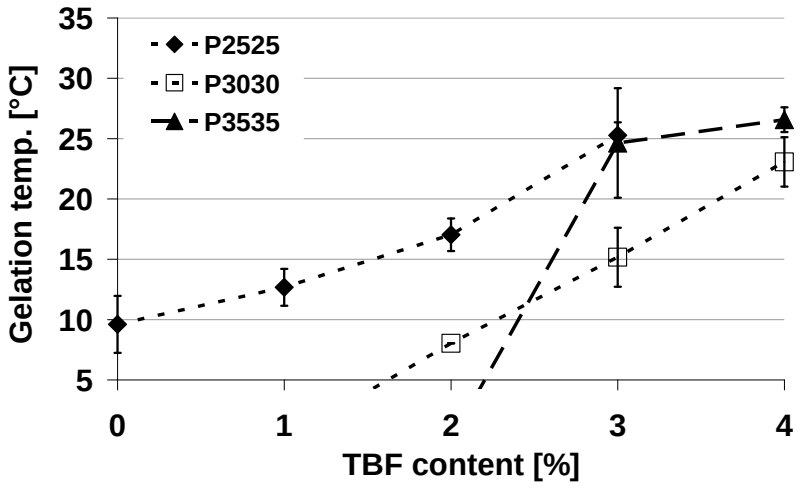

Fig. 4.6 Gelation point of several semisolid formulations (n = 3); All measurements were carried out at 100 Pa, except for POX3535 at 200 Pa [100]

Other substances, which increased POX gelation temperature, have been documented, such as diclofenac, propylene glycol, sodium dodecyl sulfate, alcohol

and also vice versa, substances which decreased it: vitamin B_{12}, sorbitol, 5-ALA and NaCl [5,127-129]. All those substances have the ability to modify particularly PPO block solubility in water, thus delaying or accelerating POX micellization process. The increase in gelation temperature upon TBF incorporation was however not in line with the expected effect of chlorine salts, which generally accelerate micellization due to their ability in reducing water activity/ salting out [130] or what has recently been described as water-structure-shaper [130-132]. Therefore, terbinafine cation must have a major role in affecting POX gelation process compared to its chloride anion. This phenomenon has also been observed from lithium chloride [132].

4.1.5 Small angle X-ray diffraction (SAXD)

SAXD enables to identify the presence of a liquid crystal structure through the scattered X-ray by an ordered crystal lattice. The hint at the liquid crystal structure has been signalized through the presence of a ringing effect in several thermogelling formulations, especially from P2525, the original thermogelling formulation. The early hypothesis led to the cubic structure since these thermogelling formulations featured a high viscosity, isotropy and ringing effect; these are characteristics of the cubic structure [87]. However, this assumption has not yet been further examined by Grüning before [2].

Small angle X-ray diffraction of the formulations with ringing effects hinted at the presence of the cubic structure Pn3m, which is displayed in Table 3.2 and Fig. 4.7 as “kub 2”. This structure was evident particularly from P2525, which reflections followed the order of Pn3m structure, i.e., according to Bragg ratio: 1: $\sqrt{2}:\sqrt{3}:\sqrt{4}:\sqrt{6}:\sqrt{8}:\sqrt{9}:\sqrt{10}$. The addition of TBF and the application of heat modified the peak intensities.

Fig. 4.7 presents the structure of P2525 upon addition with TBF and heating to 40 °C. At a constant temperature of 20 °C, the structure was still distinct upon incorporation of 1% TBF (black line). With 3% TBF at similar temperature (blue line), the intensity weakened and the spacing order could not be recognized clearly. Heating to 40 °C amplified the peak intensities so that 3P2525, which was not visible at 20 °C, became distinct (orange line). This was also the case for 1P2525, which intensity increased upon heating to 40 °C.

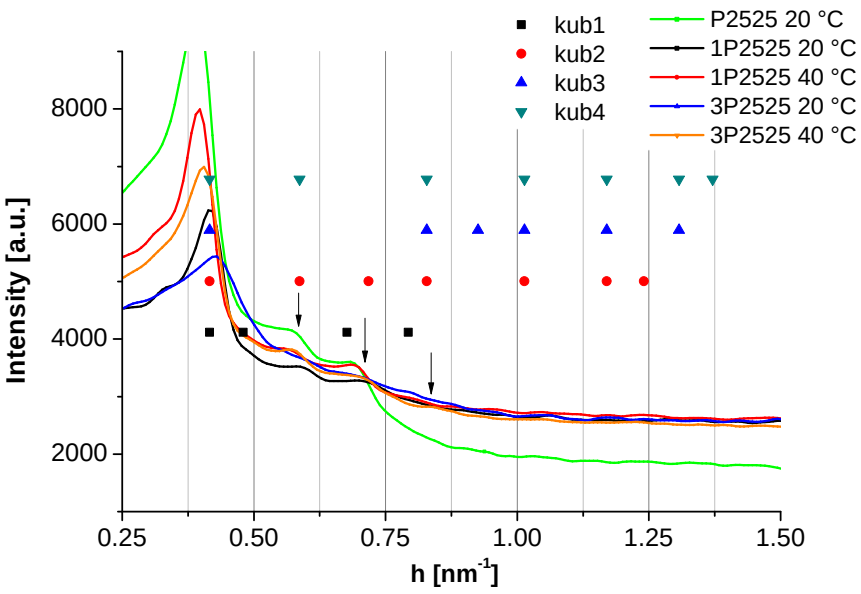

Fig. 4.7 SAXD results of P2525 with varied TBF content (0%, 1% and 3%) and upon heating (20 and 40 °C)

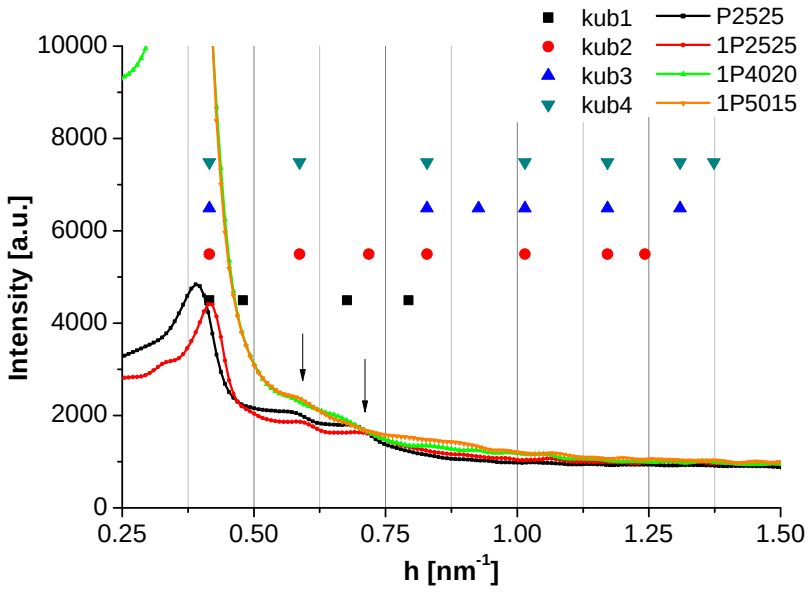

Fig. 4.8 SAXD results of P2525, 1P2525, 1P4020 and 1P5015 at 20 °C; sheet for the cubic structure estimation and calculation had been developed by van Hemelrijck [6].

In contrast to the SAXD result from P2525, SAXD results from 1P4020 and 1P5015 (Fig. 4.8) could not be interpreted due to their high intensities. However, the following two peaks (pointed with black arrows) were similar to P2525' spacing order. The assumption that 1P4020 and 1P5015 may possess a cubic structure is not completely excluded since both formulations feature the ringing effect. The structure which may be displayed by 1P4020 and 1P5015 might though be different from P2525 structure.

Liu and Chu [133] reported the transformation of the cubic structure, i.e., from face-centered cubic (fcc) within the concentration range of 20-40% to body-centered cubic (bcc), which was observed when the concentration of POX 407 aqueous hydrogel increased to 50%.

The SAXD results showed at least that the isotropic formulations with ringing effects are likely to be cubic liquid crystals although the data presented here are still limited for characterization in detail. P2525 retained its cubic structure upon addition of 1% TBF whereas the reflections disappeared after the incorporation of 3% TBF (20 °C). Since the cubic structure is a consequence of the micellization process, TBF addition will also influence the gelation temperature of the formulation; this is in agreement with the rheology result in the previous section. Briefly, TBF was shown to be a POX-structure breaker, both from rheology and SAXD measurements. Heating, on the other hand, amplifies SAXD intensity thus makes the order more visible. Increasing the temperature turns POX more hydrophobic due to the progressive PPO dehydration and at a definite point, gelation occurs [134]. TBF as a structure breaker shifts POX gelation point to a higher temperature only; this indicates that the formulation can gel. The reappearance of 3P2525 peaks upon heating to 40 °C hinted at the gelation of the formulation. Such a gelation had not happened at 20 °C.

4.2 TBF stability in aqueous media

As TBF is a relatively new drug in the market, no stability data of TBF have been reported so far. Regarding the use of aqueous media in some experiments of this study, TBF stability under the influence of different pH values and temperatures was evaluated.

4.2.1 Influence of pH on TBF stability

Lebo et al. [109] reported TBF stability in aqueous solution up to 72 h when buffered at the pH of 5.8. The degradation in aqueous solution occurred even after the addition of antioxidants, e.g., ascorbic acid and sodium metabisulfite [109]. Unfortunately, the report of TBF stability from Lebo et al. [109] did not include the information on the initial TBF concentration. TBF degradation occurred as well when methanol and acetonitrile were used as solvent [76,77]. Hitherto, the degradation mechanism of TBF has not been reported. TBF degradation apparently deals with hydrolysis since TBF in

a dry state, e.g., tablet was reported to be stable up to six months in a stress condition (40 °C, 75% RH) [77].

Two buffers at pH 5.8 (PB) and pH 7.4 (PBS) were employed in the present study to examine TBF stability for 144 h. UV spectra from both pH values can be seen in Fig. 4.9.

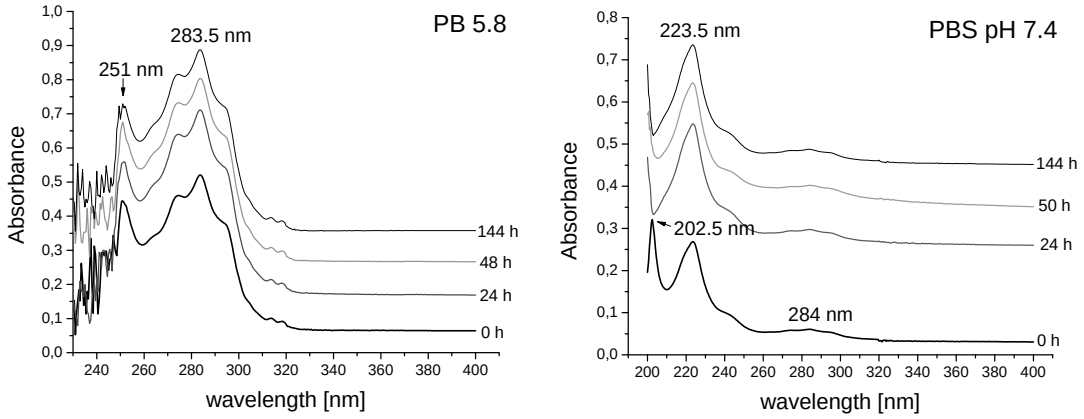

Fig. 4.9 UV spectrograms of 0.1% TBF solution in PB 5.8 and PBS 7.4 for up to 144 h

No changes were observed up to 48 h from TBF solution in PB. After 144 h, the peak at 251 nm split into two peaks. Apart from that, the maximum peak occurred at 283.5 nm and the profiles remained unchanged during the examination. In contrast to PB, the absorbance profiles in PBS changed dramatically after 24 h, marked by the disappearance of the first peak at 202.5 nm. Yet, the main peak at 223.5 nm remained unchanged. From this observation, pH 5.8 is sufficient to maintain TBF stability for the permeation study within 48 h. Changes in absorbance of TBF at 251 nm were displayed in Table 4.1. A further discussion to this finding will be given in the next section 4.2.2.

Table 4.1 Absorbance (A) of TBF in PB at ambient temperature

Time [h]	A at 251 nm
0	0.394
2	0.429
24	0.400
48	0.418
144	0.374

The different UV spectra of TBF under different pH values corresponded well with the work reported by Egle [135]. Depending on the pH value applied, TBF chromatograms

showed different patterns and peaks measured by means of HPLC with a UV detector [135].

4.2.2 Influence of temperature on TBF stability

Besides the influence of pH value, the influence of temperature on TBF stability was examined as well since permeation study is commonly carried out at higher temperatures than 20 °C to mimic the skin surface temperature (32 °C) or the body temperature of 37 °C.

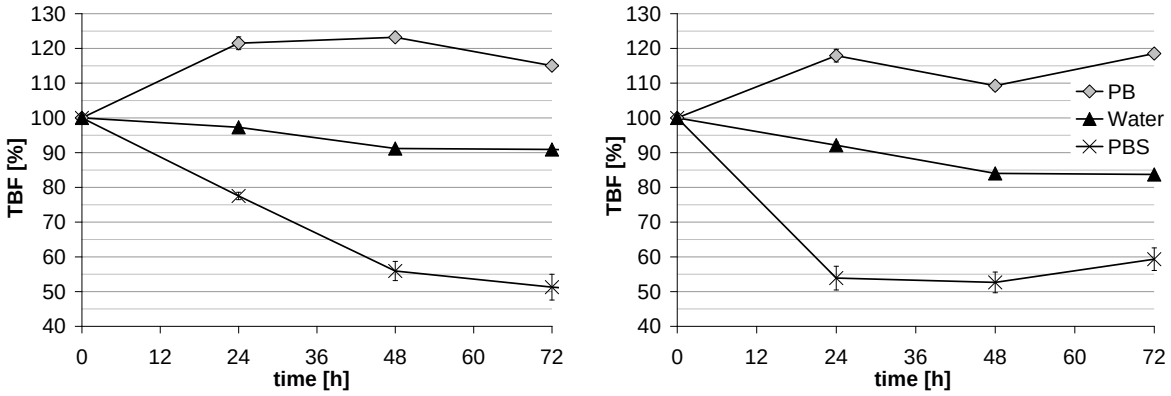

Fig. 4.10 TBF concentration in PB, water or PBS up to 72 h at 20 °C and 32 °C

Changes in TBF concentrations at two different temperatures and in 3 different media during storage are displayed in Fig. 4.10. Surprisingly, PB increased TBF concentration to 120% for both temperatures after 24 h. Solvent evaporation seemed to be impossible since all the samples were packed in gas-tight vials. Therefore, an increase in TBF molar absorptivity (ε) at both temperatures in PB (hyperchromic shifts) was suggested. A slight increase in TBF absorbance during the early storage period in section 4.2.1 was observed as well from the first 2 h in PB (see Table 4.1). Afterwards, TBF absorbances remained about constant and decreased after 48 h.

The hyperchromic shift of TBF in an acidic milieu was possibly a result of a conjugation extension of TBF's double bonds or π-stacking interaction which commonly occurs between aromatic rings [136]. Unfortunately, there is no report associated with TBF so far. A similar finding has been reported by Peters from estradiol aqueous solution [137]. The concentration of estradiol solution increased steeply during storage from day 7 to 17, whereas the degradation product estron was first detected after day 17. The concentration of estradiol increased overall from 5 to 8

µg/mL during these 10 days. Furthermore an additional peak with earlier retention time had been detected after 8 days which was considered as “ghost peak”. In contrast to estradiol, no ghost peak was detected either from the HPLC chromatograms or from the UV spectra as seen in Fig. 4.9. This increase in concentration was specific only for PB and was not observed in water and PBS. TBF solution in PB was also measured by means of photon correlation spectroscopy (ZetaSizer Nano Series ZS ZEN 3600 from Malvern Instrument Ltd.) to detect any aggregate that might have been formed in pH 5.8. However, no aggregation could be detected and thus still no further explanation to this phenomenon. Some possible explanation to this phenomenon could be π-stacking formation of TBF aromatic rings which elevated TBF molar absorptivity thus its absorbance or the formation of (a) degradation product(s) that exhibited similar absorption maxima as TBF did. A further investigation is needed to elucidate this phenomenon in detail.

TBF concentrations decreased readily in other media, i.e., water and PBS. The degradation rate was higher with increasing temperature. Nevertheless, TBF was more stable in water than in PBS. TBF content in water was reduced by 10% and 15% after 48 h at 20 °C and 32 °C, respectively. In PBS TBF deterioration was more dramatic; 45% within 48 h at 20 °C and about the same within 24 h at 32 °C. The fact that TBF degraded faster in PBS rather than in water hinted at a strong influence of electrolytes to the degradation process. In an acidic milieu of pH 5.8, however, TBF stability was sufficiently maintained for the permeation study.

4.3 TBF stability in the formulations

This study was carried out to examine TBF stability in the formulations during storage at 20 °C in a climatized room. A stability study is important since the formulation may exhibit unexpected changes during storage. Alterations which may occur encompass larvated incompatibilities and drug degradation due to the storage conditions, such as: temperature, humidity and packing material. Macroscopical changes of the formulations and TBF content were followed for six months and three months, respectively. The macroscopical observations comprised changes in appearance, physical state and phase separation meanwhile TBF contents in the formulations were determined by means of HPLC subsequent to extractions.

4.3.1 Macroscopical changes of the formulations

After one month of storage, there were no significant changes in physical appearance of the formulations containing 1% TBF except for few formulations which turned yellow. This alteration occurred to almost all formulations with IPA/DMIS of ≥40% and POX/MCT between 25-50%. After three months, the area in the phase diagram representing systems with yellow color grew; now occupying an area with POX/MCT between 25-60% including one formulation that contained 30% IPA/DMIS. After six months, almost all formulations with IPA/DMIS of ≥25% and POX/MCT between 25-60% underwent this alteration. All these changes are depicted in Fig. 4.11. In addition, the color intensity increased along with the increase in IPA/DMIS contents in the formulations as well as with the increase in storage duration. TBF loading of the formulations also increased the yellow color intensity.

Besides the yellow color alteration, there was also a fairly dynamic macroscopical change observed especially in the liquid area. After three months, all transparent mixtures in the study turned turbid/ white or inhomogeneous and one liquid formulation (1P2530) turned creamy. After six months, some liquid formulations were again observed as transparent but they were surely not exactly the same transparent formulations as in the initial state. Alteration in the semisolid area became noticeable as well after six months where the gel-like and paste-like area broadened. This was likely caused by the evaporation of volatile compounds such as IPA and water since air-tightness of the packaging was not fully guaranteed. Overall, the liquid formulation was apparently very sensitive towards storage, especially when the packaging used did not ensure air-tightness.

Since all the formulations affected by the yellow color alteration were liquid, this color change occurred somehow faster within the first three months than after the 3rd month when the semisolid formulations also started to turn yellow. Formulations without TBF did not turn yellow even after one year of storage; this was confirmed by van Hemelrijck and Müller-Goymann [91]. The alterations of the bases which have been reported before were liquefaction, microbial growth and phase separation after one year of storage in a similar storage condition [91]. Since the alteration rate was faster in liquid formulations, the high content of IPA/DMIS was suspected to be responsible for this. In addition, a low viscosity and a liquid state favor chemical reaction. Such an

alteration could also originate from a larvated incompatibility between the constituents which will be elaborated in the next section.

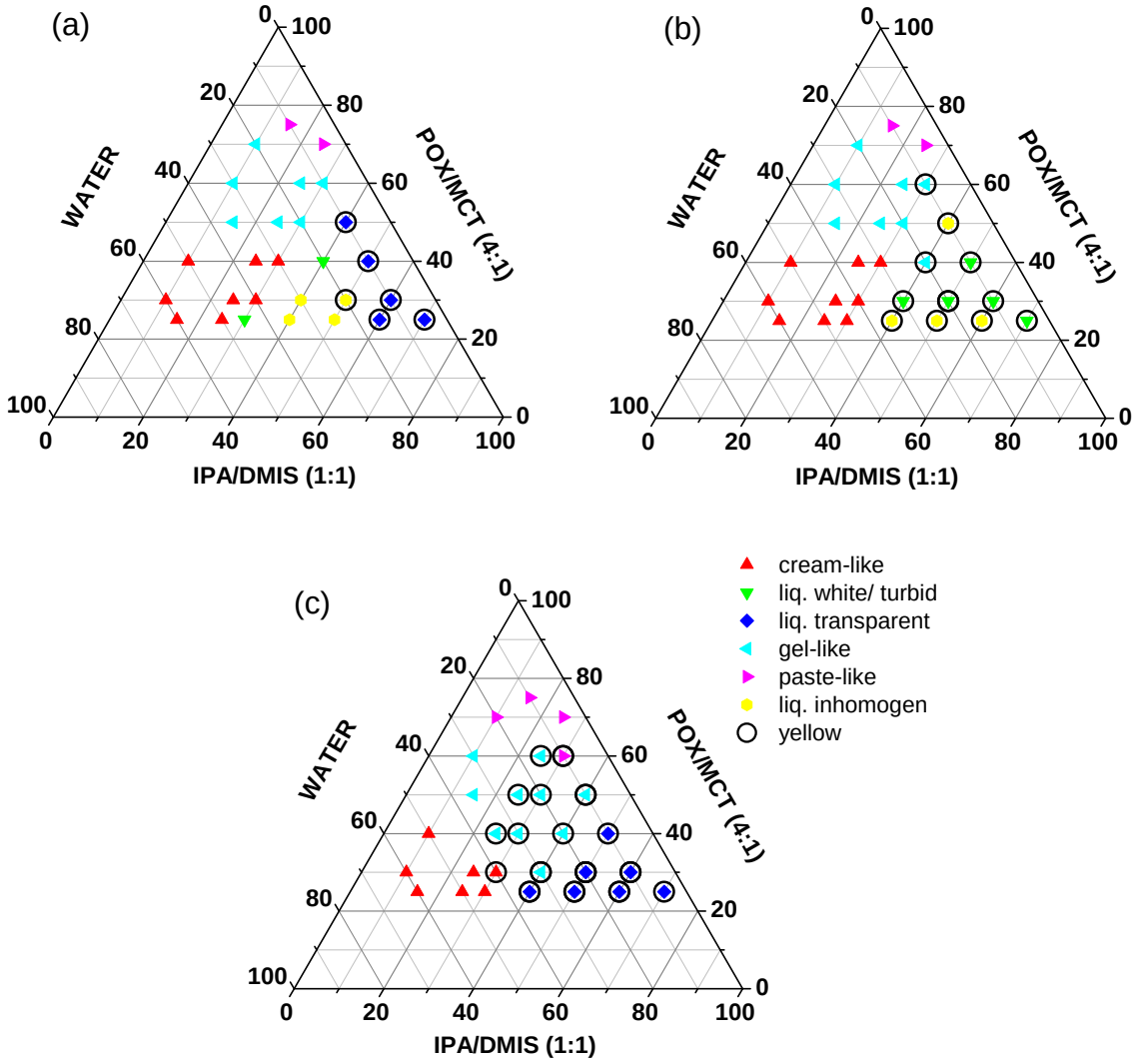

Fig. 4.11 Macroscopical changes of thermogelling formulations containing 1% TBF during storage at 20 °C after one (a), three (b) and six (c) months

4.3.2 Finding the instability and/or incompatibility trigger

Following the result of the previous section where alteration occurred during storage, it was then necessary to identify the trigger of the alteration. By having some reactive functional groups, i.e., double bonds and tertiary amine, TBF may undergo a chemical reaction with any of the formulation components (incompatibility) or degrade due to hydrolysis in the presence of water.

After one month of storage, the reason for the alteration was identified. As can be seen from Table 4.2, all the mixtures containing DMIS turned yellow. This did not

occur in other mixtures. This result hinted at a particular chemical reaction between TBF and DMIS or its major impurities since the base itself did not undergo this alteration. Since the product is observable (yellow) under visible light, it is suggested that a product with higher molecular weight was formed.

Table 4.2 Binary and multiple mixtures to identify the trigger of alteration in the formulations

Mixture	TBF	POX	MCT	IPA	DMIS	Water	Result
1	X		X				n.a.
2	X			X			n.a.
3	X				X		yellow
4	X					X	n.a.
5	X	X	X				n.a.
6	X	X		X			n.a.
7	X	X			X		yellow
8	X	X				X	n.a.
9	X	X		X	X		yellow
10	X	X		X		X	n.a.
11	X	X		X	X	X	yellow
	0.2 g	**1.96 g**	**0.49 g**	**3.43 g**	**3.43 g**	**0.49 g**	**total: 10 g**

n.a.: no alteration was observed

4.3.3 Changes in TBF concentrations during storage

TBF concentrations in the formulations after three months of storage are displayed in Fig. 4.12 and Table 4.3. After one month, the concentration decreased by about 5% and after three months, TBF final concentrations were outside the permitted area 95-105%, i.e., between 71–79%.

After one month, almost all formulations were still within the permitted concentration except 1P3040 and 1P4040 which were distinctly lower than 95%, and 1P2836 and 1P2525 which were just below 95%. The least degradation was given by 1P4412 (3.22%) and the maximum one was shown by 1P4040 (8.57%). After three months, the minimum degradation was surprisingly shown by 1P3040 with 22.56% and the highest one was given again by 1P4040 with 30.67%. Statistical analysis ANOVA revealed that TBF changes after one and three months were significantly different (p<0.05) from the initial TBF concentration C_0. Among all formulations, 1P4412 was the one with the significantly highest stability (p<0.05) with only 3.22% degradation after one month. As a note, 1P4412 was also the formulation with the least IPA/DMIS

content. TBF decreases were particularly high from formulations with high contents of IPA/DMIS, with 1P3040 and 1P4040 as examples. A high content of IPA/DMIS in the formulation produced a low viscosity, and accordingly liquid formulations, which may accelerate the degradation process.

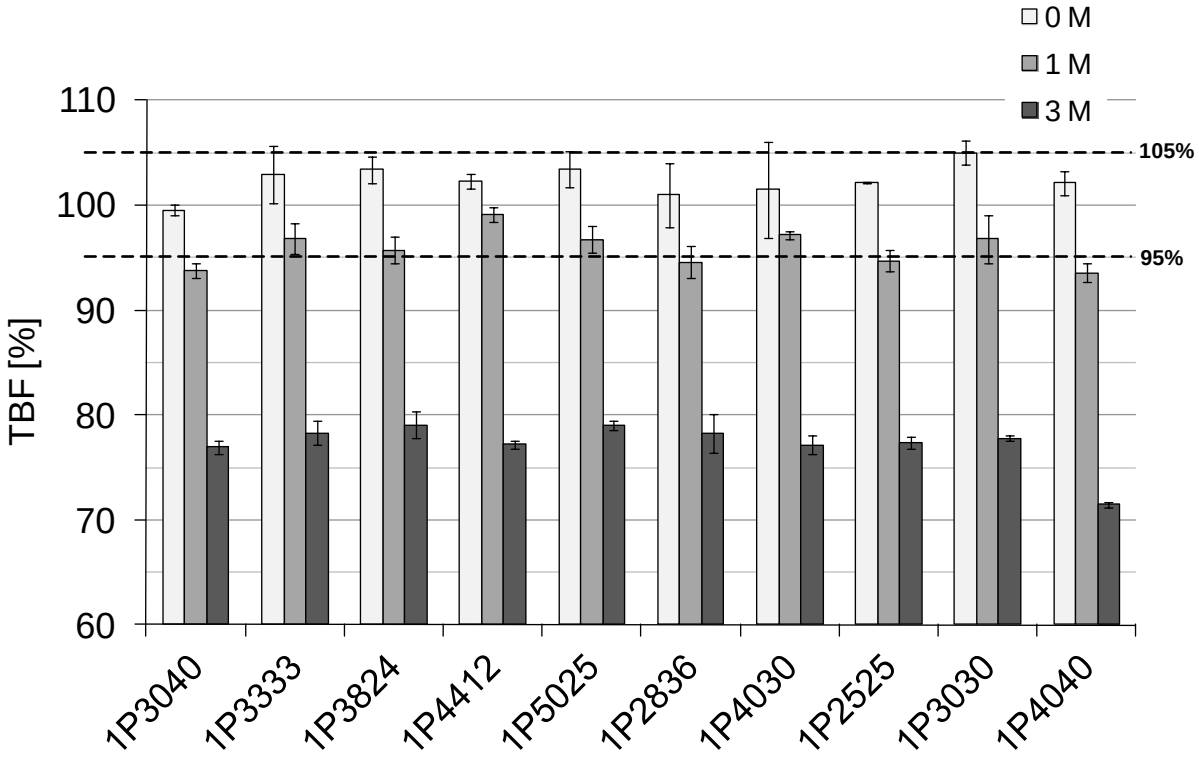

Fig. 4.12 TBF concentrations in formulations within three months of storage at 20 °C (n = 3)

Table 4.3 Changes in TBF concentration [%] from selected formulations during storage

Formulation	Initial concentration (C_0)	C after 1 month (C_1)	C after 3 months (C_3)	$C_1 - C_0$	$C_3 - C_0$
1P3040	99.51 ± 0.51	93.79 ± 0.70	76.95 ± 0.63	-5.71	**-22.56'**
1P3333	102.93 ± 2.68	96.82 ± 1.46	78.32 ± 1.09	-6.11	-24.62
1P3824	103.43 ± 1.27	95.74 ± 1.32	79.06 ± 1.25	-7.69	-24.38
1P4412	102.31 ± 0.73	99.09 ± 0.73	77.21 ± 0.40	**-3.22*'**	-25.09
1P5025	103.45 ± 1.77	96.74 ± 1.29	79.03 ± 0.40	-6.71	-24.42
1P2836	101.00 ± 3.04	94.57 ± 1.53	78.26 ± 1.81	-6.43	-22.75
1P4030	101.49 ± 4.54	97.19 ± 0.37	77.15 ± 0.90	-4.30	-24.35
1P2525	102.23 ± 0.08	94.73 ± 1.01	77.39 ± 0.61	-7.50	-24.84
1P3030	105.02 ± 1.12	96.78 ± 2.28	77.81 ± 0.30	-8.24	-27.21
1P4040	102.16 ± 1.13	93.58 ± 0.89	71.49 ± 0.28	**-8.57"**	**-30.67"**

*p<0.05 (one way ANOVA with Gabriel post-hoc test at the 0.05 level); n = 3-5; 'the least TBF degradation; "the highest TBF degradation

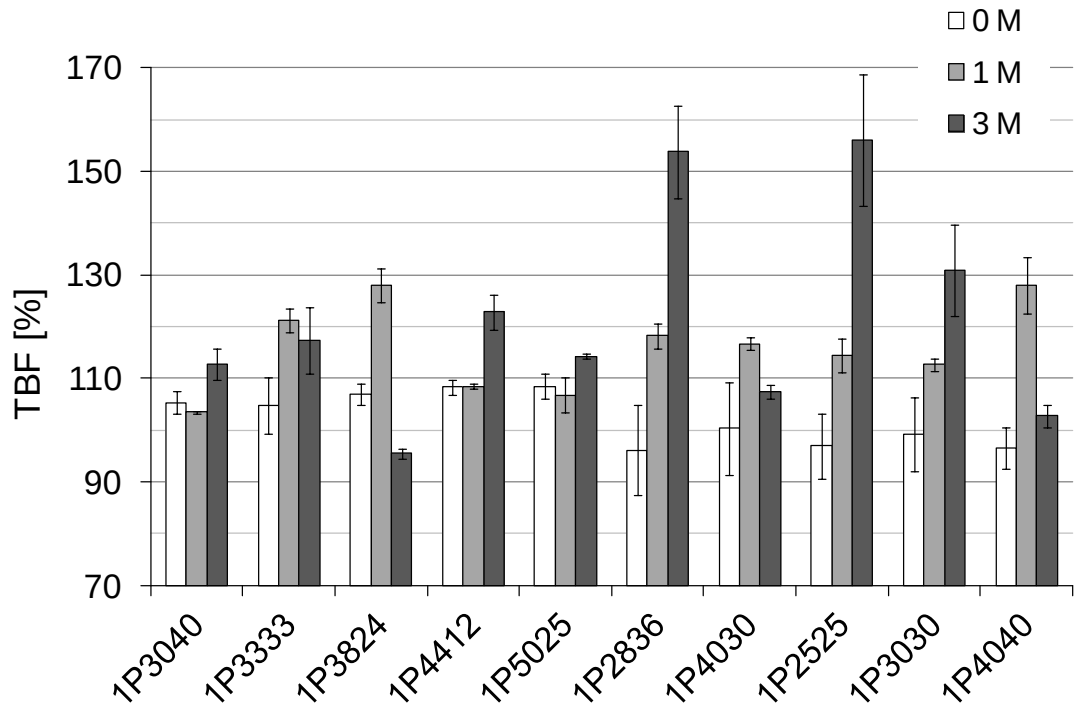

Fig. 4.13 TBF concentrations of the thermogelling formulations stored in unguator jars at 20 °C for up to three months (n = 3)

Packing the formulations in gas-tight vials has been a crucial step in this study. Without considering this, an excessive evaporation of volatile substances (IPA, water)

from the formulation occurred. As expected, TBF contents rose during the storage as depicted in Fig. 4.13. In this manner, TBF concentrations after one month increased remarkably to over 125%. After three months, TBF concentrations even reached 160%, a value which was not realistic. Thereafter, these results hinted at the importance of a proper packaging for the stability study although the unguator jars reflect the common packaging of semisolid formulations.

Referring to pharmacopoeial requirements in terms of the drug content in the formulation established, this shall generally amount to 95–105%. This requirement could be fulfilled by the thermogelling formulations containing 1% TBF up to one month only. 1P3040 and 1P4040 failed to meet this requirement. In accordance to this, the POX-based thermogelling formulations would still be suitable as vehicles for extemporaneous preparations containing TBF for up to one month at a storage temperature of 20 °C.

4.3.4 Thin layer chromatography (TLC)

TLC can separate substances from a mixture according to their polarities and affinities to either stationary or mobile phase. The stationary phase used in this study was silica gel that was immobilized on a glass plate. Silica gel is considered as polar. The mobile phase used was rich in chloroform and was considered as non-polar. In such a system, a polar substance will show a higher affinity to the polar stationary phase so that the spot will be visible earlier with a low R_F value. This is vice versa for a relatively non-polar substance. In other words, substance separation by means of TLC is a competitive process between the stationary and the mobile phase.

The result of separation from the examined formulations by means of TLC is displayed in Fig. 4.14. Generally, all formulations containing TBF showed spots at R_F 0.66-0.74. According to the reference standard (1% TBF in methanol), those spots belonged to TBF. Additionally, extra spots at lower R_F of 0.09-0.11 were shown by formulations containing TBF which have been stored for one month. The spot at lower R_F was not evident from the freshly prepared TBF solution in methanol nor from the bases without TBF (e.g., P2570, P2530, P2550 and P2560). The intensity of the spot at this low R_F was found to be dependent on TBF concentration in the formulation. As expected, the spot intensity was stronger from formulations with higher content of TBF and formulations after storage. Referring back to the system used, the spot with low R_F

value should be a polar substance. Furthermore, this spot should be much more polar than TBF and was tightly bound to the stationary phase.

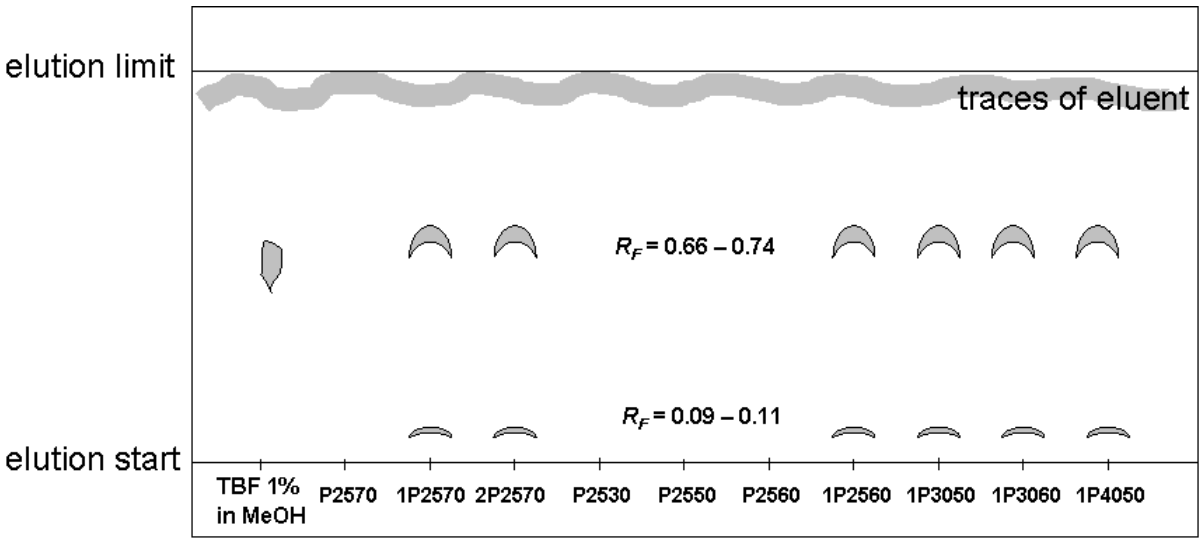

Fig. 4.14 Separation of one-month-old formulations with 1% TBF solution in methanol as reference

From the previous section, it may be concluded, that the alteration occurred due to a “larvated incompatibility” of TBF with DMIS and this new spot could be the product of this interaction. For further identification of the substance of this new spot, isolation and a further elucidation by means of other analytical methods are required.

TBF spots from the freshly prepared solution and from the formulations were slightly different in their R_F values. The R_F value of TBF spot from the freshly prepared solution was slightly lower compared to those from the formulations. Different environments of both samples can cause this phenomenon. TBF can behave differently in environments with different pH values or upon the presence of other substances. However, since TBF appeared as a single spot, this slight difference in R_F values can be considered as insignificant.

4.3.5 Resume of TBF stability study

TBF stability was proven to be pH dependent. As reported by Lebo et al. [109], pH 5.8 was found to be the most suitable pH for TBF aqueous solution since TBF degraded faster in water and PBS (pH 7.4). In this study, UV spectrograms remained unchanged for up to 48 h (Fig. 4.9). Changes occurred in PBS even earlier after 24 h. TBF degradation rate increased as the storage temperature increased from 20 °C to 32 °C. The ranking of TBF degradation rate in various aqueous media was PBS>water>PB. It

is interesting that TBF absorbance in PB increased by 20% and this remained for 48 h. Since evaporation of the solvent from the packing was rather impossible, a hyperchromic shift due to the elongation of TBF's double bonds conjugation or π-stacking interaction which commonly occurs between aromatic rings might be responsible for this phenomenon. Of course the formation of (a) degradation product(s) with similar absorption maxima to TBF is possible as well. Unfortunately this cannot be detected from either UV spectogram or HPLC chromatogram. Therefore, a further investigation is needed to elucidate this phenomenon in detail.

Changes in appearances were observed from the thermogelling formulations with and without TBF. While the alteration of the bases was in line with the report of van Hemelrijck and Müller-Goymann [91], the formulations containing TBF turned yellow during storage. The color change started earlier in formulations with high content of IPA/DMIS than in formulations with low IPA/DMIS content.

TBF was more stable in most of the formulations than in the aqueous solution. TBF concentrations from all examined formulations were over 95% after one month storage at 20 °C. A faster TBF degradation was observed for formulations with high content of IPA/DMIS. After three months, all TBF concentrations in the formulations were less than 95%. In other words, these thermogelling formulations containing TBF were only stable up to one month at 20 °C. The decrease in TBF amount correlated well with an increase in yellow color intensity happening first in formulations with high IPA/DMIS. Thereby and in accordance with observations from the binary and multiple mixtures, it was concluded that the TBF instability was triggered by a larvated incompatibility between TBF and DMIS. The presence of a degradation product was visible from TLC separation. All formulations undergoing color changes exhibited an extra spot at lower R_F. Since the eluent used was non-polar and the stationary phase was polar, this additional spot was suggested to be polar.

4.4 Permeation study across human SC [100]

Skin is the site where dermatophytosis occurs frequently. In accordance to this, the performance of POX-based formulation containing 1% TBF was examined across human SC compared with other vehicles containing 1% TBF as well. In addition, some formulations with higher TBF amounts (2% and 4%) were evaluated as well.

4.4.1 Thermogelling formulations vs. other vehicles

A formulation containing 1% TBF was chosen, i.e. 1P2525, and its permeation flux across SC was compared with Basiscreme DAC and Lamisil® Creme, with respect to their comparable creamy consistencies. A steady state flux could be achieved as shown in Fig. 4.15 for all the formulations with slight differences in their lag times. The permeated amounts were ranked 1P2525>Lamisil® Creme>Basiscreme DAC while the ranking of the fluxes was 1P2525>Basiscreme DAC>Lamisil® Creme (see Fig. 4.16). 1P2525 flux was around 1.4-fold higher compared to Lamisil® Creme and Basiscreme DAC. However, all fluxes were not significantly different (p>0.05). This was also the case for the lag times which were comparable as well (see Fig. 4.17).

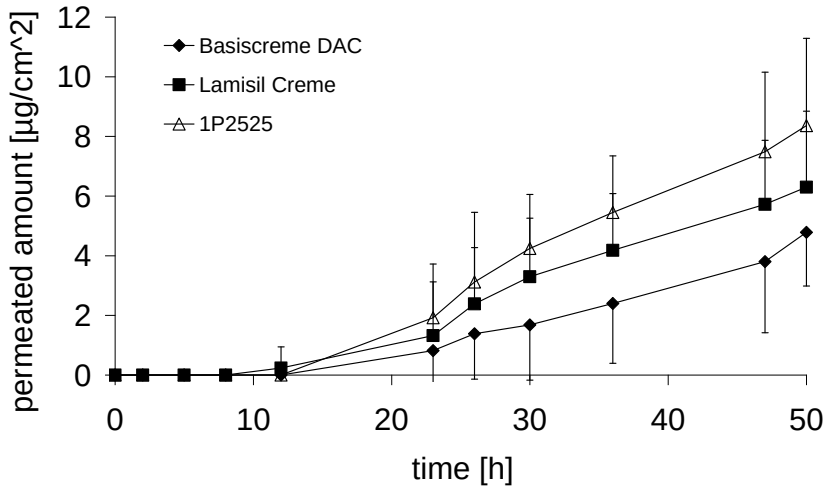

Fig. 4.15 Permeation of TBF from 1P2525, Lamisil® Creme and Basiscreme DAC across SC (n = 4-9); donor: ♀, 38-year-old [100]

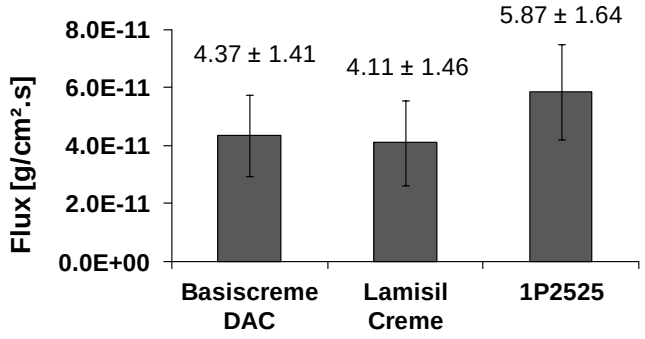

Fig. 4.16 TBF fluxes (mean ± SD) across SC from 1P2525, Lamisil® Creme and Basiscreme DAC (n = 4-9) [100]

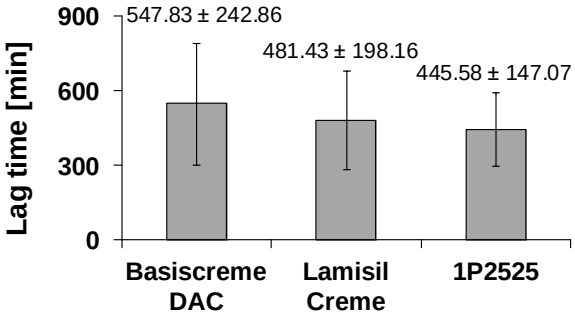

Fig. 4.17 TBF lag times (mean ± SD) across SC from 1P2525, Lamisil® Creme and Basiscreme DAC (n = 4-9) [100]

TBF was completely soluble in all the tested formulations for the permeation study, including Lamisil® Creme and the Basiscreme DAC containing 1% drug. 1P2525 contained more water than Basiscreme DAC (50% vs. 40%) and this could be an advantage for the permeation. The water content of Lamisil® Creme is unfortunately not known for comparing this result, but its flux was similar to that from Basiscreme DAC. The ability of water in increasing drug diffusion across skin has been assigned to its interaction with the SC's lipid polar head groups thus loosening the lipid packing and providing more space for diffusion [28,29].

Up to 2% TBF was dissolved in P2525, meanwhile in the Basiscreme DAC drug dissolution was only possible up to 1%. This showed that the thermodynamic activity of 1P2525 was actually lower than that in the Basiscreme DAC, whilst the drug activity in the Basiscreme DAC was close to maximum. TBF thermodynamic activity in Lamisil® Creme was close to maximum as well since the vehicle did not enable TBF loading up to 1.5%. If the permeation was only depending on the thermodynamic activity of the formulation, then Basiscreme DAC and Lamisil® Creme should have given a higher flux value than 1P2525 did, but this was not the case. The nature of the vehicle and its interaction with TBF might thus play also a major role.

Differences in vehicle type, construction of a gel network and its tortuosity will affect TBF binding with the vehicle and thus TBF release rate. For example, Gendy et al. [138] found that flurbiprofen release from carbomer gel was higher than from POX 407 gel. They suggested that this was due to the different microstructure and release mechanism from both gelling agents. Despite similar appearances of P2525, Basiscreme DAC and Lamisil® Creme, POX vehicle contains more hydrophilic ingredients than other creams so that TBF binding with this vehicle is apparently

weaker. A strong influence to the skin lipids such as their fluidization or disruption of lamellar sheets could enhance drug permeation rate as well and measurements by means of DSC could help in visualizing this (see section 4.7).

4.4.2 TBF permeation from thermogelling formulations containing more than 1% TBF

The enhancement factors from formulations with more than 1% TBF are listed in Table 4.4. Increasing TBF concentration in the formulation led to an increase in TBF permeation flux. The enhancement factor was significantly different (p<0.05) only for P4030 containing 4% TBF whereas for all formulations tested with 1% TBF the fluxes were similar. Due to high standard deviations of 2P2525 and 2P3030, a significantly different enhancement could not be deduced. Permeation profiles of formulations containing more than 1% TBF can be seen in Fig. 4.18 - Fig. 4.20.

Table 4.4 TBF fluxes (mean ± SD) and enhancement factors from thermogelling formulations containing TBF of more than 1%

Formulation	[% TBF]	Flux at steady state x 10^{-11} [g/cm^{2}s]	Enhancement factor [-fold]
1P2525	1	4.56 ± 0.84	
2P2525	2	15.00 ± 12.60	3.3
1P3030	1	3.38 ± 0.89	
2P3030	2	8.11 ± 4.14	2.4
1P4030	1	4.72 ± 0.98	
4P4030	4	17.33 ± 2.77	3.7*

*p<0.05, n = 3, donor: ♀, 55-year-old

1P2525, 1P3030 and 1P4030 were not yet saturated with TBF and higher permeation fluxes were obtained by increasing TBF amount (see Table 4.4). The enhancement factors from P4030 and P2525 were almost similar, although the latter referred to a drug content increase from 1 to 2%. This could be assigned to a difference in drug release from the vehicle depending on the composition. The dependency of POX 407 concentration and drug release has already been reported by Gilbert et al. [139] where the increase in POX concentration was followed by a decrease in the apparent diffusion coefficient (D_{app}) of the examined solutes benzoic acid and p-hydroxybenzoic acid. This was also the case for piroxicam, where its release was dependent on the POX 407 concentration in the examined gels. The permeation rate of piroxicam across synthetic cellulose membranes and rat skin decreased as the concentration of POX

increased [140]. It has been hypothesized that the growth of the micelle size due to the increase in POX content could reduce the water channels of the gel matrix and thus simultaneously increases the tortuosity. A higher tortuosity would be followed by a decrease of D_{app} from a gel with a high POX concentration [141]. Nevertheless, the drug release from a POX gel was also determined by the gel dissolution upon contact with water [142].

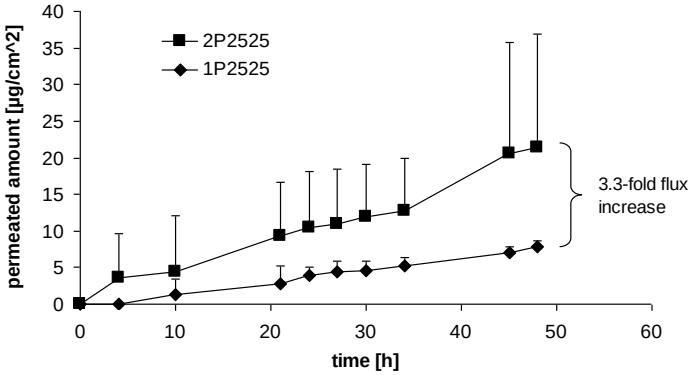

Fig. 4.18 Permeation of 1% and 2% TBF from P2525 across SC (n = 3); donor: ♀, 55-year-old

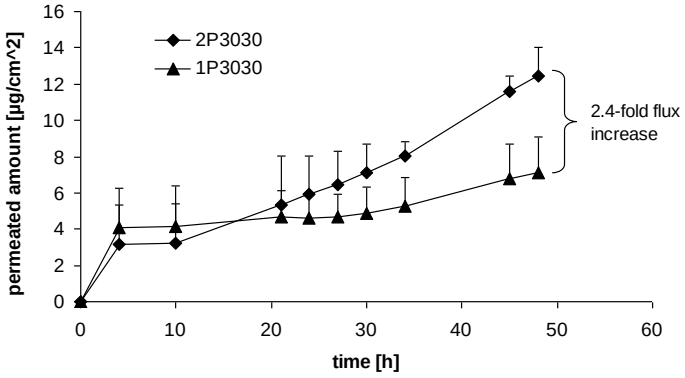

Fig. 4.19 Permeation of 1% and 2% TBF from P3030 across SC (n = 3); donor: ♀, 55-year-old

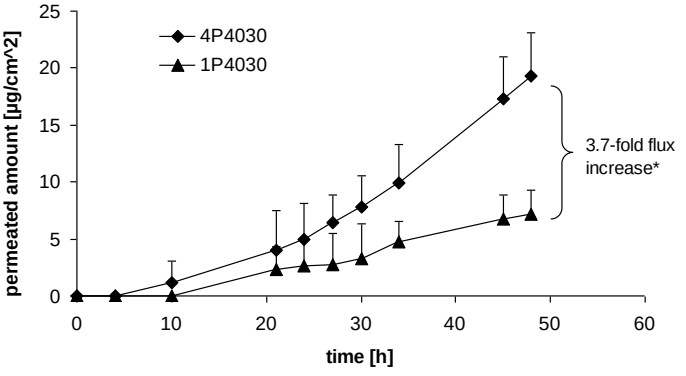

Fig. 4.20 Permeation of 1% and 4% TBF from P4030 across SC (n = 3); donor: ♀, 55-year-old; *significant difference (p<0.05)

In comparison to the flux value achieved by 5-ALA [5] which was incorporated into P2525 at an amount of 10% (w/w), the increase in TBF fluxes in the present study were not pronounced. Compared to Basiscreme DAC, the permeation enhancement across skin from P2525 was 7.5-fold for 5-ALA and 1.4-fold for TBF only (with 1% incorporated drug). TBF possibly resided inside the micelles, meanwhile the hydrophilic 5-ALA filled the aqueous channels between the micelles. The latter is the region from which the solute is directly available for release from a POX system [139]. When TBF is located inside the micelles, this could enlarge micelle size as well. As a consequence, drug diffusion should also decrease due to similar reasons as explained above.

The lag time exhibited by 1P2525 was not significantly different from other non-POX formulations suggesting that all formulations needed about the same time to penetrate and permeate across the SC. Furthermore, this implies that lag times were quite independent of the formulation ingredients, at least from 1P2525.

4.5 Permeation across hooves

Besides human skin, nail is also the site where dermatophytosis commonly occurs. Onychomycosis accounts for about 50% of all the nail disorders [143]. Since human nails were not available for this study, bovine hooves (100 µm thickness) were employed as a human nail model. Lamisil® DermGel was included in this study, instead of Lamisil® Creme, due to its hydrophilic characteristic which should be an advantage for the ungual permeation.

Steady state conditions could be achieved for TBF permeation across hooves as shown in Fig. 4.21. Different from TBF permeations across SC, those across hooves did not show any pronounced lag time, hinting at a spontaneous penetration of TBF into hooves with subsequent permeation. A lag time could only be calculated from extrapolation of the flux of the steady state part of the permeation curve.

1P2525 and POX hydrogel 20% with 1% TBF showed superior flux values over other non-POX formulations as seen in Fig. 4.22. Basiscreme DAC showed yet a flux twice as high as that of Lamisil® DermGel. The ranking of the lag times was slightly different from the fluxes being POX hydrogel<1P2525<Lamisil® DermGel<Basiscreme DAC (see Fig. 4.23). Nevertheless, all the formulations did not show any significant differences (p>0.05) in lag times compared to Lamisil® DermGel.

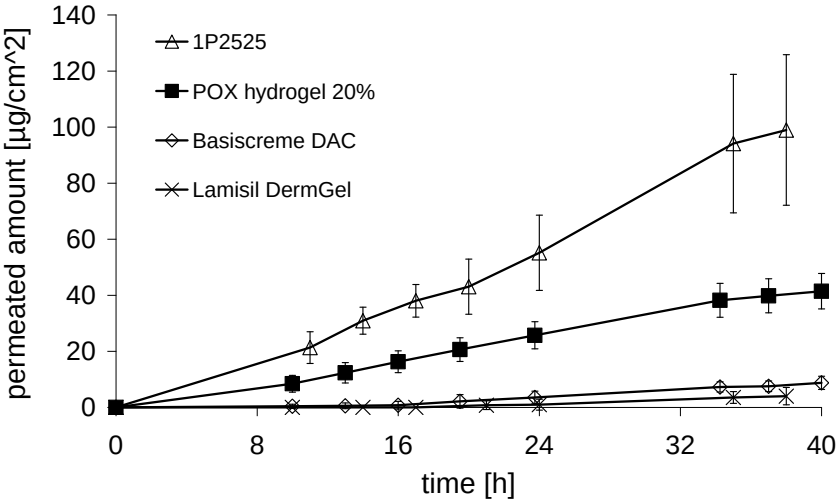

Fig. 4.21 Permeation of TBF across hooves (n = 3-5), TBF amount permeated was calculated as base since Lamisil® DermGel contains TBF base

1P2525 flux was about 2.5-fold higher than that from POX hydrogel hinting at a synergistic effect of the ingredients. 1P2525 flux was even 18-fold higher than that from Lamisil® DermGel and 10-fold from Basiscreme DAC. It is interesting to note that both enhancers (IPA and DMIS) in 1P2525 have not been acknowledged as ungual penetration enhancers yet although their penetration enhancement action in this study was evident.

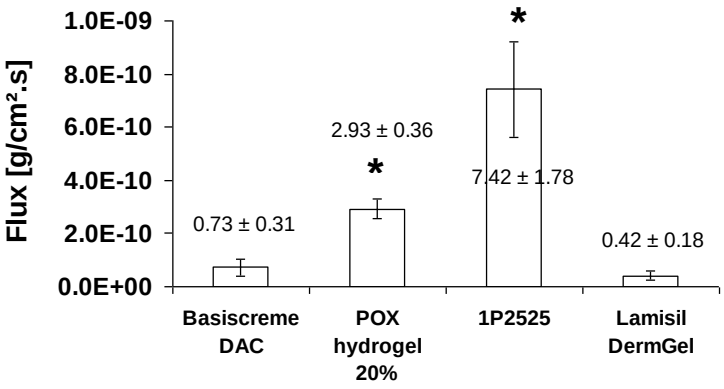

Fig. 4.22 Fluxes of TBF base (mean ± SD) across hooves (n = 3-5); *significant compared to Lamisil® DermGel (p<0.05)

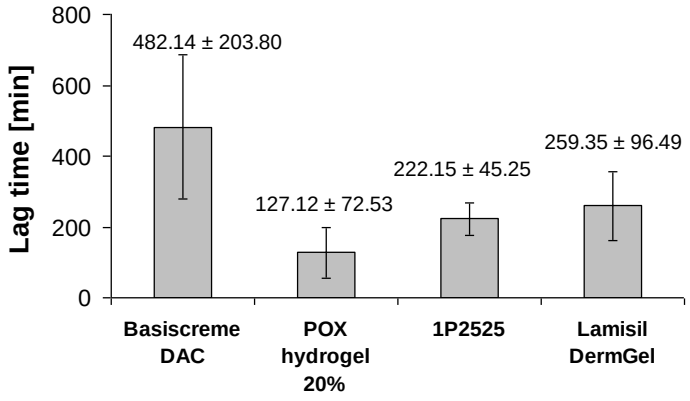

Fig. 4.23 Lag times of TBF base (mean ± SD) across hooves (n = 3-5)

Since water acts as a nail plasticizer and ungual penetration enhancer, POX hydrogel with almost 80% water content (the highest amongst all) was expected to give the highest flux. This is however not the case. The role of water in enhancing ungual penetration has been reported with ketoconazole as permeant from the work of Gunt and Kasting [144]. Ciclopirox permeated also faster through nails from a Carbomer® gel formulation than from a non-aqueous nail lacquer [145].

TBF fluxes across hooves were generally around 10-fold higher compared to those across skin (magnitude 10^{-10} vs. 10^{-11}). The lipophilic SC controlled TBF permeation more strictly than hooves did. This was even more evident since SC (~10 µm, dry) is actually much thinner than hoof (100 µm). However, in the real practice, TBF will have to permeate further along a higher distance to reach an infected nail bed. As a note, similar to the permeation across SC, TBF in 1P2525 possessed still a lower thermodynamic activity compared to other comparative standards. TBF fluxes from 1P2525 were yet still higher over the comparisons.

4.6 TBF amount retained in SC and hooves

The validation of TBF extraction process from SC and hooves resulted in recovery values of 75% and 100%, respectively. SC binds TBF stronger than hooves do; as was mirrored from the recovery results. Extending the extraction time or extraction frequency did not improve the recovery result significantly.

TBF amount extracted from both membranes after terminating the permeation experiments with different formulations was adjusted according to the recovery validation. As can be seen from Table 4.5, the ranking of the amount retained in SC is

1P2525>Basiscreme DAC>Lamisil® Creme although the difference between 1P2525 and Basiscreme DAC was not significant. A different ranking was observed in hooves: POX hydrogel>1P2525>Basiscreme DAC>Lamisil® DermGel. In this case the difference between Basiscreme DAC and Lamisil® DermGel was not significant either.

Table 4.5 The amount of TBF retained [µg/cm^2] in SC and hooves (mean ± SD)

Formulation	Stratum corneum	Hooves
Basiscreme DAC	15.60 ± 2.33**	7.81 ± 0.34
POX hydrogel	n.d.	94.78 ± 12.60**
1P2525	19.83 ± 3.18**	23.07 ± 1.66**
Lamisil® Creme/ DermGel	8.93 ± 2.11	7.16 ± 1.18

**significant compared to Lamisil® (p<0.01), n = 3-6; n.d. = not determined; skin donor: ♀, 38-year-old

In terms of 1P2525 showing the highest TBF amount retained in SC amongst all, the ranking of the TBF retained corresponded nicely with that of the fluxes. This finding indicated a higher and faster drug partition rate from the vehicle of 1P2525 into the SC.

In contrast to the permeation through skin, the water content apparently plays an important role in determining the amount of TBF retained in hooves. The high water content of POX hydrogel (~80%) compared to 1P2525 (~50%) provoked an about 4-fold TBF amount retained in hooves. Water improves hooves hydration and this provides more sites for TBF binding within the keratin molecules. Basiscreme DAC with an even lower water content of 40% also exhibited a TBF amount retained far below that of POX-based formulations although a water content difference by 10% compared to 1P2525 was not likely to account for one third TBF amount retained in hooves. TBF amounts retained from Basiscreme DAC and Lamisil® DermGel were quite similar, hinting at a better partition of TBF into hooves from the POX-based formulations.

4.7 DSC study [100]

DSC enables the visualization of the microstructural changes within SC upon contact with formulation. From Fig. 4.24, it can be seen that every formulation had its own style in affecting the lipid mobility of the SC. 1P2525 showed the weakest transitions, corresponding to the lowest transition enthalpies, i.e., T2 and T3 only, while Lamisil® Creme exhibited three transitions (T2-T4) and Basiscreme DAC exhibited an additional endothermic transition at about 45 °C belonging to residues of Basiscreme

itself on the SC. The transitions were reproducible for every tested formulation with standard deviations of maximum 1.1 °C from triple measurements. The resume from all transitions shifts can be seen in Fig. 4.25. Albeit close to the standard deviation, the ranking for T2 shifts were 1P2525>Basiscreme DAC>Lamisil® Creme. T3 shifts were about the same for 1P2525 and Basiscreme DAC, being slightly greater than Lamisil® Creme's T3 shift. However, T2 and T3 from all examined formulations were not significantly different from each other (p>0.05).

Barry [28] mentioned up to four endothermic transitions T1-T4 observed by means of DSC, when SC is heated up to 120 °C. While T1 (~40 °C) and T4 (~100 °C) are unfortunately not always visible, the presence of T2 (~70 °C) and T3 (~85 °C) are more reliable. T1 and T4 were found to be strongly dependent on the skin source and its water content during measurement [28]. Interaction of SC with a penetration enhancer is responsible for loosening its tight microstructure, thus the lipid mobility increases. This increase aids drug penetration and yields higher flux. The endothermal transition shifts, measured by means of DSC, due to the increase in lipid fluidity were also demonstrated by Glombitza and Müller-Goymann using an *in vitro* model of the skin lipid matrix [146].

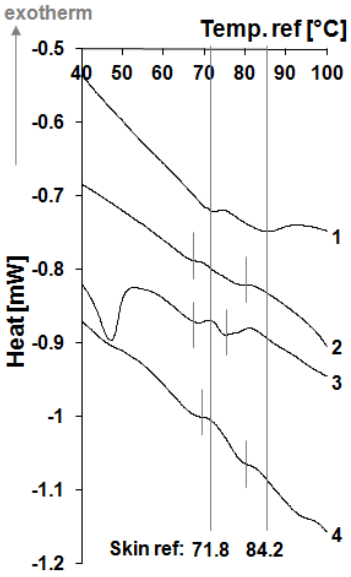

Fig. 4.24 Skin thermograms of skin reference/ hydrated to water content of 20% (1); treated with: 1P2525 (2), Basiscreme DAC containing 1% TBF (3), Lamisil® Creme (4) [100]

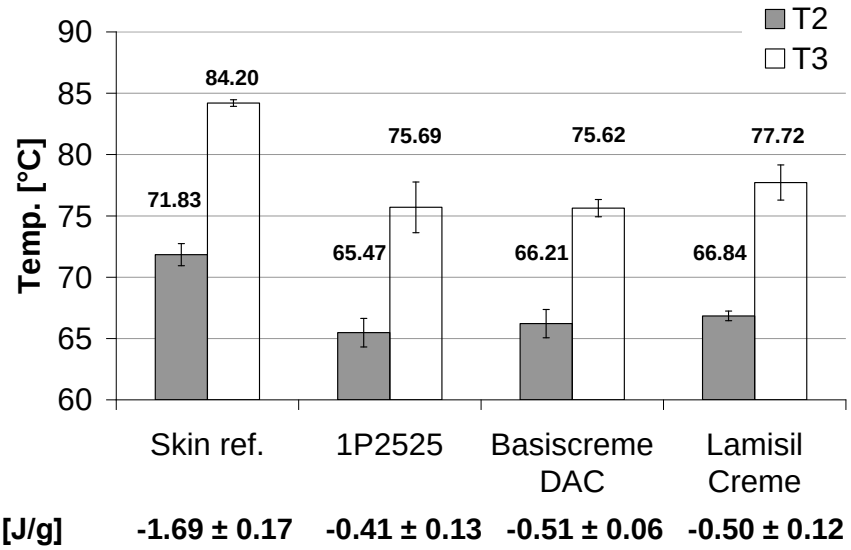

Fig. 4.25 Resume of endothermic transitions T2 and T3 as well as enthalpies ΔH (sum of T2 and T3) from SC (mean ± SD); donor: ♀, 38-year-old [100]

1P2525 produced the highest endothermic transition shifts (T2 -6.3 °C; T3 -8.5 °C) and the lowest enthalpy of the SC lipid matrix compared to other formulations. Although the difference was not statistically significant, the least negative enthalpy produced by 1P2525 indicated a relative stronger influence of the vehicle to the SC towards an increase in lipid fluidity. This influence was comparable for Basiscreme DAC and Lamisil® Creme. An additional endothermic peak given by Basiscreme DAC at 45 °C resulted from one of the vehicle components since T1 happens earlier at about 37 °C [29] whereas three endothermic peaks exhibited by Lamisil® Creme were consecutive peaks of T2-T4. Comparing both, Basiscreme DAC is likely to be relatively more effective in disrupting the SC lipid than the commercial formulation, although their TBF permeation fluxes were in the same order of magnitude. According to the DSC result, the interaction between the POX-based vehicle and SC matrix was not powerful enough in explaining the higher permeation rate of TBF. Thus the nature and the structure of the thermogelling formulation was suggested to play a more important role in enhancing TBF permeation rate despite TBF's lower thermodynamic activity in the vehicle.

Referring to the previous work of Grüning and Müller-Goymann [5], DSC measurement following SC treatment with P2525 containing 5-ALA, the decrease in endothermic shifts of T2 and T3 was greater than that for treatment with Basiscreme DAC (i.e. T2/4.6 °C, T3/4.3 °C for P2525 vs. T2/2.0 °C, T3/0.2 °C for Basiscreme

DAC). The incorporation of a lipophilic drug such as TBF into the thermogelling vehicle apparently modifies the vehicle ability in interacting with the skin lipid matrix. Thermodynamic activity of 5-ALA in this vehicle has not been determined due to its high aqueous solubility but it was evident that the vehicle interaction with skin lipid matrix played an important role for 5-ALA's remarkable penetration enhancement.

4.8 TBF permeation from formulations with different compositions across SC

The composition of the thermogelling formulation was varied to examine the influence of the ingredients on TBF permeation rate across SC. In order to investigate this systematically, two 'components' of the pseudoternary phase diagram were kept constant at the ratio 1:1. Thus, it was expected that the influence of the third 'component' on TBF permeation rate would be more visible while diminishing the interference from the other 'components'. An overview of the position of the selected formulations for this purpose is displayed in the pseudoternary phase diagram of Fig. 3.4.

4.8.1 Characteristics of the chosen formulations for the permeation study

The characteristics of the chosen formulations with different compositions for the permeation study can be seen in Table 4.6. In the first group, where the ratio of POX/MCT to water was kept constant at 1:1, from 1P3040 to 1P4412, the content of POX/MCT and water increased meanwhile IPA/DMIS decreased. Complex viscosity increased upon increasing the amount of POX and water; consistencies changed from liquid (1P3040) to semisolid (1P4412). With regard to 1P3040, networking of POX micelles was likely to be insufficient for gelation, i.e., a semisolid consistency. This may be due to the low amount of POX and water (30% each) and the rather high IPA/DMIS content of 40%. The white to off-white appearance of both liquid and semisolid formulations of this group was typical for dispersions, i.e., emulsion type systems.

Table 4.6 Properties of the examined formulations for the permeation study

Formulation	Appearance[1]	Ringing (20 °C)	Complex viscosity [Pa·s][2]	Changes in composition (downwards)
POX/MCT: water (1:1)				
1P3040	Liquid, heterogeneous, off-white	-	968 ± 30	POX/MCT ↑
1P3333	Liquid, highly viscous, off-white	-	5778 ± 103	IPA/DMIS ↓
1P3824	Semisolid, creamy, white	+	8953 ± 306	Water ↑
1P4412	Semisolid, creamy, white	+	12523 ± 530	
IPA/DMIS : water (1:1)				
1P2836	Liquid, heterogeneous, off-white[3]	-	2595 ± 97	POX/MCT ↑
1P3333	Liquid, highly viscous, off-white	-	5778 ± 103	IPA/DMIS ↓
1P4030	Semisolid, gel-like, hazy	+	8078 ± 242	Water ↓
1P5025	Semisolid, gel-like, hazy	-	7830 ± 164	
POX/MCT: IPA/DMIS (1:1)				
1P2525	Liquid, highly viscous, white[4]	-	5183 ± 85	POX/MCT ↑
1P3030	Liquid, highly viscous, off-white[4]	-	5852 ± 146	IPA/DMIS ↑
1P3333	Liquid, highly viscous, off-white	-	5778 ± 103	Water ↓
1P4040	Liquid, fairly viscous, off-white	-	255 ± 22	
POX hydrogel20% containing 1% TBF	Semisolid, gel-like, clear	-	1878 ± 43	

[1] 24 hours after manufacture at 20 °C

[2] n = 3 (32 °C); 1P3333 is the intersection of the three examined lines

[3] after stirring and elevation of the temperature to 32 °C (during the permeation study), 1P2836 remained homogeneous

[4] semisolid at 32 °C

In the second group where the ratio of IPA/DMIS to water was kept constant at 1:1, from 1P2836 to 1P5025, POX/MCT content increased meanwhile IPA/DMIS and water contents decreased. Appearances of the formulations changed from an off-white liquid to gel-like formulations. The complex viscosity increased gradually from 1P2836 to 1P5025. Formulations with gel-like appearance were only found in this group.

In the third group where the ratio of POX/MCT to IPA/DMIS was kept constant at 1:1, from 1P2525 to 1P4040, the amount of POX/MCT and IPA/DMIS increased meanwhile the amount of water decreased. A low content of water in 1P4040 led to a sudden drop in complex viscosity and the formation of a liquid system. This occurred likely due to an insufficient amount of water (20%) for POX hydration in the presence of high IPA/DMIS content of 40% and thus no gelation occurred as in the case of 1P3040 in the first group. It should be emphasized that 1P2525 and 1P3030 were semisolid at 32 °C during the permeation study.

POX hydrogel 20% containing 1% TBF was included in this study to observe the behavior of a simple mixture of POX and water only, in terms of TBF permeation rate. TBF was completely dissolved in POX hydrogel 20% as was obvious from its macroscopically clear and isotropic appearance under the polarizing microscope. POX hydrogel 20% complex viscosity was considered low when compared to 1P2525 viscosity; both formulations contained the same POX amount of 20%. This implicitly showed that the additional ingredients in 1P2525 built a different structure with a higher complex viscosity value (5183 vs. 1878 Pa.s).

POX acts as a nonionic surfactant, being able to form and stabilize emulsions [147]. POX content in almost all formulations was sufficient to stabilize both the oily and the aqueous phases so that no phase separations had been observed, except for 1P3040 which was still heterogeneous even after re-stirring and at elevated temperature of 32 °C. A high water content in the formulation allowed sufficient POX swelling so that formulations with highly dispersed oily phases and thus creamy appearance were obtained. A POX content ≥40% together with sufficient IPA/DMIS in the formulation could solubilize the whole oil phase (MCT); the system turned clear and produced a gel-like appearance (1P4030, 1P5025). IPA/DMIS contents of 40% or higher led to the formation of liquid systems, despite an elevated POX content. The complex viscosities were below 1000 Pa·s as in the case of 1P3040 and 1P4040.

From all formulations prepared for the permeation study, only three compositions exhibited ringing effects. Those were 1P3824, 1P4412 and 1P4030. Their ringing characteristics were still in line with the previous section for the bases without TBF because the formulations selected for the present permeation studies originated partly from the area of the ringing formulations. Again, it is noticeable that these ringing formulations possessed relatively high complex viscosity compared to other non-ringing formulations.

4.8.2 Permeation across SC from the series with POX/MCT : water (1:1)

Increase in POX/MCT and decrease in IPA/DMIS from 1P3040 to 1P4412 in this group, exhibiting an increase in complex viscosities, led to a decrease in fluxes (Fig. 4.26) and lag times (Table 4.7). All the formulations reached steady state after 20 h with distinct lag times except for Lamisil® Creme as depicted in Fig. 4.26. The highest flux exhibited by 1P3040 apparently originated from its low viscosity due to its high IPA/DMIS content. The second highest flux from 1P3824 was not significantly different

compared to 1P3333 or 1P4412. All fluxes from this group were higher than those from Lamisil® Creme. The change in consistency from liquid (1P3040) to semisolid (1P4412) was in agreement with an expected TBF lower release rate. POX hydrogel containing 1% TBF with only a slightly higher complex viscosity than that of 1P3040 gave about a similar flux value.

4.8.3 Permeation across SC from the series with IPA/DMIS : water (1:1)

Again within this group, a steady state could be obtained from each formulation as shown in Fig. 4.27. 1P2836 exhibited the highest TBF permeation rate and the shortest lag time within this group. In contrast to the first group, an increase in POX/MCT content was followed by a pronounced increase in lag time (Table 4.7). The change in consistency from liquid (1P2836) to a highly viscous gel (1P5025) seemed to hamper TBF permeation; this could be due to the high complex viscosity produced by this gel-like system. However, although being not significantly different, all fluxes from thermogelling formulations were higher than those from Lamisil® Creme except for 1P5025 which was significantly lower than that of Lamisil® Creme. A high standard deviation from 1P2836 obscured TBF high flux over other systems. Again, POX hydrogel containing 1% TBF with only a slightly lower complex viscosity compared to 1P2836 showed about a similar flux.

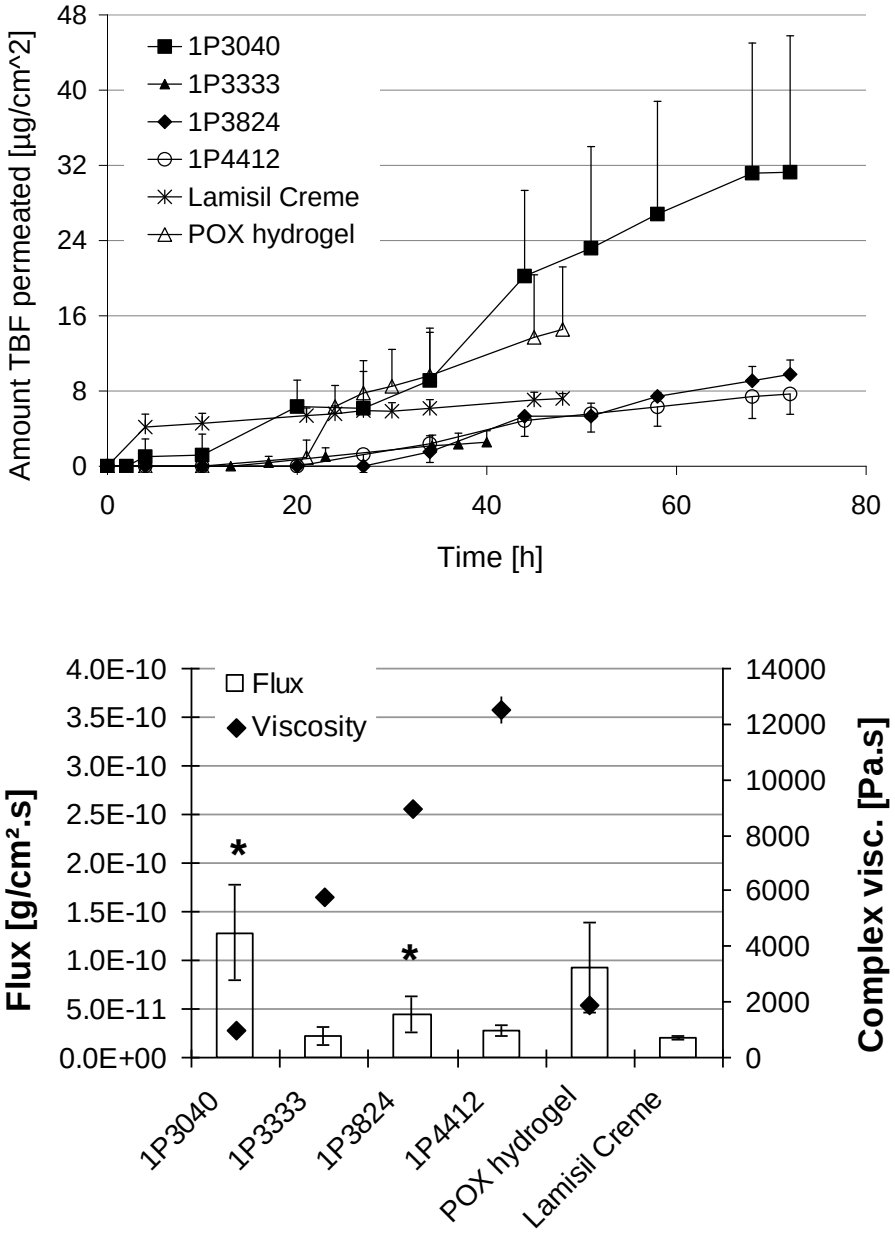

Fig. 4.26 Permeation profiles, fluxes and complex viscosities of formulations (mean ± SD) from the series of POX/MCT : water (1:1) across SC; n = 3-5; *p<0.05, compared to Lamisil® Creme; donor: ♀, 55-year-old

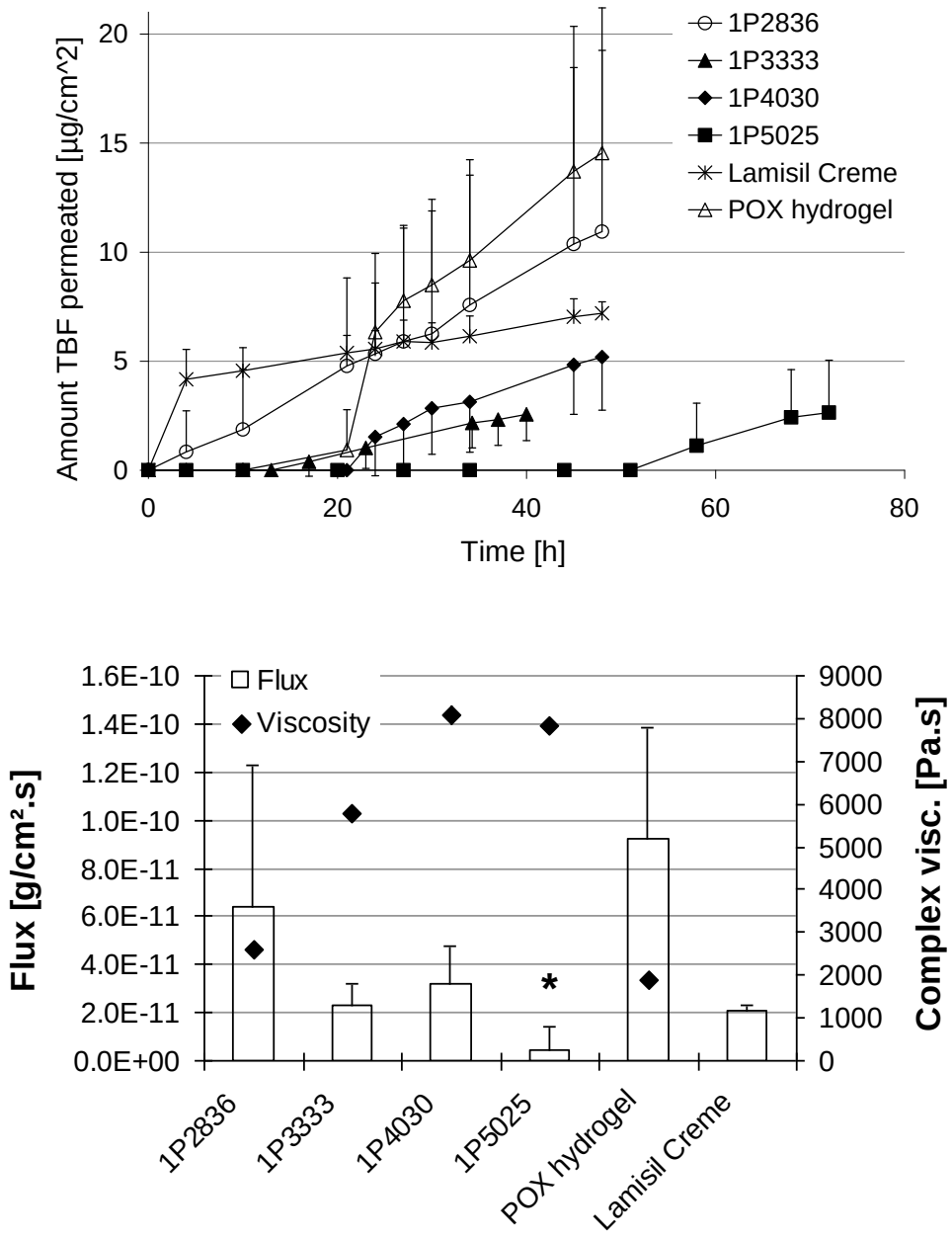

Fig. 4.27 Permeation profiles, fluxes and complex viscosities of formulations (mean ± SD) from the series of IPA/DMIS : water (1:1) across SC; n = 3-6; *p<0.05, compared to Lamisil® Creme; donor: ♀, 55-year-old

4.8.4 Permeation across SC from the series with POX/MCT : IPA/DMIS (1:1)

Steady states were also achieved by the third group and almost all formulations showed a direct release since the beginning of the permeation (see the permeation profiles in Fig. 4.28). Upon increasing POX/MCT the complex viscosities of the formulations increased slightly in the beginning and then suddenly dropped at 1P4040. Fluxes were in line with the reciprocal viscosities while decreasing first and then

increasing suddenly at 1P4040. Water amount was not sufficient for establishing the networking of POX micelles in 1P4040 so that the complex viscosity dropped. It has been well known from the previous groups that decreases in viscosities were followed by increases in fluxes. This was also the case for this third group. Again, almost all fluxes were greater than Lamisil® Creme's value except for 1P3333 which was approximately similar.

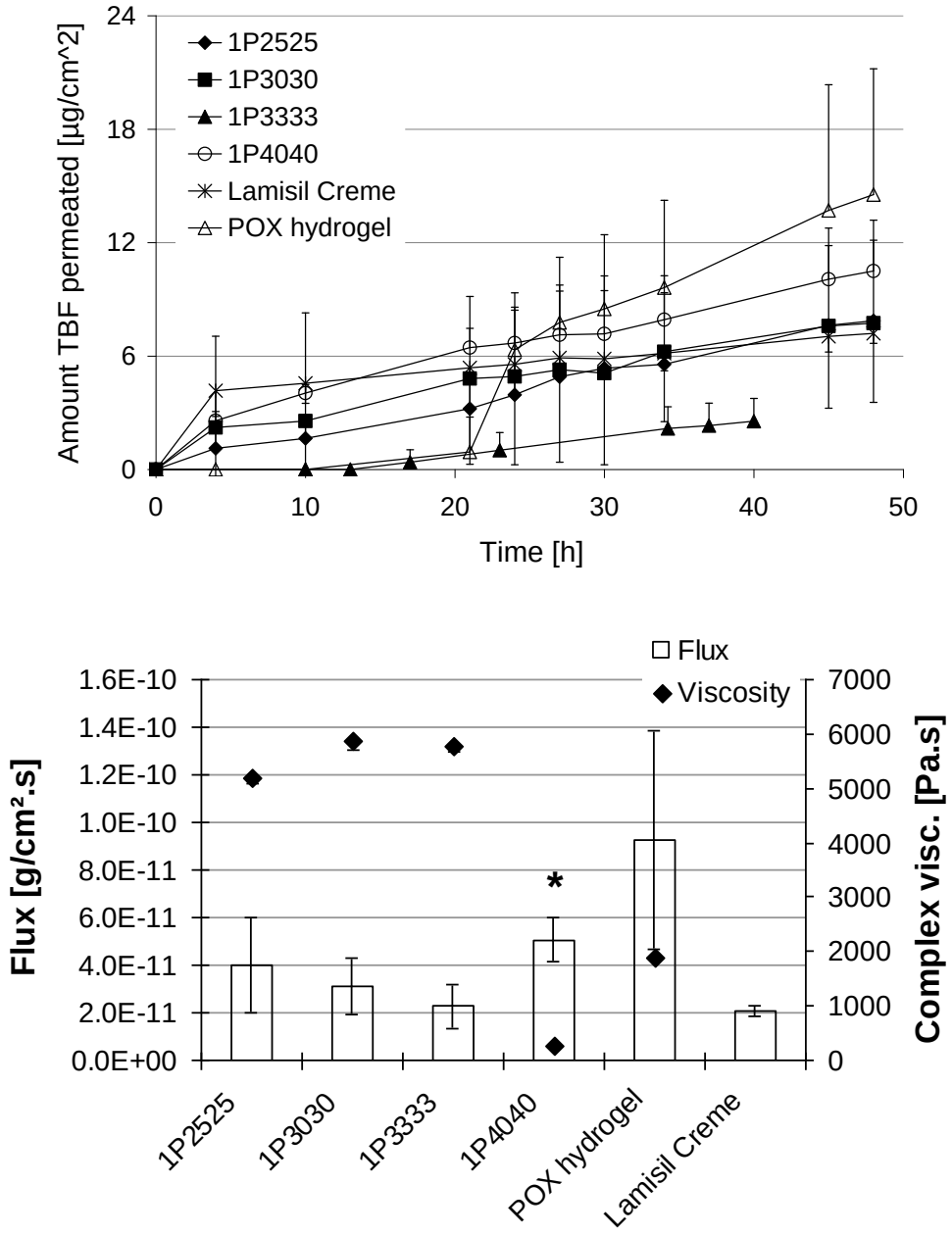

Fig. 4.28 Permeation profiles, fluxes and complex viscosities of formulations (mean ± SD) from the series of POX/MCT : IPA/DMIS (1:1) across SC; n = 3-5; *p<0.05, compared to Lamisil® Creme; donor: ♀, 55-year-old

Compared to 1P2525 with the same POX content of 20%, POX hydrogel containing 1% TBF exhibited higher flux of about 2-fold. The absence of other components in POX hydrogel may indeed have increased drug partition into SC so that the permeation rate increased. On the other hand, the low viscosity of POX hydrogel, which was about 2.8-fold lower than 1P2525, could also be the driving force for the higher drug permeation. A dependency between viscosity and flux has been though observed from other groups previously. To clarify this, a relation between complex viscosities and fluxes will be elaborated in the next section.

4.8.5 Compilation of permeation across SC

POX and water were observed to be responsible for building up the viscosity of the formulation meanwhile IPA/DMIS tended to decrease it. A nice relation between fluxes and the reciprocal viscosities was shown by most formulations. Formulations with similar viscosities exhibited fluxes in the same order of magnitude, with 1P2525; 1P3030; 1P3333 or 1P3824; 1P4030 as examples. A closer look is given in Fig. 4.29. However, this rule did not apply if IPA/DMIS content was ≥40% as in the case of 1P4040, which revealed about the same flux as 1P3824 and 1P4030 although its viscosity was far apart from those of 1P3824 and 1P4030.

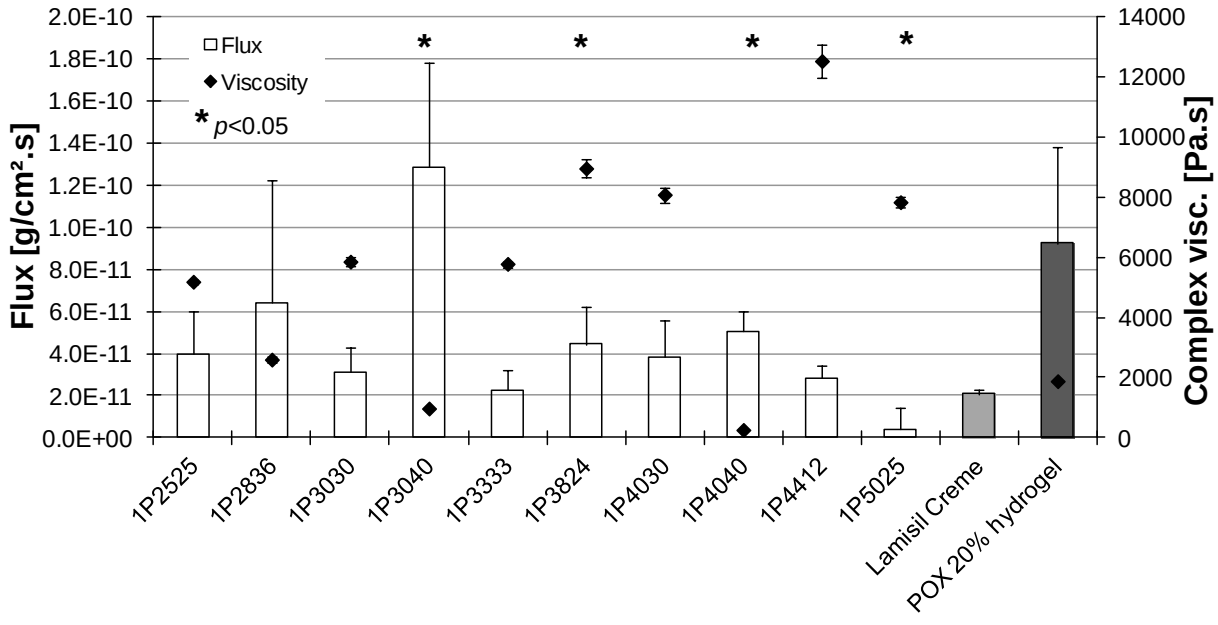

Fig. 4.29 Compilation of fluxes and complex viscosities from thermogelling formulations (mean ± SD) with different compositions across SC; n = 3-6; *p<0.05, compared to Lamisil® Creme; donor: ♀, 55-year-old

TBF fluxes from the thermogelling formulations were generally higher than Lamisil® Creme, except from 1P5025 (p<0.05). TBF flux from POX hydrogel 20% containing 1% TBF was relatively high compared to other thermogelling formulations, yet about comparable with formulations possessing low viscosities.

Lag times of TBF from this group are listed in Table 4.7. Lag times tended to decrease as the water content in the formulations increased. There is apparently no direct relation between POX/MCT or IPA/DMIS contents with changes in lag times. How water affects the lag time can for example be observed in the first group, i.e., while water increased from 1P3040 to 1P4412, the lag times decreased. This was also the case for other groups, with 1P4040 as exception.

Table 4.7 Resume of permeation data (mean ± SD) of thermogelling formulations with different compositions across SC and the amount of TBF retained in SC after 48 h of permeation; n = 3-6; *p<0.05 compared to Lamisil® Creme

Formulation	Flux [x10^{-11} g/cm²·s]	Lag time [min]	TBF amount retained[1] [µg/cm^2]
POX/MCT: water (1:1)			
1P3040	12.86 ± 4.95*	867	17.09 ± 2.76
1P3333	2.28 ± 0.92	572	20.31 ± 7.26
1P3824	4.44 ± 1.78*	483	8.93 ± 1.59
1P4412	2.83 ± 0.58	193	6.21 ± 0.57
IPA/DMIS : water (1:1)			
1P2836	6.43 ± 5.82	351	16.85 ± 4.72
1P3333	2.28 ± 0.92	572	20.31 ± 7.26
1P4030	3.83 ± 1.76	511	14.08 ± 4.61
1P5025	0.42 ± 1.02*	1347	6.69 ± 1.85
POX/MCT: IPA/DMIS (1:1)			
1P2525	4.00 ± 2.02	12	15.07 ± 3.31
1P3030	3.11 ± 1.17	285	9.48 ± 2.73
1P3333	2.28 ± 0.92	572	20.31 ± 7.26
1P4040	5.06 ± 0.92*	0	15.98 ± 6.72
Lamisil® Creme	2.08 ± 0.22	0	10.75 ± 3.63
POX hydrogel 20%	9.25 ± 4.57	225	32.92 ± 3.33*

[1] data was corrected according to the recovery of the extraction procedure (75%); 1P3333 is highlighted as the intersection point from all groups

There was, however, no unlimited permeation enhancement from the three examined lines. Nevertheless, a local maximum flux from each group was evident and this was

strongly dependent on the composition of the formulation. The permeation data in the previous section signalized a dependency between TBF fluxes and the reciprocal complex viscosities. Therefore, both parameters were plotted in Fig. 4.30.

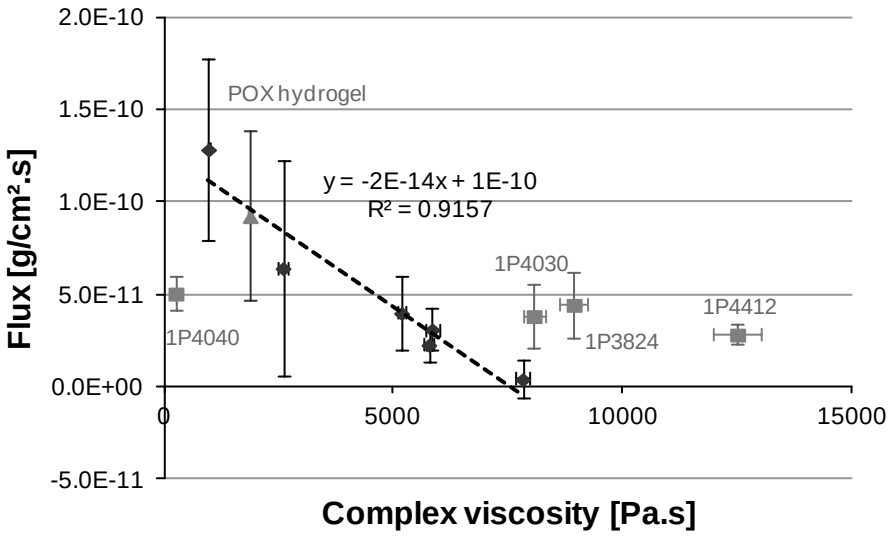

Fig. 4.30 Relation of fluxes - complex viscosities from thermogelling formulations with different compositions across SC

Plotting all data in one graph, a fairly linear relation between fluxes and complex viscosities could be drawn within the viscosity range from 1000 to 8000 Pa·s only. Outside this range, fluxes seemed to be independent of the complex viscosities with a tendency to a higher flux value when POX was about or exceeded 40%, as shown by 1P4030, 1P3824 and 1P4412. In contrast, the flux shown by 1P4040 was apparently lower than expected. POX hydrogel containing 1% TBF followed this linear relation.

Within the viscosity range from 1000-8000 Pa·s, the permeation rate was inversely dependent on the complex viscosity of the formulation. It might be hypothesized that the release seemed to control the permeation because the lower the viscosity was, the higher the release rate from the formulation would be. Outside 1000-8000 Pa·s, other factors played an additional role so that TBF permeation did not follow the linear relation with the reciprocal viscosities anymore. At lower viscosity, i.e., less than 1000 Pa·s, the high content of IPA/DMIS made POX swell insufficiently so that the gel matrix was not built at all. When the complex viscosity exceeded 8000 Pa·s, a highly ordered structure could have been built thus the matrix might have turned more complex or the tortuosity of the matrix could simply have increased.

Three formulations with noticeable high viscosities -1P4030, 1P3824 and 1P4412- were particularly interesting since their fluxes were higher than those from other formulations with lower viscosities. It is a coincidence that these three formulations also featured a ringing effect. The existence of the ringing effect could be an indication for the presence of a cubic structure and this could also be the reason why their fluxes were higher as their expected values.

The application of lyotropic liquid crystal phases (LLC) as drug vehicle for transdermal delivery has been reported before and the permeation enhancement was rather specific for a particular drug. As example, the hexagonal phase has been reported to increase the permeation rate of diclofenac sodium and paracetamol whereas propanolol permeated better from the lamellar phase [85]. Last but not least, in order to draw a relation between the high fluxes from the three formulations mentioned above with the possible existence of the LLC, a further elucidation of the LLC structure is needed.

4.8.6 TBF amount retained in SC

The amount of TBF retained in SC was determined after terminating the permeation and the overview from all formulations can be seen in Fig. 4.31. All data presented have been corrected by the recovery of the extraction process. The amounts of TBF retained from the thermogelling formulations were about comparable and mostly higher yet not significantly higher than the amount retained from Lamisil® Creme. POX hydrogel 20% showed a significantly higher amount retained compared to Lamisil® Creme. Thermogelling formulations with low amount retained have been identified as those with relatively high viscosities, as shown by 1P4412 and 1P5025. Furthermore, there was no peculiarity of formulations with ringing effect with regard to their amount retained (1P3824, 1P4412 and 1P4030).

Assuming that a high drug permeation rate originates from a high drug partition rate into SC, there was, however, no correlation at all between TBF fluxes and the amounts of TBF retained in SC. On the contrary, a fairly linear reverse correlation was found between the amount of TBF retained in SC and the complex viscosity of the formulation as shown in Fig. 4.32 with r^2=0.5123. As was hypothesized for fluxes and complex viscosities, the increase in complex viscosity could reduce TBF partition into SC and thus subsequently both the penetration and permeation. However, TBF amount retained from POX hydrogel was much higher and outside the linear

correlation. A high water content or possibly the absence of other ingredients apparently increased TBF binding to SC.

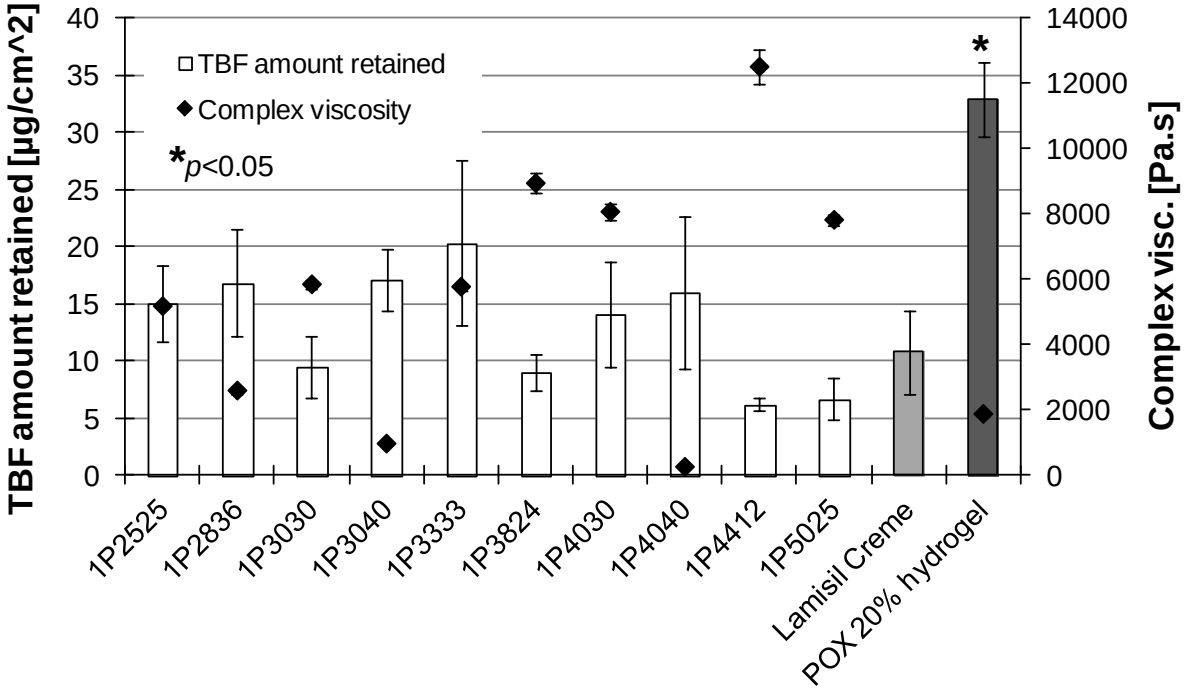

Fig. 4.31 Amount of TBF retained (mean ± SD) in SC after 48 h permeation; n = 3-6; *p<0.05, compared to Lamisil® Creme; donor: ♀, 55-year-old

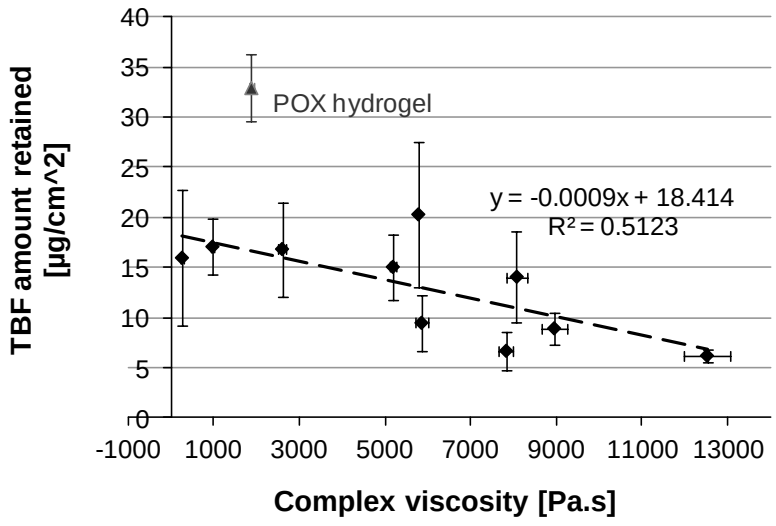

Fig. 4.32 Relation of TBF amount retained in SC and complex viscosity of the formulation

Referring to the influence of a single component or a mixture of components on the TBF amount retained, there is also no apparent correlation between composition and TBF amount retained (compare the different series where only one component or

component mixture was varied in concentration while the ratio of the other components was kept constant (Table 4.7)). The content of POX, IPA/DMIS or even water did not give a pronounced correlation with the amount retained in SC. Resuming all, TBF binding with SC seems to be a multiple process which cannot be predicted from a single component of the formulation. However, the complex viscosity – which is the product of the entire constituents – gives at least an explanation for this case.

4.9 TBF permeation from formulations with different compositions across hooves

Permeation experiments across hooves revealed fluxes with high standard deviations in some cases. This could be due to the high variability of hooves themselves or due to an irregular drug release from the formulation. For data analysis, mean and median of fluxes from each formulation were displayed together. But, medians were used instead of means for further analysis. Fluxes from Lamisil® DermGel were not included in the upcoming section since it has previously been shown that TBF permeated lesser (p<0.05) from Lamisil® DermGel than from 1P2525 (see Fig. 4.22). To assist interpretation, TBF fluxes across hooves were displayed using box plot as shown in Fig. 4.33. Therefore, all the important values (five-number summary) such as the minimum, 25th percentile (Q1), median (Q2), 75th percentile (Q3) and the maximum can be depicted all at once.

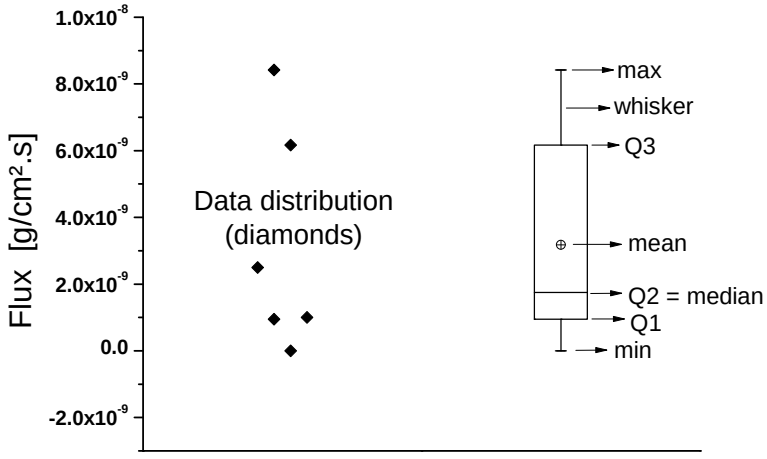

Fig. 4.33 Box plot

4.9.1 Permeation across hooves from the series with POX/MCT : water (1:1)

By increasing POX/MCT and water content in the formulation, complex viscosities of the formulations rose, as known from the previous section. Medians of the fluxes

remained constant from 1P3040 to 1P3333 and then dropped at 1P3824 and 1P4412 (Fig. 4.34). By observing the data distribution from each formulation, it can be seen that fluxes tended to decrease when POX/MCT contents increased. Among all formulations, 1P4412 exhibited the lowest mean and median. One-way ANOVA could not be used to test any difference between the means of the samples since their variances were unequal (Levene's test, p<0.05). Furthermore, as summarized in Table 4.8, Welch's test and Brown-Forsythe's test were used instead. Post-hoc test Games-Howell was applied to track the formulation which gave significantly different result. Unfortunately, for this group, Welch's test and Brown-Forsythe's test gave contradictory results: Yet, Games-Howell's test showed no differences between the fluxes. High standard deviations from 1P3040, 1P3333 and 1P3824 were responsible for this result.

Increase in complex viscosity did not result in a significant change in TBF fluxes as seen in Fig. 4.34. Interestingly to note that 1P4412 with the highest water content (44%) showed no TBF permeation at all. IPA/DMIS content decreased from 1P3040 to 1P4412 while the complex viscosity increased along with POX/MCT increase.

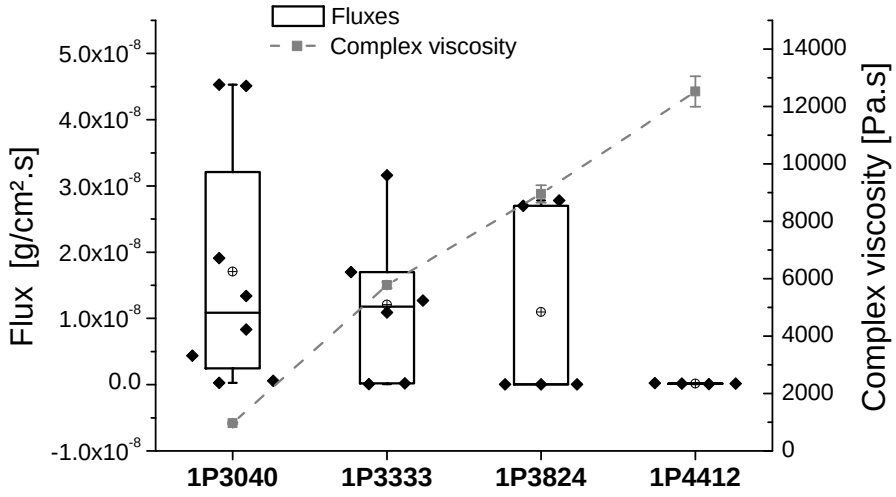

Fig. 4.34 TBF fluxes across hooves and complex viscosities of formulations with POX/MCT : water (1:1) across hooves; n = 4-8

4.9.2 Permeation across hooves from the series with IPA/DMIS : water (1:1)

As depicted in Fig. 4.35, complex viscosities increased from 1P2836 to 1P4030 and were then followed by a slight drop at 1P5025. Fluxes were about 1 x 10^{-8} g/cm^2·s for

1P2836 and 1P3333 and then steeply dropped at 1P4030 and 1P5025. 1P3333 produced the maximum fluxes although the lowest complex viscosity was shown by 1P2836. Similar to section 4.9.1, one-way ANOVA could not be carried out since variances of the samples were unequal (Levene's test, $p<0.05$). Again, Welch's test and Brown-Forsythe's test showed different conclusions as summarized in Table 4.8. Yet, the post-hoc test according to Games-Howell indicated that 1P2836 revealed significantly different fluxes from the other three formulations. According to this, the assumption of significant differences between formulations could be drawn.

Fluxes in Fig. 4.35 corresponded well with the reciprocal complex viscosities of the formulations. Especially when 1P3333 high deviation is not considered, fluxes decrease from 1P2836 to 1P4030 being reversely in accordance with the increase in complex viscosities. Medians and complex viscosities were about constant for 1P4030 and 1P5025.

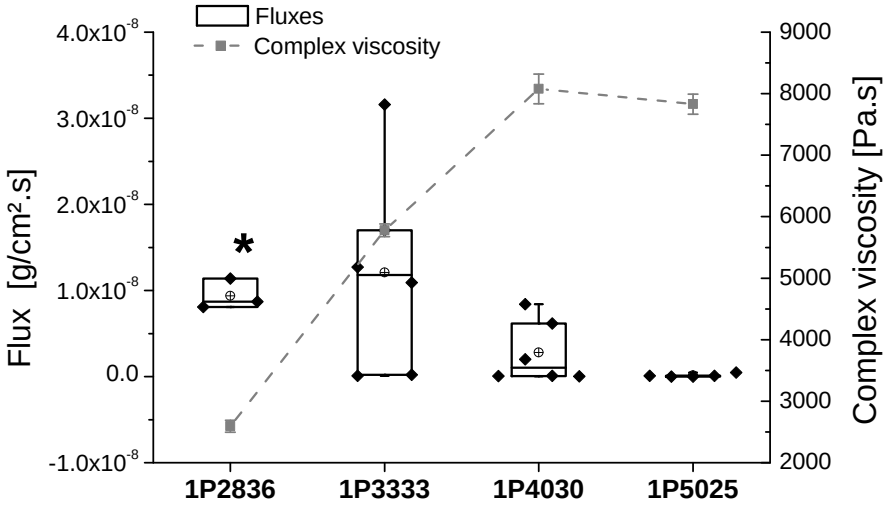

Fig. 4.35 TBF fluxes across hooves and complex viscosities of formulations with IPA/DMIS : water (1:1) across hooves; n = 3-6, *1P2836 revealed significantly different fluxes.

4.9.3 Permeation across hooves from the series with POX/MCT : IPA/DMIS (1:1)

From 1P2525 to 1P4040, fluxes were similar for the first two formulations and then increased at 1P3333 although the complex viscosities were about similar. A drop in complex viscosity of 1P4040 was followed by a slight decrease in 1P4040 flux (Fig. 4.36). From this group, there was no linear or reciprocal correlation observed between fluxes and complex viscosities, possibly obscured by 1P3333's high deviation. Again,

one-way ANOVA could not be used to test this group since sample variances were unequal (Levene's test, $p<0.05$). Since the post-hoc test according to Games-Howell revealed no differences between the formulations, fluxes within this group were considered as insignificantly different. Nevertheless, the low complex viscosity of 1P4040 was in line with its fairly high TBF flux. In addition, this flux apparently correlated with the high IPA/DMIS content, similar to the group of POX/MCT : water at 1:1.

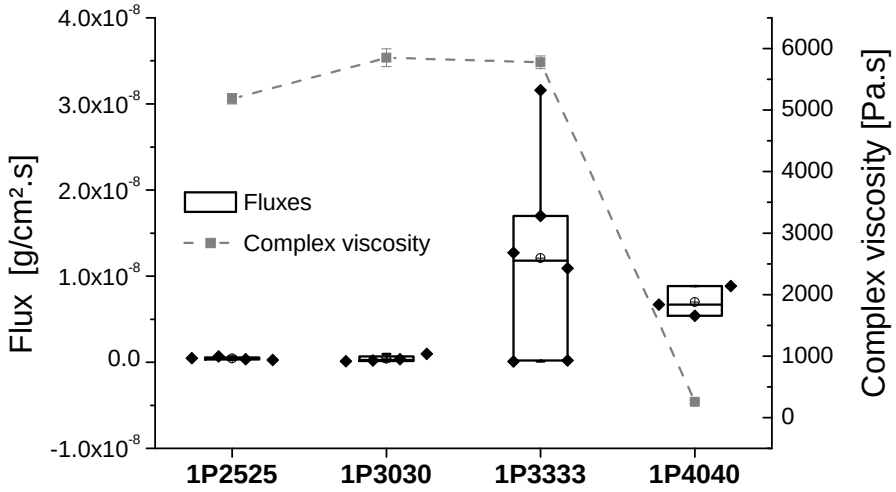

Fig. 4.36 TBF fluxes across hooves and complex viscosities of formulations with POX/MCT : IPA/DMIS (1:1) across hooves; n = 3-6

Table 4.8 Statistics of TBF fluxes across hooves

Group	Sample variances (Levene's test)	Alternative test	Post-hoc test (Games-Howell's test)
POX/MCT : water (1:1)	unequal	**W**: $F(3,8.43) = 4.44$, $p=0.038$ (different) **B-F**: $F(3,14.83) = 1.53$, $p=0.249$ (not different)	no difference
IPA/DMIS : water (1:1)	unequal	**W**: $F(3,5.61) = 24.56$, $p=0.001$ (different) **B-F**: $F(3,6.24) = 4.51$, $p=0.053$ (not different)	1P2836 was significantly different
POX/MCT : IPA/DMIS (1:1)	unequal	**W**: $F(3,5.31) = 12.81$, $p=0.007$ (different) **B-F**: $F(3,5.29) = 5.12$, $p=0.051$ (not different)	no difference

W: Welch's test, B-F: Brown-Forsythe's test

4.9.4 Compilation of permeation across hooves

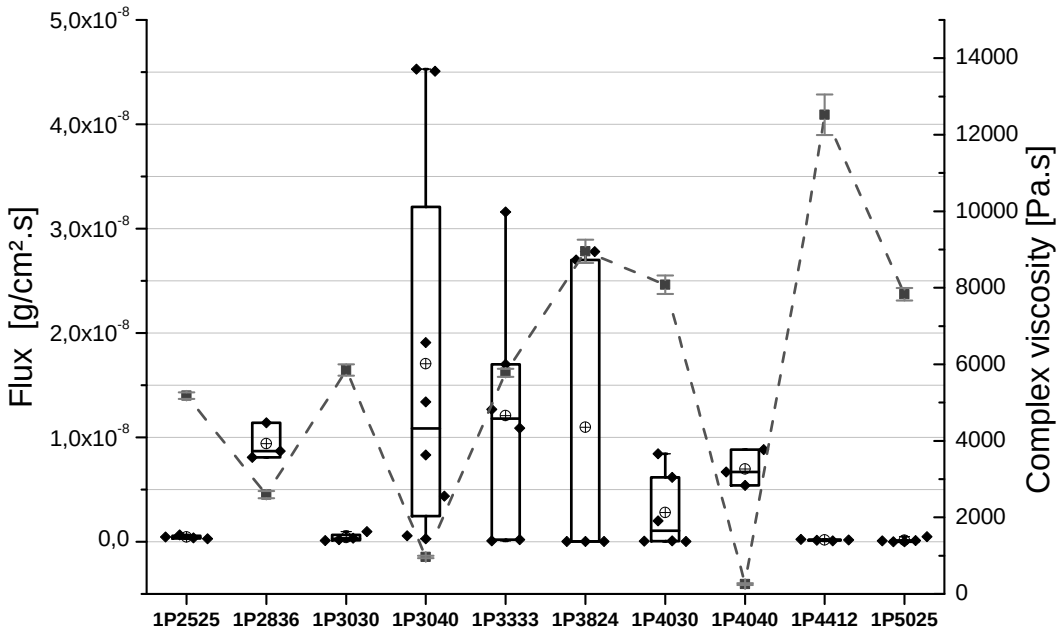

Fig. 4.37 Compilation of TBF fluxes across hooves and complex viscosities of thermogelling formulations with different compositions; n = 3-8

The reverse correlation between complex viscosities and fluxes was fairly evident if all data were displayed together as in Fig. 4.37. This relation was not obvious from each single group due to the high standard deviations from several formulations (1P3040, 1P3333 and 1P3824). Statistical analysis revealed that only 1P2836 showed significantly different fluxes among all formulations. All means and medians from each formulation are summarized in Table 4.9.

To analyze the relation between both parameters, medians and complex viscosities of the formulations are plotted in Fig. 4.38. Medians and complex viscosities of the formulations did not show a similarly good linear correlation as in the case of SC permeation. The correlation coefficient was r^2 = 0.4616 for hooves whereas that for SC was r^2 = 0.9157.

Table 4.9 Permeation data of TBF across hooves (n = 3-8): means, medians and amounts retained

Formulation	Mean $x10^{-9}$ [g/cm²·s]	Median $x10^{-9}$ [g/cm²·s]	TBF amount retained[1] [µg/cm²]
POX/MCT: water (1:1)			
1P3040	17.05 ± 18.48	10.84	22.4 ± 6.7
1P3333	12.09 ± 11.75	11.82	12.7 ± 2.9
1P3824	10.98 ±14.99	0.04	14.0 ± 1.6
1P4412	0.17 ± 0.06	0.17	10.8 ± 1.6
IPA/DMIS : water (1:1)			
1P2836	9.41 ± 1.79	8.69	14.0 ± 1.2
1P3333	12.09 ± 11.75	11.82	12.7 ± 2.9
1P4030	2.79 ± 3.64	1.05	12.3 ± 1.0
1P5025	0.14 ± 0.19	0.09	7.3 ± 0.5*
POX/MCT: IPA/DMIS (1:1)			
1P2525	0.44 ± 0.17	0.41	13.9 ± 1.4
1P3030	0.41 ± 0.39	0.28	18.6 ± 4.9
1P3333	12.09 ± 11.75	11.82	12.7 ± 2.9
1P4040	6.98 ± 1.74	6.69	11.3 ± 1.3

[1] recovery of the extraction procedure was 100%; *1P5025 revealed significantly different amount (one-way ANOVA at α=0.05, followed by Games-Howell post-hoc test); 1P3333 is the intersection of the three examined lines

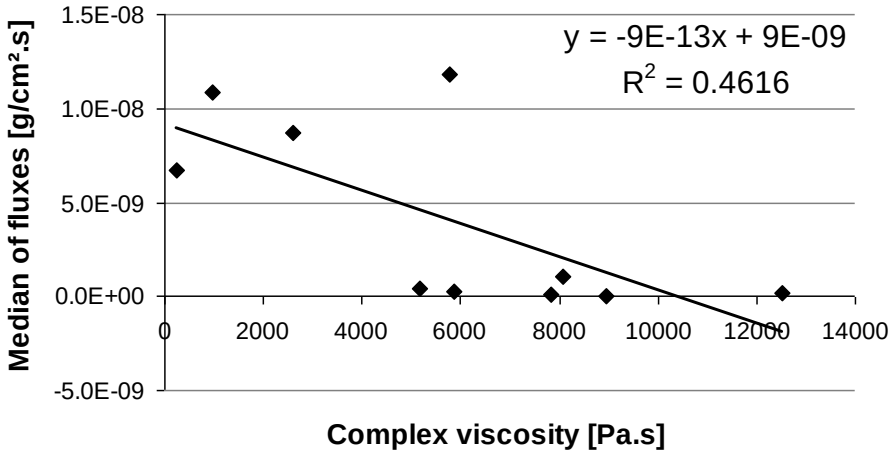

Fig. 4.38 Medians of TBF fluxes across hooves and complex viscosities of thermogelling formulations containing TBF

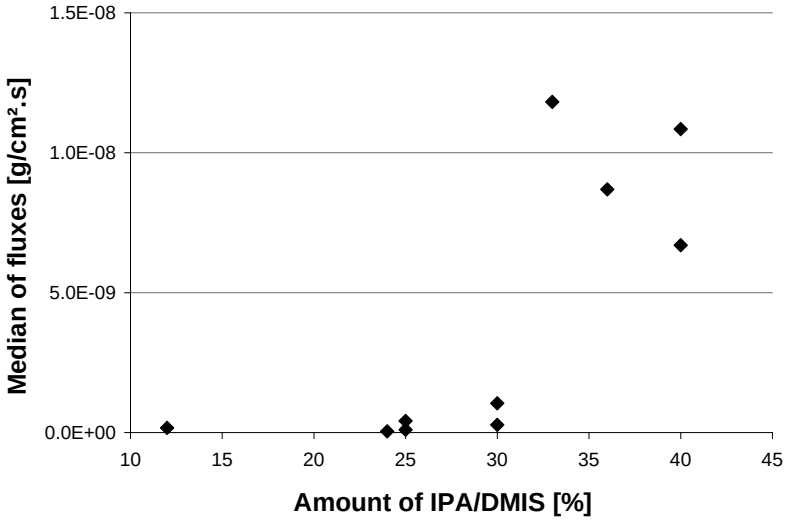

Fig. 4.39 Medians of TBF fluxes across hooves from thermogelling formulations containing TBF -in dependency of IPA/DMIS contents-

Previous permeation experiments from different bases showed that the presence of IPA/DMIS granted a benefit to TBF permeation across hooves. In this context, TBF flux from 1P2525 was 2.53-fold higher than that from POX hydrogel 20% although 1P2525's complex viscosity was 2.76-fold higher than POX hydrogel's complex viscosity (5183 vs. 1878 Pa.s). The important role of IPA/DMIS for TBF permeation across hooves can be further explored through Fig. 4.39. In contrast, there were no apparent correlations between medians and the other components of the formulations (water or POX/MCT) if they were plotted together. Unless IPA/DMIS reached 25%, TBF did not permeate across hooves. Above 25%, TBF fluxes increased and reached a maximum flux at higher IPA/DMIS content of the formulation. In this case, a sufficient amount of IPA/DMIS was essential to initiate TBF permeation across hooves. This phenomenon was still evident even if the high standard deviations were considered. A possible mechanism of IPA/DMIS in promoting TBF permeation across hooves from these formulations has not been reported before. However, dimethyl sulfoxide, also a transdermal penetration enhancer, has been reported to increase econazole permeation into deeper nail layers. Yet, the high concentration used (99%) prohibits its further administration due to its irritant effect [38].

The role of water in the ungual permeation was not seen from this section. Water as a potent ungual penetration enhancer has been reported by Walters et al. [10,51]. They found that the homologous alcohols permeated to a higher extent from aqueous

solutions than from the neat liquids (undiluted). Hence, IPA/DMIS likely played a more important role than water in this study.

Compared to the permeation across SC, the ringing formulations did not show a noticeable permeation enhancement across hooves. Actually there has not been any report associated with the use of LLC for ungual penetration enhancement. Since the lipid content of human nail, and accordingly hooves, is low (0.1-1%) [10], a modification of the ungual permeation process via LLC is rather unlikely. Therefore, the strategy in ungual penetration enhancement deals rather with the cleavage of the disulfide bonds within nail keratin and/or the increase in nail swelling [72].

4.9.5 TBF amount retained in hooves

TBF amounts retained in hooves after 12 h of permeation are displayed in Table 4.9. For a better visualization, all data were plotted together with the complex viscosities of the formulations in Fig. 4.40. Generally, TBF amounts retained in hooves were all about on the same level except for 1P3030 and 1P3040 which were relatively high, yet not statistically significant, and 1P5025 which was the lowest among all. Statistical analysis showed that 1P5025 was the only formulation which was significantly different from other formulations.

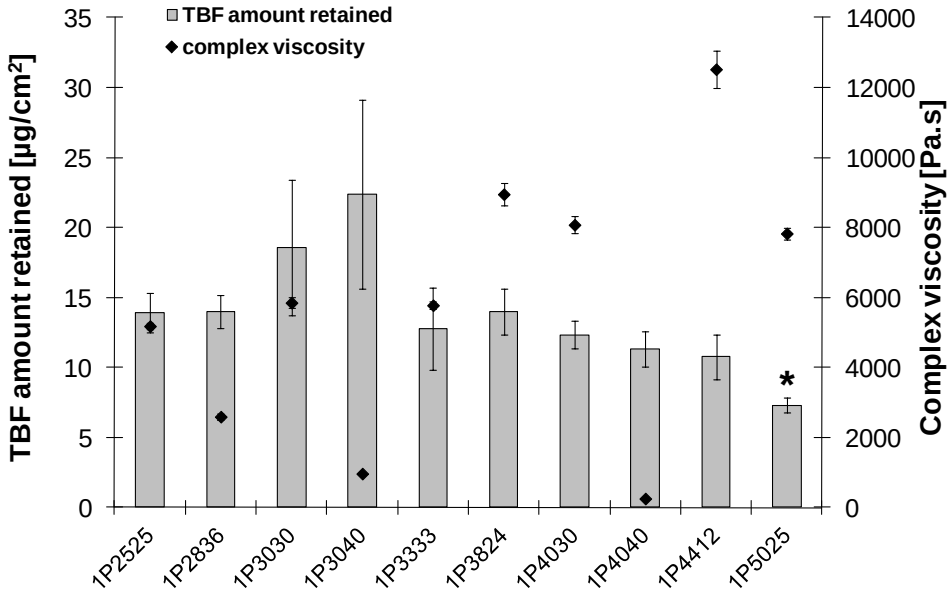

Fig. 4.40 TBF amounts retained in hooves and complex viscosities of the thermogelling formulation (mean ± SD), *1P5025 revealed significantly different amount (one-way ANOVA at α=0.05, followed by Games-Howell post-hoc test).

The relation between TBF amount retained in hooves and the complex viscosity of the formulation is not evident. As can be seen in Fig. 4.40, the amounts of TBF retained were generally constant although complex viscosities varied. A decrease in complex viscosity from 1P3030 to 1P3040, for example, did not influence the amount of TBF retained. This has been observed with other formulations as well. In addition, the influence of other components of the formulation on the amount of TBF retained was not evident either.

4.10 Resume of TBF permeation across SC and hooves from thermogelling formulations with different compositions

TBF permeation fluxes from 1P2525 across SC were 1.4-fold higher than those from Basiscreme DAC and Lamisil® Creme, yet not significantly different. Since TBF's thermodynamic activity was the lowest in 1P2525, the nature of the thermogelling vehicle might play a major role for the permeation enhancement. A higher permeation flux was achieved by incorporating higher TBF contents into the vehicle. The latter was only possible due to the specific composition of the formulation. Furthermore, the enhancement factor is found to be specific for each composition (Table 4.4).

DSC study on SC displayed comparable T2 and T3 shifts for all the vehicles examined. In other words, they showed a comparable influence on the melting of the lipid bilayer and to the disruption of protein-lipid association. These comparable results of T2 and T3 corresponded well with the permeation results in terms that there were no significantly different fluxes across SC from various vehicles either. Nonetheless, DSC thermograms revealed that 1P2525 eliminated T1 and T4 completely whilst Basiscreme DAC still showed a specific transition close to T1 which belonged to residues of the base itself. T4 was also evident from Lamisil® Creme. Summarizing all, the influence of the thermogelling formulation on the skin lipids seemed to be stronger than that from the other non-POX bases.

1P2525 showed higher permeation fluxes across hooves compared to POX hydrogel 20%, Basiscreme DAC and Lamisil® Dermgel. Fluxes from 1P2525 and POX hydrogel 20% were significantly higher than those from Lamisil® Dermgel (p<0.05). POX-based formulations favored TBF permeation across hooves which characteristics are hydrophilic as well. Besides, the presence of other constituents in the thermogelling formulations improved TBF permeation, hinting at the synergistic action of all constituents.

The greatest benefit of the thermogelling formulations among other vehicles is the high amount of TBF retained both in SC and hooves after the permeation. Although the highest amount of TBF retained in hooves was given by POX hydrogel 20%, TBF amount retained both in SC and hooves from 1P2525 was significantly higher than that from Lamisil® Creme (p<0.05) (see p. 78).

Permeation study from thermogelling formulations with different compositions arrived in the conclusion that high fluxes across SC can be achieved with increasing IPA/DMIS content. Indeed, a high content of IPA/DMIS reduced the complex viscosity of the formulation; thus, TBF permeation were favored. A reverse linear correlation between fluxes and complex viscosities was observed between 1000 to 8000 Pa·s. POX hydrogel 20% containing 1% TBF obeyed this relation as well. The viscosity of the formulation is not necessarily the rate limiting step of the percutaneous absorption; but it determines drug diffusion and drug release from the vehicle [37]. 1P4030, 1P3824 and 1P4412 with their noticeably high viscosities gave higher fluxes than expected. The latter phenomenon might be the result of their ringing properties, possibly due to the existence of a liquid crystalline phase, e.g. a cubic system. The amount of TBF retained in SC was apparently dependent on the complex viscosity as well (r^2 = 0.5123) whereas there was no direct correlation between each single constituent and the amount of TBF retained in SC.

TBF permeation across hooves varied considerably for some formulations (1P3040, 1P3333 and 1P3824) although there is still no explanation for this high standard deviation since TEER values of hooves used were checked prior to the permeation study. It can only be hypothesized that there was an unknown interaction between the formulations and the hooves. TBF only permeated when IPA/DMIS exceeded 25%. Below this content, medians were close to zero. TBF fluxes across hooves (see Fig. 4.39) seemed to be constant between 33 and 40% of IPA/DMIS.

As it has been shown in section 4.1.3, TBF solubility in various thermogelling formulations was not uniform. According to Fig. 4.4, TBF solubility ranged from less than 2% to 4%. Since most of the permeation experiments in this study were carried out with 1% TBF, TBF thermodynamic activity (α) in the formulations varied. Therefore, differences in TBF fluxes from the examined formulations might be also caused by differences in their α independent of a systematic variation of a simple component or a component mixture. For this assessment, α of TBF in the vehicles are

displayed in Table 4.10. As a basic calculation, a saturated TBF amount in a formulation (according to Fig. 4.4) gives the highest α, i.e., it reaches unity. When a saturation condition was achieved with 4% TBF, a formulation containing 1% TBF gave α of 0.25.

Table 4.10 Thermodynamic activity of TBF in several thermogelling formulations

Formulation	TBF thermodynamic activity in the formulation
1P2525	0.5
1P2836	*n.d.* (app. <0.25)
1P3030	0.25
1P3040	*n.d.* (app. <0.25)
1P3333	0.25
1P3824	0.5 (app.)
1P4030	0.25
1P4040	*n.d.* (app. <0.25)
1P4412	<0.5 (app.)
1P5025	0.33

n.d.: not known; app.: approximation according to Fig. 4.4

The relation between TBF fluxes across SC and the respective α is displayed in Fig. 4.41, except for α of some formulations which were not determined. In terms of similar α, two groups of formulations produced similar fluxes. The first group consisted of 1P2525 and 1P3824 only. The second group encompassed 1P3030, 1P3333 and 1P4030. This relation was not visible before. Meanwhile 1P3030 and 1P3333 had comparable complex viscosities, the viscosity of 1P4030 was much higher. This was also the case for 1P2525 and 1P3824. Therefore, the thermodynamic activity is able to explain the comparable fluxes from some thermogelling formulations.

Exception is given by 1P5025; meanwhile its α is between 0.25 and 0.5, its flux was far lower than that from all the other formulations. Although its viscosity was comparable with 1P4030, both fluxes were different. Regarding this, fluxes of 1P5025 should have been higher than those of 1P3030 or 1P3333 or 1P4030. Since this is not the case, POX content of 1P5025, which was the highest among all, obviously played a more important role. As discussed before, assuming that TBF binding to the vehicles was comparable for all formulations, an increase in POX content would increase the tortuosity of the diffusion pathway and reduce D_{app} of TBF [141].

Employing saturated system for the permeation study would probably be the best choice. However, this is not reflected by commercial TBF formulations which

commonly contain 1% TBF for topical application. Thereafter, by incorporating 1% TBF in all the cases, TBF permeation across SC was suggested to depend on several factors, i.e., viscosity of the formulation, TBF thermodynamic activity and the complexity of the gel network.

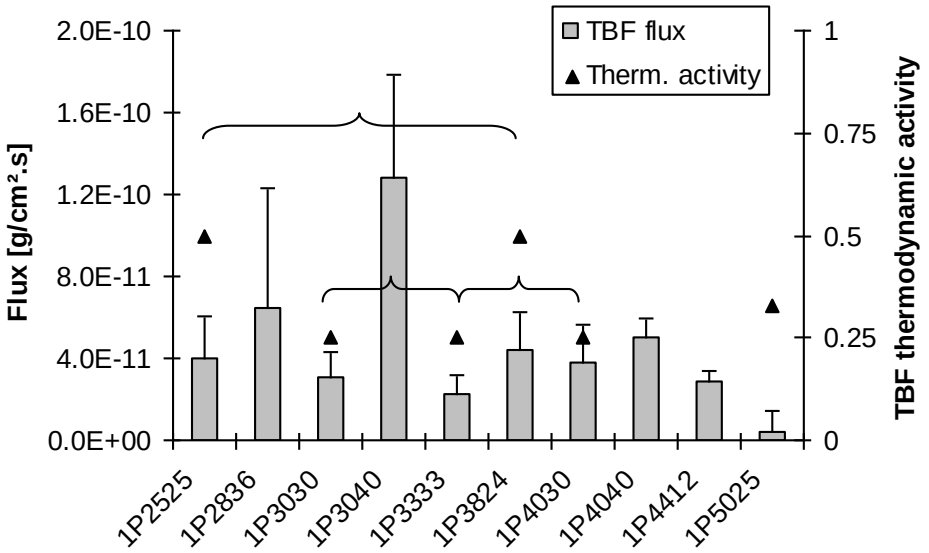

Fig. 4.41 TBF fluxes across SC and its thermodynamic activity in the formulation

A formulation with high solubilizing capacity for TBF will give a low α; this means a lower driving force for penetration. A compromise between drug solubility in the formulation and in the skin will enhance drug's transdermal delivery [148]. This consideration is especially valid for DMIS, a liquid substance with a high solubilizing capacity. Lin and Nash [149] determined the solubility of various drugs with different physicochemical properties and showed that their solubilities in DMIS were always much higher than in water. The examined drugs were benzoic acid, camphor, ephedrine, lidocaine, methylparaben, testosterone and theophylline with DMIS solubility enhancement of 92-, 259-, 16-, 138-, 131-, 4165- and 1.6-fold, respectively (all compared to water). DMIS high capability in dissolving various drugs, especially non-polar drugs, is related to its low dielectric constant [150]. A single use of DMIS was not proven to be efficient as a penetration enhancer [148,151] but in combination with a penetration enhancer it could enhance the penetration and permeation of some drug [2]. Funke et al. [152] have shown that DMIS has only a negligible effect to the skin lipids by means of DSC measurements on the treated full skin of hairless mice. Rossi et al. [153] reported that DMIS supported the delivery of hydrophilic actives by increasing the polarity of SC. Besides, DMIS is able to reduce the contact angle of

some cosmetic oils; this is advantageous for the cosmetic purpose by spreading the constituents homogeneously [153].

As cosolvent, DMIS is prone to increase drug solubility in the formulation and this will reduce drug thermodynamic activity. But, in combination with a penetration enhancer, DMIS may increase drug partition coefficient, accordingly drug solubility, in the sub-stratum corneum region. This phenomenon is suggested from evidence of DMIS traversing the skin after a topical application [152,154]. This effect has been reported “solvent drag” in the literature, as in the case of ethanol [155] and propylene glycol [156,157]. A high drug accumulation in the skin is a benefit for the treatment of antifungal infection, acne, psoriasis etc. where a systemic effect is not desired [148]. The amounts of TBF retained in the SC after permeation from the thermogelling formulations correlated well with DMIS content. Formulation with high DMIS content tended to produce high accumulated amount in the SC, e.g. 1P3030 vs. 1P3040 or 1P4030 vs. 1P4040 (Table 4.7). Finally, the thermogelling formulations revealed significantly higher amounts of TBF retained in the SC compared with non-POX based formulation.

The relation between α and TBF fluxes across hooves has been explored as well. Unfortunately, due to the high variation in fluxes, no relation between both could clearly be drawn as in the case of permeation across SC. Since TBF flux across hooves was higher with an increased content of IPA/DMIS (compare Fig. 4.39), it is suggested that DMIS may play an important role. With its high solubilizing capacity and its hydrophilic property, DMIS diffuses as easily as water across hooves. However, the presence of water is a prerequisite for the action of an ungual penetration enhancer because pure organic solvents, e.g., ethanol and acetone cannot cause sufficient swelling of the nail, a common precondition of ungual permeation enhancement [11]. Walters et al. [51] reported that permeation rates of neat homologues alcohols were about 5-fold smaller than from their diluted aqueous solutions. In conjunction to this, the permeation enhancement of TBF across hooves along with high content of IPA/DMIS is a part of the synergistic action between water and DMIS.

4.11 Human nail plate model made of human hair keratin [114]

In the next upcoming sections, the manufacture process and the physicochemical characterization of the keratin film will be discussed in detail.

4.11.1 Keratin film manufacture

The lyophilization of the dialysate yielded ~60% of the dry hair weight used in the keratin extraction procedure (section 3.2.8.1). This was in accordance with data reported by Nakamura et al. [55], who found more than 65% with the same method. However, this method was time-consuming in terms of determining the extraction efficiency. Therefore the Bradford method [115], a quicker method, was further performed to determine the protein content of the keratin dialysate using bovine serum albumin as standard. The protein content of the keratin dialysate was found to be 13 ± 3.7 mg/mL. This refers to approximately 26% from initial hair weight being distinctly lower than what had been detected with the lyophilization method (~60%). However, the Bradford method is easier to perform and sufficiently reliable to monitor the recovery of the extraction process.

With 2 mL of keratin dialysate mixture, different KF thicknesses of 90-120 µm were obtained. This range remained the same for different batches. However, as expected, this range decreased when the protein content in the keratin dialysate was lower, and vice versa. Variation in KF with similar thicknesses can be seen later on from the standard deviation of the marker P_{app} in the permeation study (without PE) in Table 4.12.

After evaporating the solvent from the keratin solution, a clear, translucent and brownish film was achieved. The subsequent curing process gave this film a water-resistant property as well as mechanical stability due to an oxidation of disulfide bonds between keratin molecules. The intermediate product, finished keratin films and bovine hoof membranes are displayed in Fig. 4.42 (a-c).

During dialysis, the keratin molecules aggregated together, changing the appearance of a clear solution into an opaque one, hinting at the growing size of keratin aggregates. Further solvent evaporation led to film formation. Curing was essential to oxidize the disulfide bonds between keratin molecules, and thus produced water-resistant films.

The drying process and the plasticizer amount played an important role. A mild evaporation at 40 °C for 24 h was the optimum condition. A higher drying temperature led to a rapid evaporation and evoked trapped air bubbles, producing uneven films. Insufficient plasticizer (i.e., glycerol) resulted in brittle KF, whereas an excessive use led to a moist film. The optimum concentration for this purpose was found to be 1% glycerol.

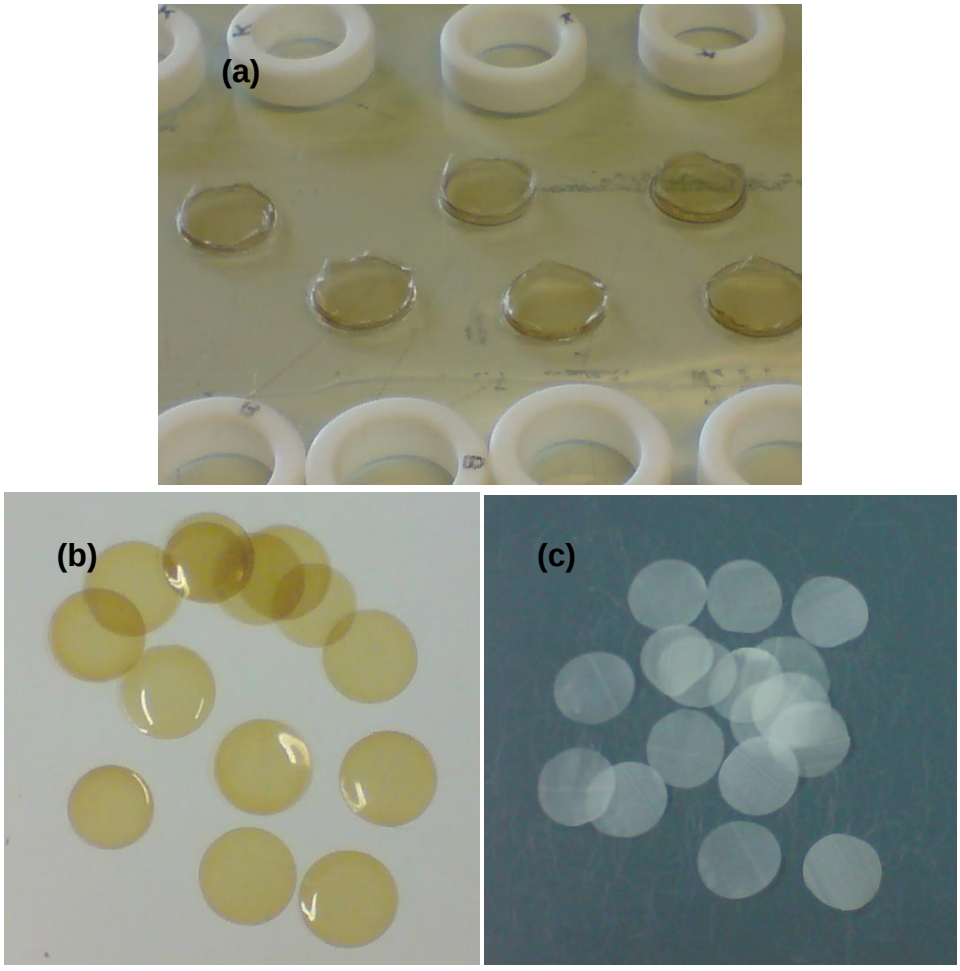

Fig. 4.42 (a) The intermediate products of keratin films before punching and curing; (b) Keratin films after curing; (c) Bovine hooves for the permeation study; membrane diameter = 15 mm; Teflon rings are shown in (a) [114]

4.11.2 Water absorption profile from keratinous materials

The water absorption profiles of all materials under study can be seen in Fig. 4.43. The water uptake of hoof was the greatest, by about 45%, followed by nail and keratin film, around 30% and 5%, respectively (referred to the initial dry weight).

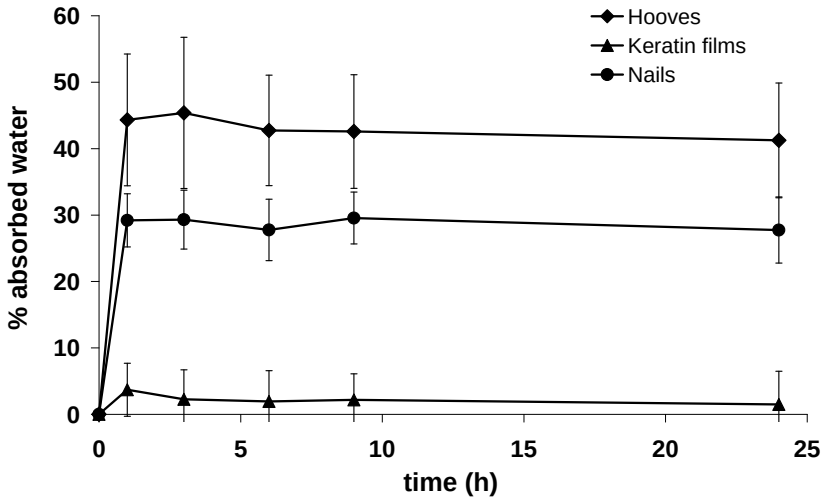

Fig. 4.43 Water absorption profiles from hooves, keratin films and human nail clippings – a comparison (n = 5) [114]

4.11.3 SDS-PAGE

The protein content of KF, its raw and intermediate materials were separated using SDS-PAGE and the respective protein bands were compared to those of human nail and bovine hoof extracts. The gel matrix after the separation is depicted in Fig. 4.44. All human keratin materials from hair and nail showed similar band profiles. Major fragments at approximately 42 and 52 kDa were clearly observed in both hair and nail. Further bands from nail extract (b) were situated at approximately 11, 16 and 24, 95 and 135 kDa. The protein from hair extract (c) and its aqueous suspension after dialysis (a) showed similar major fragments, although the other bands were slightly diffuse. The finished KF (d) resembled the characteristic hair bands from hair extract in the same position. Curing altered the intensities of these protein bands (e) and increased the intensity of diffuse bands in the lower molecular weight area (10-26 kDa), which hinted at fragment cleaving to smaller sizes. Hoof extract (f) showed a different profile to that of human hair and nail. Two diffuse major fragments were obvious at 20-26 and around 42 kDa. Another thin band appeared at 95 kDa.

The major protein bands from KF at around 42 and 52 kDa were similar to those from human nail. This finding is in accordance with a previous study from Baden et al. who also found similar SDS-PAGE patterns for human keratinized tissues [53]. In addition, they also found that human hair and nail showed nearly equivalent water absorption profiles at various relative humidities.

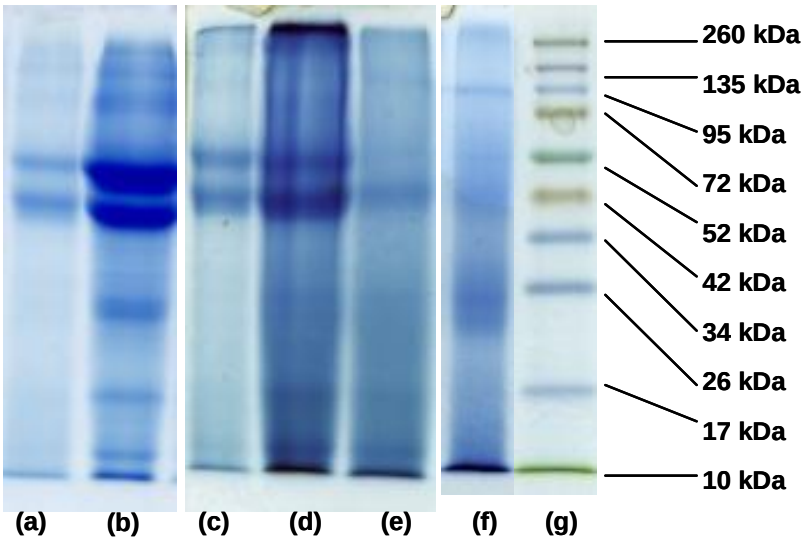

Fig. 4.44 SDS-PAGE of (a) aqueous keratin suspension after dialysis; (b) human nail extract; (c) hair extract; (d), (e) keratin film before and after curing, respectively; (f) hoof extract; (g) molecular weight marker [114]

Therefore and because of the discrepancy between human and bovine keratin, KF made of human hair is suggested as a strong candidate for a nail plate substitute. KF still retained its SDS-PAGE pattern after film formation while a reduction in intensity occurred after curing. This could hint at the denaturation of KF protein into smaller sizes, which appeared as diffuse bands throughout the lane. Reichl [12] investigated human hair keratin as cell culture/tissue engineering substrate and showed that the arrangement of the keratin filament in KF produced with this method did not resemble that in the native hair or nail. The arrangement was observed as a tightly packed and well-connected nanostructure of the keratin dialysate, as has been verified with cryo-TEM micrographs [12]. This artificial arrangement explains the susceptibility of KF to all PEs.

4.11.4 Finding the analogue of KF

In order to find the thickness analogue of KF versus bovine hoof, permeation studies were carried out with SF, first. The permeation data showed that the KF of 120 µm thickness resembled hooves of 100 µm thickness, as can be seen in Fig. 4.45. The 120 µm thick KF was further tested for the permeation of FD4 and RB and those permeability coefficients were then compared to the 100 µm thick bovine hoof again. A similar profile was shown by FD4, but a significant discrepancy (p<0.01) was obvious with RB (Table 4.12). Nevertheless, both bovine hooves and KFs revealed the same rank order of marker permeability coefficients (i.e., RB>SF>FD4).

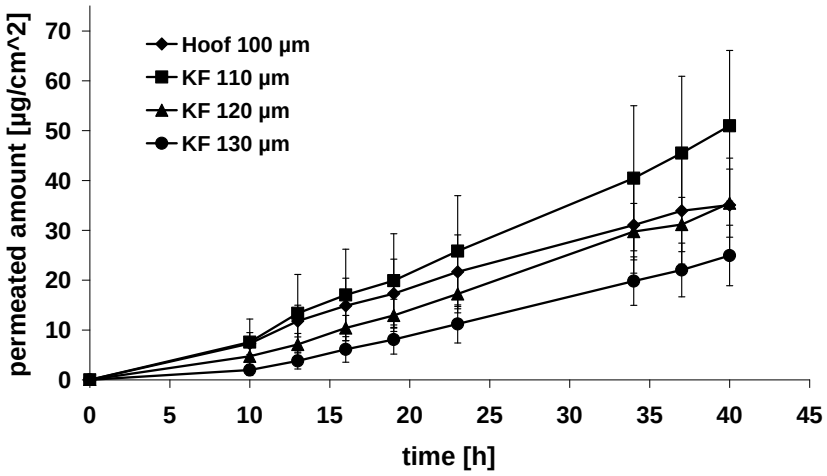

Fig. 4.45 Permeation of SF in dependence of KF thickness (110-130 µm), comparison: 100 µm thick hoof (n = 4-6) [114]

The recoveries of the marker extraction process were between 63% and 100% (Table 4.11). The actual accumulated amount for every marker can be seen in Table 4.13. A great affinity of keratin to the lipophilic RB is also obvious from this table. Both membranes retained more RB than the hydrophilic markers. KF bound more RB than hoof (42% vs. 26%, $p<0.01$) as well as SF ($p<0.05$). The accumulation of FD4 in hoof and KF was comparable and amounted to only 0.8% from the initial donor concentration.

Table 4.11 Recovery of the extraction process

Marker	Recovery of extraction [%]	
	Hoof	KF
SF	93	82
RB	63	68
FD4	100	77

The KF/hoof ratios, in terms of P_{app} (without PE treatment) and accumulated amount, for every individual marker were about in the same magnitude. The KF/hoof ratios were about 1.2 for SF, 1.6-1.8 for RB and 0.7-0.98 for FD4 (see Table 4.12 and Table 4.13).

Table 4.12 P_{app} of the markers [x 10^{-7} cm/s] (mean ± SD)

Marker	Hoof 100 µm	KF 120 µm	KF/hoof ratio
SF	5.00 ± 1.35	5.85 ± 1.12	1.2
RB	17.68 ± 2.22	32.29 ± 3.94	1.8**
FD4	0.56 ± 0.15	0.41 ± 0.11	0.7

**p<0.01; n = 4-12

Table 4.13 Percentage of the accumulated marker in the membranes (mean ± SD) after 20 h permeation study (40 h for RB)

Marker	Accumulated amount in hoof 100 µm (%)	Accumulated amount in KF 120 µm (%)	KF/hoof ratio
SF	1.52 ± 0.12	1.93 ± 0.16	1.27*
RB	25.97 ± 5.73	42.13 ± 5.14	1.62**
FD4	0.83 ± 0.06	0.82 ± 0.11	0.98

*p< 0.05; **p< 0.01; n = 3-6

The search for a KF analogue revealed an optimal thickness of about 120 µm, compared to the 100 µm thick hoof. This was confirmed by the permeability coefficients of two markers (SF and FD4) as well as by their accumulated amounts in the membranes. A significant discrepancy was shown for RB, where its permeability coefficient across hoof was lower than that across KF (p<0.01). Again this discrepancy was shown for the RB accumulated amount as well. A strong binding of lipophilic RB to KF hinted at some specific binding of hair-type keratin compared to hoof keratin. This could be attributed to the different amino acid compositions from both materials, as reported by Baden et al. [53,158]. Furthermore, the graph shown in Fig. 4.46 emphasizes that a large discrepancy between hoof and KF permeabilities could be expected when the solute is a lipophilic substance, although this explanation is in contrast to some literature reports [8,9,42,72].

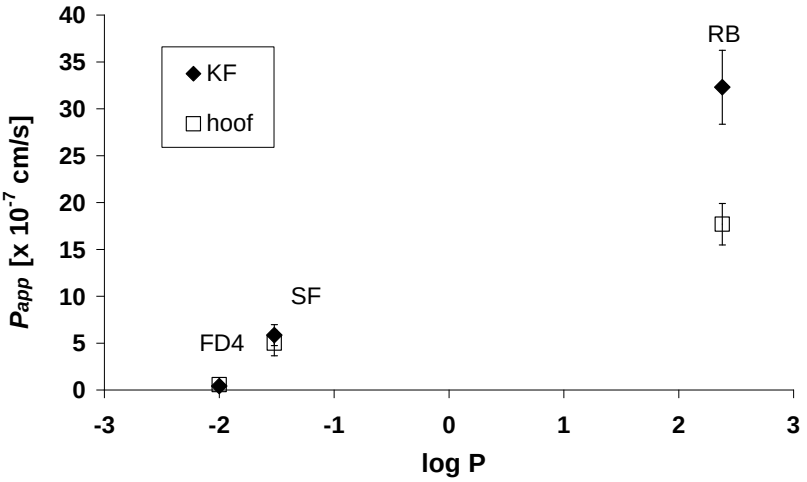

Fig. 4.46 Plot of permeability coefficients (*Papp*) and log octanol water partition coefficients (log P) of the markers [114]

It has been acknowledged that human nail, hooves and accordingly KFs behave as hydrophilic membranes [9,10,42], where the permeation should not be controlled by the lipophilicity of the substance, but rather by its molecular weight [8,9,42,72]. Both SF and RB are not very different in their sizes (376 and 443, respectively), but SF is an acidic dye and RB is a basic one. Keratin, with a pI around 5 [54], is negatively charged in a neutral environment and supports the diffusion of a positively charged molecule, e.g., RB at pH 7.4. This explains the greater P_{app} of RB compared to SF across hoof and KF in this milieu as shown in Table 4.12. This phenomenon has been described by Mertin and Lippold before [9] and was attributed to the Donnan equilibrium phenomenon [7,159]. The electrostatic repulsion between the SF anion and the negative co-ion of keratin in this milieu at the membrane interface is responsible for its smaller P_{app} compared to RB.

The amounts of SF and FD4 bound in both membranes were inconsiderable (maximum 1.9%) whereas the amount of bound RB was much higher. This was in agreement with the work of DeLauder and Kidwell [160], who found no binding between fluorescein and hair samples after exposure of 10 mg/mL dye in 10 mM phosphate buffer, pH 5.6 at 37 °C for 2 h. They found that anionic substances such as SF could not be absorbed into hair due to the electrostatic repulsion at the hair interface, which was negatively charged in this milieu (pH>5). Rhodamine 6G, a cationic dye, was found to be almost completely absorbed in the hair samples after the same defined exposure. This finding supported once more the phenomenon of

Donnan equilibrium and confirmed the great influence of environmental pH to the diffusion of charged or dissociated molecules across nail or hoof.

Interestingly, the ratio of KF/hoof from each marker was almost similar in terms of P_{app} and accumulated amount. As example, despite the discrepancy shown by RB between KF and hoof, the ratios remained constant for the permeated (P_{app}) and accumulated amount (ratio KF/hoof 1.6–1.8). This implies that KF and hoof were comparable by a factor, which was determined by the physicochemical properties of the marker.

4.11.5 Influence of PE on permeability of the markers

All the permeability coefficients after treatment with PEs can be seen in Table 4.14. The permeability coefficients of the three markers were generally higher in KFs compared to hooves after treatment with PEs. Exceptions, however, refer to SF after treatment with urea and RB after treatment with TA, where the P_{app} in hooves were higher than those in KFs.

The P_{app} of SF across hooves and KFs increased after PE treatment. KF was more susceptible to PEs, especially after treatment with TA, as well as after PE combination and serial treatment. The ratios of KF versus hoof permeation after the application of PEs in the case of SF were at maximum 2.1-fold.

All PEs increased FD4 permeability across KF although the urea impact was not significant. Interestingly, the single treatment of both TA and urea decreased FD4 permeability across hooves, but its combination and serial treatment enhanced it. Papain was able to increase FD4 permeation across hooves as well. The highest ratio of KF versus hoof permeability was observed by TA treatment being 16.8-fold.

Table 4.14 *Papp* of the markers (mean ± SD) after treatments with PEs [x 10^{-7} cm/s] and its ratios [114]

Marker	PE	P_{app} Hoof	P_{app} KF	Enhancement Factor (vs. no PE)		KF/ hoof ratio
				Hoof	KF	
SF	no PE	5.00 ± 1.35	5.85 ± 1.12	-	-	1.2
	Urea 3d	22.49 ± 8.50	9.67 ± 2.80	4.5*	1.7*	0.4
	TA 15h	55.63 ± 8.26	88.41 ± 14.15	11.1**	15.1**	1.6**
	Combination urea-TA	53.62 ± 5.25	95.20 ± 7.51	10.7**	16.3**	1.8**
	Serial urea-TA	45.82 ± 5.77	83.09 ± 11.16	9.2**	14.2**	1.8**
	Papain 15h	9.78 ± 4.09	20.80 ± 3.62	2.0	3.6**	2.1*
FD4	no PE	0.56 ± 0.15	0.41 ± 0.11	-	-	0.7
	Urea 3d	0.19 ± 0.08	0.51 ± 0.24	0.3**	1.2	2.7*
	TA 15h	0.31 ± 0.04	5.20 ± 2.48	0.6**	12.7**	16.8**
	Combination urea-TA	2.19 ± 1.53	6.87 ± 2.22	3.9**	16.8**	3.1*
	Serial urea-TA	8.13 ± 5.19	11.60 ± 0.13	14.5**	28.3**	1.4
	Papain 15h	1.62 ± 1.29	2.79 ± 1.19	2.9**	6.8*	1.7
RB	no PE	17.68 ± 2.22	32.29 ± 3.94	-	-	1.8**
	Urea 3d	9.62 ± 6.10	43.07 ± 11.26	0.5*	1.3*	4.5*
	TA 15h	86.48 ± 28.92	68.32 ± 19.21	4.9**	2.1**	0.8
	Combination urea-TA	17.02 ± 11.95	93.55 ± 15.26	1.0	2.9**	5.5**
	Serial urea-TA	5.97 ± 2.11	119.10 ± 35.20	0.3**	3.7**	19.9**
	Papain 15h	10.40 ± 5.83	59.90 ± 50.29	0.6*	1.9	5.8

*p< 0.05; **p< 0.01; n = 3 – 12

RB permeability across hooves increased after TA treatment, whilst the urea treatment, the serial treatment and papain reduced it. KF was susceptible to all treatments, although the papain treatment was not statistically significant. Remarkable differences between KF and hoof were observed with urea when its combination and serial treatment were applied (i.e., KF versus hoof ratios 4 - 19.9-fold).

From the preliminary experimental set up papain was expected to be a potential PE because concentrations of 3% and 5% damaged both membranes within one hour (data not shown). Therefore, a papain concentration of 2% was chosen for the further permeation study. However, a penetration enhancement could not be shown for RB

across hooves. This phenomenon is not fully understood considering that there has not been reported any proof for the interaction of papain with other substances.

4.11.6 Resume of marker permeability across KF and hoof

The application of PE astonishingly did not always increase the permeability coefficient of tested marker. While the application of urea increased the P_{app} of SF across hooves, this was not the case for FD4 and RB. Again the P_{app} of SF and RB across hooves increased after treating hooves with TA, but this was not the case for FD4.

4.11.6.1 Permeation across hoof

PEs could increase the amount of permeated SF (up to 11.1-fold) across hooves. In the case of FD4 only papain, the combination and serial applications of urea-TA were effective. The permeability coefficient of RB increased after treating hooves with TA only.

4.11.6.2 Permeation across KF

All PEs increased marker permeability coefficients, although for both urea and papain, the impact on FD4 and RB permeation was not significant, respectively.

4.11.6.3 KF versus hoof

In the case of SF permeation, hooves and KF permeability differed only up to 2.1-fold when PE treatment was performed. Greater discrepancies of 16.8- and 19.9-fold were found for FD4 and RB permeation when TA and serial application were used, respectively. KF versus hoof ratios of 2- to 3-fold were observed when urea and its combination with TA were applied to FD4. Urea and its combination with TA resulted in about 5-fold ratios for RB. Fig. 4.46 shows the relation between permeability (P_{app}) and octanol/water partition coefficient of the markers (log P) under study. As a note, Fig. 4.46 is actually not intended to explain a dependency of the markers' partition coefficients (lipophilicities) on their permeation coefficients, as it was clear that both parameters were independent in terms of permeation across nail and hoof. Rather, this plot is an effort to explore the behavior of the tested membranes, especially their response to markers with different physicochemical properties.

4.12 Microbiological assay

This assay was aimed to assess the efficacy of the formulation quantitatively by measuring the growth inhibition of *T. rubrum* after TBF application on the human nail model bovine hoof or keratin film. The nail model hoof/ keratin film simulates the nail plate in place of a real application of the formulation. The efficacy of the formulation is a function of the growth inhibition after incubation of the membrane with the formulation. An aseptic condition is essential for conducting this assay since any microbial contamination will influence the growth of *T. rubrum*. For that reason, all steps must be done in an aseptic condition under a laminar air flow. Furthermore, safety issues must be seriously considered since human pathogenic fungi produce spores and these can further transmit the disease.

T. rubrum strain DSM 19959 was chosen since this strain grows faster (within 10-15 days) than other strain, e.g., *T. mentagrophytes* which needs more than one month to grow. *T. rubrum* preferably colonizes skin and can be isolated thereof while *T. mentagrophytes* is mainly isolated from nails. Actually, skin fungus generally grows faster than nail fungus. That is probably why the clinical manifestations of the skin fungal infection are usually more acute than nail fungal infection is, which is rather chronic and hard to be cured.

First of all, the membranes were treated with TBF loaded formulation to allow for TBF diffusion -vertical penetration and permeation- across the membrane. Subsequent to the permeation across the membrane, TBF also diffuses laterally within the agar. Both residual TBF within the membrane and TBF diffused into the agar should be able to inhibit the growth of *T. rubrum*. For this purpose, only one side of the membrane was treated. The untreated side faced the agar medium which had previously been inoculated with *T. rubrum*. It is important to restrict the treated area so that the formulation will not flow over the boundary of the membrane during the incubation. Any spread of the formulation would enlarge the treated area in an uncontrolled manner. The use of the donor-part of the Franz diffusion cell which was affixed together with the silicon paste was successful to control the treated area.

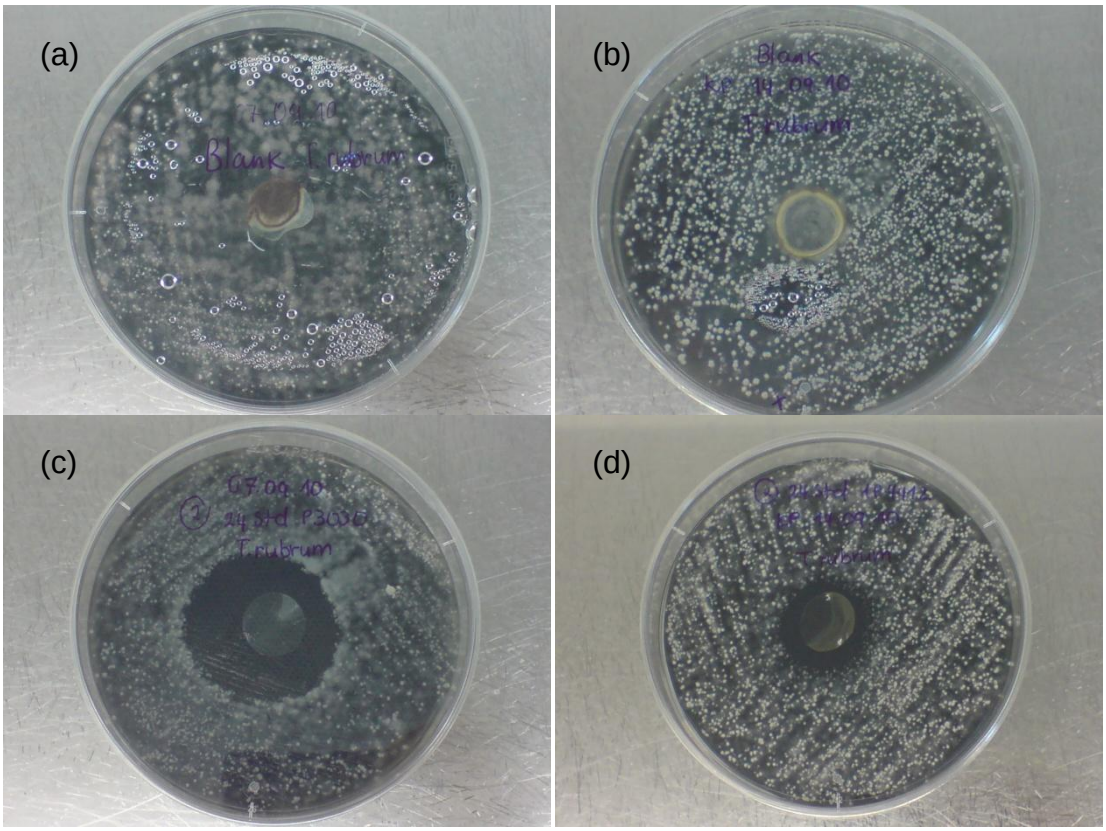

Fig. 4.47 Agar plates after 9 days of incubation: (a) hoof blank, (b) keratin film blank, (c) hoof after 24 h treatment with 1P3030, (d) keratin film after 24 h treatment with1P4412

Results showed that *T. rubrum* colonized not only the medium surface, but also the membrane as there were fungal colonies at the border of the membranes as depicted in Fig. 4.47 (a-b). The colonization of the membrane was further recognized as a visual alteration: hoof turned brownish (a), keratin film turned pale (b). This alteration hinted at the digestion of keratin by *T. rubrum*.

The diameter of an inhibition zone could be measured initially after 9 days of incubation. Otherwise, no distinct border could be observed as a zone of inhibition. Examples of inhibition zones can be seen in Fig. 4.47 (c) and (d). By means of this assay, the power of the formulation in inhibiting the fungal growth could be distinguished, e.g., between 1P3030 and 1P4412 across hoof and keratin film, respectively. Collecting the diameters of inhibition zones from the examined formulations revealed a ranking of their efficacies.

1P3030, 1P2525 and 1P4412 were chosen since they revealed different permeation fluxes and the amounts of TBF retained in hooves. Consequently, TBF diffusion rates from these formulations were expected to be different as well. In addition, standard deviations were low and their semisolid consistencies enabled convenient applications

in this assay. A zone of inhibition could be observed even after 1 h of treatment with1P3030 as displayed in Fig. 4.48. As expected, the diameters initially increased up to 5-h-treatment interval. Surprisingly, the diameters decreased after 15 h of treatment and then increased again after 24 h of treatment. This fluctuation was more distinct from hooves than from keratin films where the inhibition diameters of keratin films after 5 and 15 h were similar. It is still unclear why hooves' diameters of inhibition suddenly dropped after 15 h of incubation before it increased again after 24 h incubation. However, since the deviation from each time point was larger compared to the fluctuation observed within the sampling time, there were no significant differences between the treatment times for both membranes (one way ANOVA, alpha = 0.05, p>0.05).

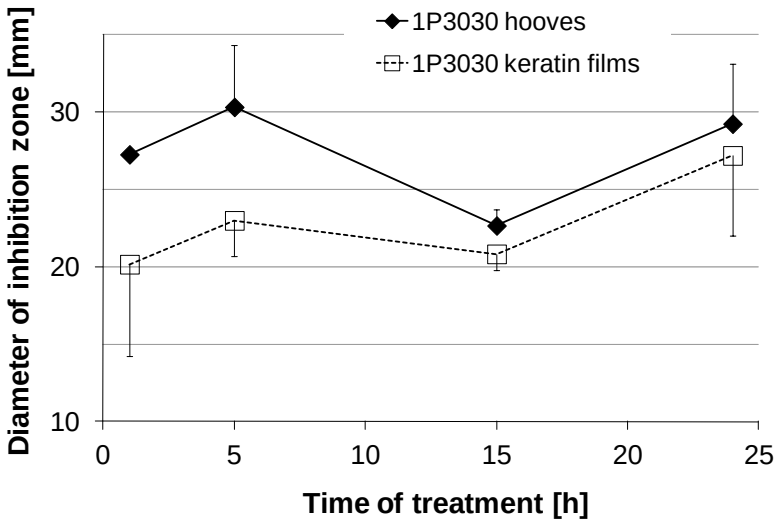

Fig. 4.48 Diameter of inhibition zone (mean ± SD) on day 9 after treatment with 1P3030 for 1, 5, 15 and 24 h (n = 3)

In order to compare the effects of different formulations in more detail, diameters of inhibition zones from the three chosen formulations across hooves and keratin films were measured after 24 h incubation. The diameters of inhibition zones from both membranes are depicted in Fig. 4.49 and Fig. 4.50. Generally, no significant differences could be observed from the three formulations across hooves or keratin films (one way ANOVA, alpha = 0.05, p>0.05). A trend was shown by hooves where the diameters of inhibitions increased along with increase in POX/MCT content from 25% to 30% and remained constant up to 44%. The inhibition diameters from keratin films revealed no distinct trend since the shortest diameter resulted from 1P3030. The

inhibition diameters resulting from TBF diffusion across hooves were against the expectation.

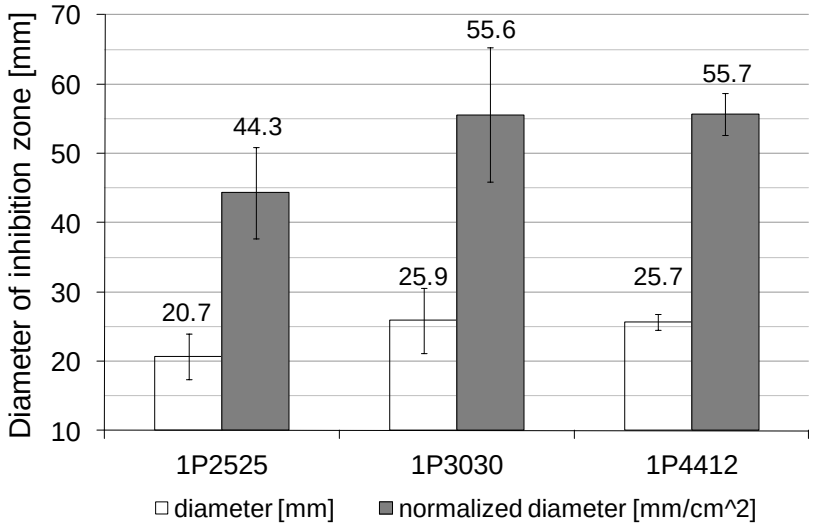

Fig. 4.49 Diameter of inhibition zone (mean ± SD) on day 9 after 24 h-treatment of hooves with 1P2525, 1P3030 and 1P4412 after 24 h (n = 3)

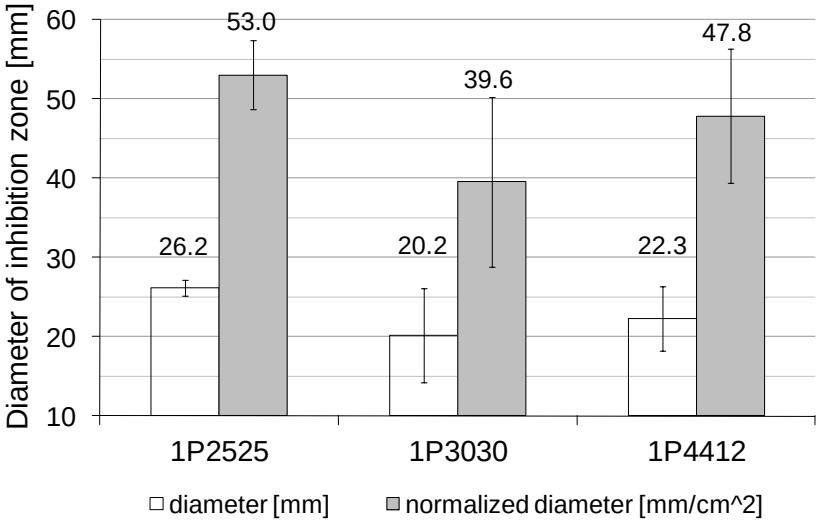

Fig. 4.50 Diameter of inhibition zone (mean ± SD) on day 9 after 24 h-treatment of keratin films with 1P2525, 1P3030 and 1P4412 (n = 3)

With increasing POX/MCT content, the median of the permeation flux decreased whereas the amount of TBF retained in hooves increased first and then decreased again (compare section 4.9.4 and 4.9.5). As a consequence, it was expected that the ranking of the inhibition zones would be either 1P2525>1P3030>1P4412 (from the permeation data) or 1P3030>1P2525>1P4412 (from the amount of TBF retained). Normalized diameters were calculated as compensation for slight differences in Franz

cell donor's orifice by dividing the diameter per opening area of the Franz cell. Nevertheless, in both cases of hooves and keratin films, diameters of inhibition and the normalized ones delivered similar trends and fluctuations.

From the result of the microbiological assay, it could be deduced that there was no distinct difference in the diameter of the inhibition zone observed from the chosen formulations. However, this assay showed that TBF was released from the formulation and permeated across hooves and keratin films although the formulation was given in a finite dose and in a short treatment of 24 h at maximum. Albeit different from the trend of the permeation flux, the presence of a diameter of inhibition zone indicated that this assay works but demands an improvement.

Improvement of the assay could be done by quantifying the amount of fungus spores seeded on the agar plate. By doing this, a more reliable and reproducible result is expected. Clinical and Laboratory Standards Institute/ CLSI (formerly NCCLS), a nonprofit educational organization in the United States, published a method M38-A2 which is applicable for the antifungal susceptibility test for molds or filamentous fungi. The inoculum is prepared from a conidial or sporangiospores suspension which is later adjusted to 0.4 - $5 \cdot 10^4$ cfu/mL to give a reproducible result. The optical density (OD) of the suspension is then measured spectrophotometrically at wavelength 530 nm. RPMI-1640 medium is recommended for diluting the suspension which is afterwards seeded on the agar plate for the assay purpose. Without standardization, the fungal amount which was seeded on the agar plate would vary so that as expected, the growth inhibition may vary as well. Yet, this procedure is time consuming and out of the scope of the current study. Still, without quantifying the spores amount seeded on the agar plate for the microbiological assay, a proof of concept was successful in demonstrating the efficacy of the formulations loaded with TBF.

4.13 Final Discussion

One aim of this work was the further characterization of the poloxamer 407-based thermogelling formulation with the highlight of TBF incorporation as a representative of a lipophilic drug. This study was carried out based on the previous work of Grüning [2] and van Hemelrijck [3] who had investigated the physicochemical properties of this vehicle and the incorporation of the hydrophilic 5-ALA for the photodynamic therapy purpose. As expected, upon the incorporation of a lipophilic drug, the behavior of this

vehicle was different from that upon the incorporation of a hydrophilic drug. Besides the characterization of the formulations, this work also emphasized the permeation of TBF from various formulations, including thermogelling formulations, across human stratum corneum and bovine hooves. The stability of TBF during the storage at 20 °C was investigated as well. Finally, to ensure that TBF in the formulation can inhibit the growth of the fungal infection causative, *T. rubrum*, microbiological assays were carried out. For this purpose, bovine hooves and keratin films made of human hair were employed as nail plate models.

4.13.1 Physicochemical characterization of thermogelling formulations containing TBF

The physicochemical properties of POX-based thermogelling formulations changed upon TBF incorporation in a different manner from 5-ALA incorporation. TBF increased the gelation temperature of the vehicle and thus extended the area of the liquid formulations in a phase diagram at room temperature as shown in Fig. 4.1. Despite the large increase in gelation temperature, the complex viscosity of the formulations remained the same up to 2% TBF addition. The increase in gelation point upon TBF addition was unexpected insofar as most chloride ions tend to decrease POX gelation temperature. Hence, terbinafine cation is suggested to give a greater influence on affecting POX gelation process compared to its chloride anion.

The influence of 5-ALA on the ringing effect and the isotropy of the vehicle has not yet been explored but TBF shifted the area of systems with ringing effect and extended the area of anisotropic systems in the phase diagram. Grüning and Müller-Goymann [5] mentioned that the shear moduli of these ringing formulations were too low (magnitude of 10^3 Pa) to be categorized as cubic system which generally reaches 10^4-10^6 Pa [126]. However, SAXD measurements disclosed the existence of the cubic system for the original thermogel P2525 [6]. The intensity of the reflections of this cubic structure (Pn3m) of P2525 was weakened upon the addition of TBF and was amplified upon higher temperature. Unfortunately, the structures of other ringing formulations 1P4020 and 1P5015 could not be elucidated due to their high primary peaks.

The ability of the vehicle in dissolving up to 4% TBF is a benefit since a maximum thermodynamic activity of TBF in the formulation can be achieved. A higher drug thermodynamic activity will be followed by a higher flux rate. Above the saturation

concentration in the vehicle, the permeation flux will be independent of the drug concentration and the vehicle used. Accordingly, a drug with similar thermodynamic activities in different vehicles should give similar fluxes as well [84]. TBF incorporation of more than 1% was not possible in Basiscreme DAC or Lamisil® Creme or Lamisil® DermGel. The high solubility of TBF in the POX-based formulations was dependent on the IPA/DMIS and POX/MCT contents in the formulations. The maximum TBF solubility can only be achieved in the area of the phase diagram with POX/MCT 30-50% and IPA/DMIS 30-40%. Outside this area, TBF solubility was less than 4% (Fig. 4.4).

4.13.2 Stability study of TBF

In this study, UV spectrograms of aqueous TBF solutions remained unchanged up to 48 h. TBF stability was lower in higher pH, e.g., in neutral and pH 7.4 than in acidic medium (pH 5.8). Furthermore, the electrolytes in PBS gave a negative influence on TBF stability compared to water. As expected, a higher storage temperature increased the degradation rate rapidly in line with the Arrhenius equation.

As described in the literature, a TBF suspension can apparently decrease TBF's degradation rate. TBF contents remained above 95% within 28 days of storage at 4° and 25 °C in an extemporaneous suspension prepared in a mixture of sweetened vehicles [161]. The initial TBF concentrations in both temperatures were 26.5 and 27.7 mg/mL, respectively. These concentrations were much higher than TBF concentration examined in this study which was 50 µg/mL (see section 3.2.3.3). Therefore, degradation seems to occur faster from a diluted aqueous TBF solution than from a saturated solution, i.e., a suspension. Unfortunately, TBF stability in various pharmaceutical solvents has not been reported in literature so far. Since TBF is commonly administered perorally as tablet, the need of such stability studies is obviously not that urgent.

In contrast to TBF's poor stability in aqueous solutions, TBF was proven to be stable in the thermogelling formulations up to 1 month (TBF content ≥95%). Despite high water contents (20-50%) and TBF's complete dissolution in all examined formulations, the thermogelling vehicle could maintain TBF stability within one month. A suggested location of TBF within the POX micelles might be advantageous for the protection from degradation. Within the micelles, a direct contact with water can be avoided. The incorporation of a hydrophobic drug into a poloxamer-based vehicle may enhance its

stability against degradation. As a general rule, poloxamers with higher PPO contents offer higher protection, e.g., camptothecin was more stable against hydrolysis with Pluronic® L92 than with Pluronic® F127 [162]. The ability of poloxamer hydrophobic core to protect drugs from degradation has been observed from indomethacin in Pluronic® F68 and F127 [163] as well as from simvastatin in various Pluronics and Tetronics [164].

4.13.3 TBF permeation across SC

TBF fluxes from 1P2525 were about 1.4-fold higher than those from Basiscreme DAC loaded with 1% TBF or from the marketed product Lamisil® Creme, yet not statistically significant (p>0.05). This minor enhancement was in line with their comparable effect on SC skin lipids which was measured by means of DSC. 1P2525 was however still more effective than other vehicles by eliminating T1 and T4 transitions completely. The thermogelling characteristics of the formulation as well as the thermodynamic activity of TBF were suggested to play an important role in TBF delivery. Thermodynamic activities are in agreement with higher drug content in the formulation and thus higher flux.

TBF permeation enhancement was not pronounced when compared to 5-ALA. The flux of the latter was 7.5-fold higher from the thermogel than from Basiscreme DAC. As reason, it is suggested that both drugs, i.e., a hydrophilic and a lipophilic one, are differently located within the POX gel network. Nevertheless, POX-based formulation still offers an advantage by revealing the highest TBF amount retained in SC after permeation. This amount plays an important role for the complete cure of fungal infection since the fungal burden is mainly located in SC.

Thermodynamic activity of TBF in the formulation can be used to further explain the influence of different vehicle compositions on the TBF fluxes. Since the TBF concentration was fixed at 1%, its thermodynamic activity varied within the examined formulations due to different saturation limits. Yet, it could be shown that formulations with similar thermodynamic activities exhibited about similar fluxes (Fig. 4.41). Finally, the most appropriate vehicle for delivering TBF was decided for from a compromise between flux, viscosity of the formulation and stability during storage. So far, it was shown that viscositiy and thermodynamic activity played important roles in delivering TBF from the thermogelling formulations across SC. Therefore, both parameters can be a useful tool in predicting/ calculating TBF permeation across SC.

DMIS, a solvent for transdermal formulation, was proven to be advantageous in improving the amount of TBF retained in SC. Although TBF permeations across SC were not pronounced compared to other non-POX vehicles, DMIS presence in the thermogelling formulations was prone to increase TBF accumulation in SC. The hydrophilic property and the high solubilizing capability of DMIS in combination with a postulated penetration into the skin are considered to be responsible for this solvent drag effect.

4.13.4 TBF permeation across hooves

Different from the permeation across SC, TBF fluxes from POX-based formulations across hooves were remarkably higher than those from other non-POX vehicles (p<0.05). Bovine hoof served in this study as a human nail plate model. TBF was delivered across hooves and its fluxes were higher from 1P2525 than from POX hydrogel hinting at a synergistic effect of all constituents. In contrast, the amount of TBF retained in hooves was ~4-fold higher from POX hydrogel than that from 1P2525. The high water content in POX hydrogel seemed to provoke TBF binding to hooves' keratin.

High experimental standard deviations from the permeation across hooves made a conclusion difficult to be drawn. However, the influence of viscosity and IPA/DMIS content on TBF fluxes was apparent (Fig. 3.36 and 3.37). Interesting to note that TBF permeated only when IPA/DMIS exceeded 25%; below this concentration, medians of fluxes remained at about zero. IPA/DMIS was proven in this study as ungual penetration promoter. The amounts of TBF retained in hooves at the end of the permeation experiment did not depend on the composition of the formulations. As an exception, only 1P5025 revealed a significantly low TBF amount retained in hooves whereas TBF amounts from 1P3030 and 1P3040 were relatively high, yet not significantly different. It might be possible that those amounts retained after 12 h of the permeation experiment could not be distinguished due to an insufficient experiment time.

A different anatomical organization of the nail from that of the skin requires different strategies for permeation enhancement in both cases. The lipid-protein-partitioning theory from Barry [30] explains that skin penetration enhancers work via one or up to three main mechanisms: alteration of intercellular skin lipids or skin protein, increase of the drug partition into skin or any combination of them. Human nail has been

described as a hydrophilic gel membrane in contrast to skin that behaves as a lipophilic partition membrane [8-10,42]. Therefore, hydrophilicity, drug molecular size and molecular charge are important parameters for the passive diffusion across nail [40] unlike skin permeation where drug lipophilicity plays a major role.

In this study, POX-based thermogelling formulations have been shown to be a potential vehicle for delivering TBF across both SC and hooves. The high amounts of TBF retained after the permeation, especially in hooves, are a great benefit for the fungal infection treatment. Therefore, this formulation could be a promising substitute and adjuvant in mycosis therapy of dermatophyte infections.

4.13.5 Human nail plate model made of human hair keratin versus bovine hoof [114]

Keratin belongs to the family of water-insoluble proteins [165]. Furthermore, it is insoluble in many solvents and even robust against digestion of enzymes, such as pepsin and trypsin. The keratin extraction requires reducing agents which turn keratin into a more soluble form via cleavage of the keratin disulfide bonds [43]. The Shindai solution is appropriate to extract the keratin from human hair to produce the keratin film (KF) under study. Blond or gray hair was the best raw material for KF production because colored hair may influence or disturb the extraction process (according to the preliminary study), due to the rich content in melanin. Bleaching could however be applied before extraction to diminish this problem.

There are two major protein groups of hair and nail keratin, i.e., low-sulfur and high-sulfur proteins. The former has higher apparent MW in the range of 55-76 kDa whereas the latter is in the range of 26.5-43 kDa [40,54]. Human hair and nail share similar proteins in both groups although their amino acid and half-cystine contents are slightly different [53]. At least seven proteins are common to hair and nail in the high-sulfur group with additional proteins for nail at MW 38.5 and 32 kDa. On the other hand, six proteins in the low-sulfur group have been identified in both materials including additional proteins at MW 61 kDa in hair and 72 or 76 kDa in nail [54]. Both groups were evident in our study from the hair and nail samples. However, to identify each single keratin protein, further application of two-dimensional electrophoresis in different pH is needed. The thick bands at around 52 kDa presented the low-sulfur proteins group meanwhile those at around 42 kDa belong to the high-sulfur proteins

group. Additional bands from each keratin group were shown distinctly by the nail extract compared to hair or KF at e.g., 76 kDa.

Cooper and Sun [166] listed some bovine proteins in previous reports. Hoof keratin comprises proteins with MW of 48, 50, 51, 52, 54, 56, 58, 60, 63 and 68 kDa. In addition to this, Kvedar et al. [167] found specific keratin proteins in bovine hoof, labeled as a_1-a_4 and b_2 with MW of 44-58 kDa and pI 5.2-6. These descriptions can however not explain the thick band with MW 20-26 kDa appeared from the hoof extract lane (f) in the present study. On the other hand, the additional band at around 42 kDa belongs to the protein group which is about similar to human keratin from hair and nail. A more detailed discussion to bovine hoof keratin contents and its immunoblotting assay are given in ref. [166,167].

Penetration enhancers (PE) were previously found to be penetrant specific [72], and this is confirmed by our study. A careful conclusion must be made if the tested substance is a large or a lipophilic molecule. The different water uptakes from hoof and KF and their different inner structures (natural vs. artificial) were possibly responsible for all discrepancies found after PE application. Hoof with the water uptake up to 45%, in contrast to KF (5%), is accordingly able to retain the PE solution within the matrix longer; this would retain the matrix acidity/ alkalinity after PE application as well. This environment will affect the solute permeation across the membrane. Human nail absorbs water up to around 30% and this is between the water uptake values observed for hoof and KF. Just considering the water uptake only, one would underestimate the permeability of KF in comparison to nail. This was actually not the case, as indicated by an even higher KF permeability compared to hoof, despite its low water uptake.

KF is supposed to be less susceptible to urea, which works via an increase in hydration. This was indeed seen for all markers across KF, where the increases after urea application were the lowest among other PE applications. However, the different water uptake between hoof and KF did not contribute to any distinct difference when the hydrophilic marker was applied. Finally, KF was very susceptible to TA, a common permanent waving agent [168].

To cleave disulfide bonds in hair, TA must reach the cortex through the hair cuticle [169]. Following this, Cannell [168] explained the reaction mechanism as follows:

$$kSSk + RSH \leftrightarrow kSH + kSSR$$

In this step, hair keratin disulfide bond (kSSk) is cleaved upon addition of thiol compound (RSH) and produces a cysteine residue (kSH) and the mixed disulfide of the thiol compound with the hair keratin (kSSR). Upon contact with the second thiol molecule, a second cysteine residue and the symmetrical disulfide of the thiol RSSR are formed:

$$kSSR + RSH \leftrightarrow kSH + RSSR$$

In the final step, the application of an oxidizing agent restores hair disulfide cross-links (kSSk) via the following reaction:

$$kSH + HSk \xrightarrow{\text{oxidizing agent}} kSSk + H_2O$$

To explain the synergistic works of TA and urea, TA as waving agent is usually employed in alkaline pH of about 9-10 to maximize disulfide bonds cleavage by the thiolate ion [168-170]. At acidic pH, heat is required to carry out the waving process. In low pH, the dominant species in the system is the un-ionized molecule $HS\text{-}CH_2\text{-}COOH$. The presence of thiolate ion $^{-}S\text{-}CH_2\text{-}COO^{-}$ in alkaline pH plays the main role for the reduction of the keratin disulfide bonds [170]. This explains the P_{app} increases across KF upon application of serial urea-TA or in combination with urea where the environments of these systems were less acidic. Meanwhile the pH of 5% TA solution was 1.63, in combination with urea the pH increased to 2.93. The pH increases of TA solutions were followed by P_{app} increases across KF except those for SF which were comparable.

Single, serial or combination of TA did not give any differences to SF's P_{app} across hooves meanwhile urea incorporation or serial application reduced RB's P_{app} across hooves. Urea in aqueous solution acts as electron donor and keratin is negatively charged in this milieu due to the alkaline pH. Theoretically, this alkaline environment should actually support RB permeation as in the case of its permeation without PE at pH 7.4. However, this was not proven. Thereafter, the electrostatic repulsion with urea molecule at the diffusion interface when RB is entering hooves, could be responsible for this phenomenon. This phenomenon was not seen in KF where urea application led to permeation enhancements for all markers.

Interestingly, although the water uptake of hooves was high, the application of urea did not always increase the permeation of markers, which can be seen with FD4 and

RB. The permeated amounts of FD4 and RB decreased, respectively, suggesting the unsuitability of urea as PE in these cases.

Papain was proven to be a potential PE, with a concentration of 2% still showing permeation enhancements across both membranes. The mechanism of papain in increasing diffusion was not clear until now. Quintanar-Guerrero et al. [123] suggested a passage formation by papain and salicylic acid, whereas Mohorčič et al. [122] proposed a hydrolysis of the keratin network by a keratinolytic enzyme, as was shown by keratinase in their study. KF was found to be more susceptible to papain compared to hooves indicating that keratin bonds in KF were more fragile than the ones in hoof.

There is unfortunately no universal ungual PE for all penetrants. In fact, the permeation of the penetrant is strongly depending on the PE concentration, treatment duration and the physicochemical character of the penetrant itself. Brown et al. [72] reported that all tested PEs (TA, urea H_2O_2, sequential and reversal TA-urea) showed no universal enhancements to all their tested substances (caffeine, methylparaben and terbinafine HCl). Caffeine as a model of a small hydrophilic drug did not show any enhanced penetration after the sequential application of 15% urea-H_2O_2 followed by 5% TA, but in the present study SF did. Indeed one should consider the influence of environmental pH to the dissociation of penetrant as well. Mertin and Lippold [9] found that benzoic acid permeated to a higher extent across nail at pH 2.0 than at pH 7.4. Vice versa, this was also the case for pyridine, a basic substance, which permeated to a higher extent and faster at pH 7.4 than at pH 2.0. This phenomenon indicated that the undissociated form facilitated the permeation across nail.

4.13.6 Microbiological assay

The microbiological assay conducted in this study revealed that TBF was released from the formulation before it further penetrated and permeated across the nail plate model. This was a preliminary study to evaluate the efficacy of the formulation against *T. rubrum in vitro*. SC would be an interesting model as well since this fungus infects human skin as well. However, the handling of SC for this purpose would be difficult due to its thickness which is about 8 µm only (from the abdomen part) [171]. Nevertheless, hoof and keratin film are valuable models since this fungus colonizes the nail plate. The evidence that TBF was delivered across the nail plate model could be ascertained from the inhibition on fungal growth.

Two main points can be drawn from this microbiological assay. First, hooves and keratin films showed similar inhibition profiles over the treatment and incubation time applied. Yet, hooves were slightly more permeable than keratin films for TBF despite their similar thicknesses (100 µm). This is evident from the higher diameter of the inhibition zone exhibited by hooves. The second point emphasizes that the formulations examined did not show any significant difference in their inhibition zones although the amounts of TBF retained in hooves after permeation were different. The use of a fungal suspension with defined number of spores in high dilution could probably improve the result of this assay, i.e., deliver distinct differences in growth inhibition.

TBF has proven successful to inhibit the growth of dermatophytes and some other causative pathogens of onychomycosis *in vitro* when applied as solution [172-176]. This growth inhibition has been shown from formulations containing TBF as well [110]. Unfortunately, the latter study was carried out without any representative barrier. An attempt to mimic the real infection condition has been performed by adding nail powder into the medium as a representative nutrient for T. rubrum in a pathological condition [177,178]. The MIC value (minimum inhibitory concentration) of antifungal agents increased upon the addition of nail powder hinting at a reduction in cidal activity in an *in vivo* situation. For that reason, the MIC values reported in the literature e.g., [69] will not reflect the efficacy of the antifungal agents when these actives are not tested under a representative condition, e.g., upon the presence of keratin as the essential nutrient of dermatophytes. Hence, the existence of a barrier (skin/ nail plate) for this assay plays an important role since in the real infection, the drug must be able to diffuse across the keratinous material (skin or nail plate) which is the main site of the infection.

Chapter 5
Conclusion

Succeeding the previous work of Grüning on poloxamer 407-based formulations as vehicles for 5-ALA in photodynamic therapy, this study aimed at the incorporation of TBF as a lipophilic antifungal agent into thermogelling poloxamer formulations and the physicochemical characterization thereof. Permeation across human stratum corneum, bovine hooves and a nail plate model as well as stability studies during storage were conducted within the framework of this study.

In contrast to 5-ALA which is hydrophilic, the lipophilic TBF changed the characteristics of the vehicles to likewise different extents. TBF increased the area of the liquid systems of the phase diagram which was likely due to the insufficient networking of POX micelles. Furthermore, the incorporation of TBF into these systems moved the area of the systems with ringing effect to higher POX/MCT contents. The anisotropic systems were found in an area with POX/MCT contents higher than 70%. This area was broader after TBF addition (2% in this study). Solubility of TBF varied in these systems, depending on the composition of the formulation, ranging from less than 2% to 4%. Gelation temperature of the POX-based formulations increased to a higher temperature after the addition of TBF. In contrast, TBF addition did not give any pronounced change in complex viscosity of the formulation. It is suggested that TBF cation has a more dominant role than its chloride anion in altering the physical properties of the formulations.

SAXD diffractograms hinted at a structural change upon addition of TBF. The cubic structure Pn3m which was shown by P2525 (the original composition of the thermogelling formulation) intensified with increasing temperature, e.g., from 20 to 40 °C, and weakened upon TBF incorporation (e.g., from 1% to 3%). All of these evidences suggest that TBF rather disorganizes and perturbs the networking of POX micelles.

The stability study revealed that TBF in selected thermogelling formulations was stable only up to one month at 20 °C. Since TBF showed a larvated incompatibility with DMIS, an alternative solubilizer would be necessary.

Permeations of TBF from the thermogelling formulations across stratum corneum and hooves showed that this vehicle gave advantages over other non-POX formulations in terms of TBF fluxes and the amount of TBF retained in both membranes. The permeation enhancement across the stratum corneum was not significantly increased by factor 1.4; yet, the amount of TBF retained in the stratum corneum was significantly higher than that from the standards of comparison (1.3- and 2.2-fold higher than from Basiscreme DAC and Lamisil® Creme, respectively). In conjunction to the fungal infection treatment, a high drug accumulation in the infected site is valuable for a complete eradication of the fungus.

While TBF permeation across stratum corneum was apparently dependent on the complex viscosity of the formulation that across hooves correlated well rather with the IPA/DMIS content. Furthermore, a synergistic action of water with DMIS is suggested to be responsible for the high TBF diffusion across hooves. The efficacy of TBF from this formulation in inhibiting the growth of *T. rubrum* has been proven *in vitro* by means of a microbiological assay although this assay needs further improvement. Nevertheless, a representative biological barrier has been employed for this experiment. A suitable and representative model for skin or nail infection will permit the translation of the *in vitro* result to the *in vivo* pathological condition.

A nail plate model made of human hair keratin has been successfully manufactured. The produced keratin film (KF) was appropriate for permeation experiments with regard to its mechanical stability and water-resistant property. This model showed similarity with bovine hooves in terms of permeability for different hydrophilic markers; the amounts of markers retained within both membranes were comparable as well. The study involving lipophilic drug and any application of ungual penetration enhancer must be carefully interpreted because the use of KF could overestimate the permeated amount in comparison to bovine hoof. Although the water uptake of this keratin film was lower than that from hooves, this film was more susceptible to the penetration enhancers. Therefore, a further improvement is still needed upon testing lipophilic substances and increasing film strength as well as a further comparative study with human nail.

References List

[1] Gupta AK, Cooper EA. Update in antifungal therapy of dermatophytosis. Mycopathologia. 2008;166:353–367.

[2] Grüning N. Entwicklung und Charakterisierung eines halbfesten Systems zur Verbesserung der Permeation von 5-Aminolävulinsäure durch exzidiertes humanes Stratum corneum. PhD Thesis. TU Braunschweig; 2007. Available from: http://www.digibib.tu-bs.de/?docid=00021704

[3] van Hemelrijck C, Müller-Goymann CC. Physikochemische Charakterisierung von Poloxamer 407-haltigen Systemen für die dermale Applikation. In: Poster for DPhG Jahrestagung, Bonn; 2008. Available from:

http://www.pharmtech.tu-bs.de/files/muegoy/CHemelrijckBonn0810.pdf

[4] van Hemelrijck C, Müller-Goymann CC. Physicochemical Characterization of Poloxamer-407 Systems for Potential Dermal Application of 5-Aminolevulinic Acid. In: Poster for DPhG Doktorandentagung, Pichlarn-Aigen; 2009. Available from:

http://www.pharmtech.tu-bs.de/files/muegoy/CHemelrijckPichlarn0911.pdf

[5] Grüning N, Müller-Goymann CC. Physicochemical characterisation of a novel thermogelling formulation for percutaneous penetration of 5-aminolevulinic acid. J Pharm Sci. 2008;97:2311–2323.

[6] van Hemelrijck C. personal communication and PhD thesis in preparation; 2011.

[7] Murdan S. Drug delivery to the nail following topical application. Int J Pharm. 2002;236:1–26.

[8] Kobayashi Y, Komatsu T, Sumi M, Numajiri S, Miyamoto M, Kobayashi D, Sugibayashi K, Morimoto Y. In vitro permeation of several drugs through the human nail plate: Relationship between physicochemical properties and nail permeability of drugs. Eur J Pharm Sci. 2004;21:471–477.

[9] Mertin D, Lippold BC. In-vitro permeability of the human nail and of a keratin membrane from bovine hooves: Influence of the partition coefficient octanol/water and the water solubility of drugs on their permeability and maximum flux. J Pharm Pharmacol. 1997;49:30–34.

[10] Walters KA, Flynn GL, Marvel JR. Physicochemical characterization of the human nail: Permeation pattern for water and the homologous alcohols and differences with respect to the stratum corneum. J Pharm Pharmacol. 1983;35:28–33.

[11] Khengar RH, Jones SA, Turner RB, Forbes B, Brown MB. Nail swelling as a pre-formulation screen for the selection and optimisation of ungual penetration enhancers. Pharm Res. 2007;24:2207–2212.

[12] Reichl S. Films based on human hair keratin as substrates for cell culture and tissue engineering. Biomaterials. 2009;30:6854–6866.

[13] Harding CR. The stratum corneum: Structure and function in health and disease. Dermatol Ther. 2004;17:6–15.

[14] Madison KC. Barrier function of the skin: "La Raison d'Être" of the epidermis. J Invest Dermatol. 2003;121:231–241.

[15] Wickett RR, Visscher MO. Structure and function of the epidermal barrier. Am J Infect Control. 2006;34(suppl. 10):S98–S110.

[16] McGrath JA, Eady RAJ, Pope FM. Anatomy and Organization of Human Skin in Rook's Textbook of Dermatology. Burns T, Breathnach S, Cox N, Griffiths C, (eds.) Blackwell Science Ltd.; 2004.

[17] Proksch E, Brandner JM, Jensen JM. The skin: An indispensable barrier. Exp Dermatol. 2008;17:1063–1072.

[18] Williams AC. Transdermal and Topical Drug Delivery. Pharmaceutical Press; 2003.

[19] Ya-Xian Z, Suetake T, Tagami H. Number of cell layers of the stratum corneum in normal skin relationship to the anatomical location an the body, age, sex and physical parameters. Arch Dermatol Res. 1999;291:555–559.

[20] Egelrud T. Desquamation in the stratum corneum. Acta Derm Venereol. 2000;(suppl. 208):44–45.

[21] Weinstein GD, McCullough JL, Ross P. Cell proliferation in normal epidermis. J Invest Dermatol. 1984;82:623–628.

[22] Reddy MB, Guy RH, Bunge AL. Does epidermal turnover reduce percutaneous penetration? Pharm Res. 2000;17:1414–1419.

[23] Kalinin AE, Kajava AV, Steinert PM. Epithelial barrier function: Assembly and structural features of the cornified cell envelope. Bioessays. 2002;24:789–800.

[24] Nemes Z, Steinert PM. Bricks and mortar of the epidermal barrier. Exp Mol Med. 1999;31:5–19.

[25] Wertz PW, Van Den Bergh B. The physical, chemical and functional properties of lipids in the skin and other biological barriers. Chem Phys Lipids. 1998;91:85–96.

[26] Dubey V, Mishra D, Nahar M, Jain NK. Vesicles as tools for the modulation of skin permeability. Expert Opin Drug Deliv. 2007;4:579–593.

[27] Elias PM. Epidermal lipids, barrier function, and desquamation. J Invest Dermatol. 1983;80(suppl. 1):44s–49s.

[28] Barry BW. Mode of action of penetration enhancers in human skin. J Control Release. 1987;6:85–97.

[29] Bouwstra JA, De Vries MA, Gooris GS, Bras W, Brussee J, Ponec M. Thermodynamic and structural aspects of the skin barrier. J Control Release. 1991;15:209–220.

[30] Barry BW. Lipid-protein-partitioning theory of skin penetration enhancement. J Control Release. 1991;15:237–248.

[31] Guy RH, Hadgraft J. Physicochemical aspects of percutaneous penetration and its enhancement. Pharm Res. 1988;5:753–758.

[32] Barry BW. Action of skin penetration enhancers - The lipid protein partitioning theory. Int J Cosmet Sci. 1989;10:281–293.

[33] Subedi RK, Oh SY, Chun MK, Choi HK. Recent advances in transdermal drug delivery. Arch Pharm Res. 2010;33:339–351.

[34] Wepf RA, Neubert RHH. Struktur und Morphologie einer hoch effizienten Barriere. Pharm Ztg. 2007;17:1506–1513.

[35] Friend DR. In vitro skin permeation techniques. J Control Release. 1992;18:235–248.

[36] Higuchi WI. Analysis of data on the medicament release from ointments. J Pharm Sci. 1962;51:802–804.

[37] Wiechers JW. The barrier function of the skin in relation to percutaneous absorption of drugs. Pharm Weekbl Sci. 1989;11:185–198.

[38] Murdan S. Enhancing the nail permeability of topically applied drugs. Expert Opin Drug Deliv. 2008;5:1267–1282.

[39] Jiaravuthisan MM, Sasseville D, Vender RB, Murphy F, Muhn CY. Psoriasis of the nail: Anatomy, pathology, clinical presentation, and a review of the literature on therapy. J Am Acad Dermatol. 2007;57:1–27.

[40] Gupchup GV, Zatz JL. Structural characteristics and permeability properties of the human nail: A review. J Cosmet Sci. 1999;50:363–385.

[41] De Berker D, Mawhinney B, Sviland L. Quantification of regional matrix nail production. Br J Dermatol. 1996;134:1083–1086.

[42] Kobayashi Y, Miyamoto M, Sugibayashi K, Morimoto Y. Drug permeation through the three layers of the human nail plate. J Pharm Pharmacol. 1999;51:271–278.

[43] Bragulla HH, Homberger DG. Structure and functions of keratin proteins in simple, stratified, keratinized and cornified epithelia. J Anat. 2009;214:516–559.

[44] Hendry KAK, MacCallum AJ, Knight CH, Wilde CJ. Laminitis in the dairy cow: A cell biological approach. J Dairy Res. 1997;64:475–486.

[45] Ghannoum MA, Hajjeh RA, Scher R, Konnikov N, Gupta AK, Summerbell R, Sullivan S, Daniel R, Krusinski P, Fleckman P, Rich P, Odom R, Aly R, Pariser D, Zaiac M, Rebell G, Lesher J, Gerlach B, Ponce-de-Leon GF, Ghannoum A, Warner J, Isham N, Elewski B. A large-scale North American study of fungal isolates from nails: The frequency of onychomycosis, fungal distribution, and antifungal susceptibility patterns. J Am Acad Dermatol. 2000;43:641–648.

[46] Vejnovic I, Simmler L, Betz G. Investigation of different formulations for drug delivery through the nail plate. Int J Pharm. 2010;386:185–194.

[47] Scher RK. Onychomycosis is more than a cosmetic problem. Br J Dermatol. 1994;130(suppl. 43):15.

[48] Elkeeb R, AliKhan A, Elkeeb L, Hui X, Maibach HI. Transungual drug delivery: Current status. Int J Pharm. 2010;384:1–8.

[49] Kitahara T, Ogawa H. Variation of differentiation in nail and bovine hoof cells. J Invest Dermatol. 1994;102:725–729.

[50] Kitahara T, Ogawa H. The extraction and characterization of human nail keratin. J Dermatol Sci. 1991;2:402–406.

[51] Walters KA, Flynn GL, Marvel JR. Physicochemical characterization of the human nail: Solvent effects on the permeation of homologous alcohols. J Pharm Pharmacol. 1985;37:771–775.

[52] Kitahara T, Ogawa H. Cellular features of differentiation in the nail. Microsc Res Tech. 1997;38:436–442.

[53] Baden HP, Goldsmith LA, Fleming B. A comparative study of the physicochemical properties of human keratinized tissues. Biochim Biophys Acta. 1973;322:269–278.

[54] Marshall RC. Characterization of the proteins of human hair and nail by electrophoresis. J Invest Dermatol. 1983;80:519–524.

[55] Nakamura A, Arimoto M, Takeuchi K, Fujii T. A rapid extraction procedure of human hair proteins and identification of phosphorylated species. Biol Pharm Bull. 2002;25:569–572.

[56] Brasch J. Current knowledge of host response in human tinea. Mycoses. 2009;52:304–312.

[57] Baeza LC, Bailão AM, Borges CL, Pereira M, Soares CMdA, Mendes Giannini MJS. cDNA representational difference analysis used in the identification of genes expressed by Trichophyton rubrum during contact with keratin. Microbes Infect. 2007;9:1415–1421.

[58] Moreno G, Arenas R. Other fungi causing onychomycosis. Clin Dermatol. 2010;28:160–163.

[59] Dahl MV. Suppression of immunity and inflammation by products produced by dermatophytes. J Am Acad Dermatol. 1993;28:S19–S23.

[60] Weitzman I, Summerbell RC. The dermatophytes. Clin Microbiol Rev. 1995;8:240–259.

[61] Dahl MV. Dermatophytosis and the immune response. J Am Acad Dermatol. 1994;31:S34–S41.

[62] Drake LA, Dinehart SM, Farmer ER, Goltz RW, Graham GF, Hordinsky MK, Lewis CW, Pariser DM, Skouge JW, Webster SB, Whitaker DC, Butler B, Lowery BJ. Guidelines of care for superficial mycotic infections of the skin: Tinea corporis, tinea cruris, tinea faciei, tinea manuum, and tinea pedis. J Am Acad Dermatol. 1996;34:282–286.

[63] Baran R, Hay RJ, Garduno JI. Review of antifungal therapy and the severity index for assessing onychomycosis: Part I. J Dermatolog Treat. 2008;19:72–81.

[64] Arrese JE, Piérard GE. Treatment failures and relapses in onychomycosis: A stubborn clinical problem. Dermatology. 2003;207:255–260.

[65] Tosti A, Piraccini BM, Stinchi C, Colombo MD. Relapses of onychomycosis alter successful treatment with systemic antifungals: A three-year follow-up. Dermatology. 1998;197:162–166.

[66] Baran R, Hay RJ, Garduno JI. Review of antifungal therapy, part II: Treatment rationale, including specific patient populations. J Dermatolog Treat. 2008;19:168–175.

[67] Binstock JM. Molecular biology techniques for identifying dermatophytes and their possible use in diagnosing onychomycosis in human toenail: A review. J Am Podiatr Med Assoc. 2007;97:134–144.

[68] Fuglseth E, Otterholt E, Høgmoen H, Sundby E, Charnock C, Hoff BH. Chiral derivatives of Butenafine and Terbinafine: synthesis and antifungal activity. Tetrahedron. 2009;65:9807–9813.

[69] Ryder NS. Terbinafine: Mode of action and properties of the squalene epoxidase inhibition. Br J Dermatol. 1992;126(suppl. 39):2–7.

[70] Schuster I, Ryder NS. Allylamines - Mode and selectivity of action compared to azole antifungals and biological fate in mammalian organisms. J Dermatolog Treat. 1990;1(suppl. 2):7–9.

[71] Ryder NS. The mechanism of action of terbinafine. Clin Exp Dermatol. 1989;14:98–100.

[72] Brown MB, Khengar RH, Turner RB, Forbes B, Traynor MJ, Evans CRG, Jones SA. Overcoming the nail barrier: A systematic investigation of ungual chemical penetration enhancement. Int J Pharm. 2009;370:61–67.

[73] Beutler U, Penn G; Purification process. 2006/0076227 A1; 2006.

[74] USP34 NF29 Revision Bulletin; 2009, April 1. Available from:

http://www.usp.org/USPNF/revisions/revisions.html

[75] Kazakov PV, Golosov SN. A simple method for obtaining terbinafine hydrochloride. Pharm Chem J. 2004;38:206–208.

[76] Matysová L, Solich P, Marek P, Havlíková L, Nováková L, Šícha J. Separation and determination of terbinafine and its four impurities of similar structure using simple RP-HPLC method. Talanta. 2006;68:713–720.

[77] Ahmad S, Jain GK, Faiyazuddin M, Iqbal Z, Talegaonkar S, Sultana Y, Ahmad F. Stability-indicating high-performance thin-layer chromatographic method for analysis of terbinafine in pharmaceutical formulations. Acta Chromatographica. 2009;21:631–639.

[78] European Pharmacopoeia, 6th ed., Govi Verlag, Eschborn; 2008.

[79] Abdel-Moety EM, Kelani KO, Abou Al-Alamein AM. Chromatographic determination of terbinafine in presence of its photodegradation products. Saudi Pharmaceutical Journal. 2003;11:37–45.

[80] Guillard EC, Laugel C, Baillet-Guffroy A. Molecular interactions of penetration enhancers within ceramides organization: A FTIR approach. Eur J Pharm Sci. 2009;36:192–199. Corrigendum to the author is available.

[81] Hadgraft J, Wolff M. Physicochemical and Pharmacokinetic Parameters Affecting Percutaneous Absorption in Dermal and Transdermal Drug Delivery - New Insight and Perspectives. Gurny R, Teubner A (eds.). Wissenschaftliche Verlagsgessellschaft mbH Stuttgart; 1993.

[82] Higuchi T. Physical chemical analysis of percutaneous absorption process from creams and ointments. J Soc Cosmet Chem. 1960;11:85–93.

[83] Moser K, Kriwet K, Froehlich C, Kalia YN, Guy RH. Supersaturation: Enhancement of skin penetration and permeation of a lipophilic drug. Pharm Res. 2001;18:1006–1011.

[84] Ishii H, Todo H, Sugibayashi K. Effect of thermodynamic activity on skin permeation and skin concentration of triamcinolone acetonide. Chem Pharm Bull. 2010;58:556–561.

[85] Muzzalupo R, Tavano L, Nicoletta FP, Trombino S, Cassano R, Picci N. Liquid crystalline Pluronic 105 pharmacogels as drug delivery systems: Preparation, characterization, and in vitro transdermal release. J Drug Target. 2010;18:404–411.

[86] Kossena GA, Charman WN, Boyd BJ, Porter CJH. A novel cubic phase of medium chain lipid origin for the delivery of poorly water soluble drugs. J Control Release. 2004;99:217–229.

[87] Brinon L, Geiger S, Alard V, Doucet J, Tranchant JF, Couarraze G. Percutaneous absorption of sunscreens from liquid crystalline phases. J Control Release. 1999;60:67–76.

[88] van Hemelrijck C, Müller-Goymann CC. Influence of the content of isopropyl alcohol and dimethylisosorbide on the thermogelification of semisolid and liquid poloxamer 407-systems. In: Poster for 6th World Meeting on Pharmaceutics, Biopharmaceutics and Pharmaceutical Technology, Barcelona; 2008. Available from:

http://www.pharmtech.tu-bs.de/files/muegoy/CHemelrijckBarcelona0804.pdf

[89] Gradzielski M, Bergmeier M, Müller M, Hoffmann H. Novel gel phase: A cubic phase of densely packed monodisperse, unilamellar vesicles. J Phys Chem B. 1997;101:X–1722.

[90] Gradzielski M, Hoffmann H, Oetter G. Ringing gels: Their structure and macroscopic properties. Colloid Polymer Sci. 1990;268:167–178.

[91] van Hemelrijck C, Müller-Goymann CC. Stability aspects of Poloxamer 407-based drug delivery systems in photodynamic therapy. In: Poster for Skin and Formulation, 3rd Symposium & Skin Forum, 10th Annual Meeting, Versailles; 2009. Available from:

http://www.pharmtech.tu-bs.de/files/muegoy/CHemelrijckVersailles09.pdf

[92] Sachdeva V, Siddoju S, Yu YY, Kim HD, Friden PM, Banga AK. Transdermal iontophoretic delivery of terbinafine hydrochloride: Quantitation of drug levels in stratum corneum and underlying skin. Int J Pharm. 2010;388:24–31.

[93] Fussnegger B. Poloxamers (2) Lutrol® F 127 (Poloxamer 407) in BASF ExAct No. 4; 2000:7. Available from:

http://worldaccount.basf.com/wa/NAFTA/Catalog/Pharma/doc4/BASF/exact/-lutrol_f_127/-.pdf?title=Poloxamers%20%282%29%20Lutrol%20F%20127%20%28Poloxamer%20407%29.&asset_type=pi/-pdf&language=EN&urn=urn:documentum:eCommerce_sol_EU:09007bb28001ac1d.pdf

[94] Escobar-Chávez JJ, López-Cervantes M, Naïk A, Kalia YN, Quintanar-Guerrero D, Ganem-Quintanar A. Applications of thermo-reversible Pluronic F-127 gels in pharmaceutical formulations. J Pharm Pharm Sci. 2006;9:339–358.

[95] Sasol Germany GmbH. Miglyol 812N Product information; 2009.

[96] Hoepfner EM, Lang S, Reng A, Schmidt PC (eds.), Fiedler Encyclopedia of Excipients for Pharmaceuticals, Cosmetics and Related Areas. vol. 2., 6th ed. Editio Cantor Verlag; 2007.

[97] Deutscher Arzneimittel-Codex (DAC), Govi Verlag, Eschborn; 2009.

[98] O'Neil MJ (ed.), The Merck Index., 14th ed., Merck Research Laboratories; 2006.

[99] Sigma-Aldrich Co., Product information of FLUORESCEIN ISOTHIOCYANATE-DEXTRAN. E; 23.02.11, Available from:

http://www.sigmaaldrich.com/etc/medialib/docs/Sigma/-Product_Information_Sheet/1/fd150spis.Par.0001.File.tmp/fd150spis.pdf.

[100] Lusiana, Müller-Goymann CC. Preparation, characterization, and in vitro permeation study of terbinafine HCl in poloxamer 407-based thermogelling formulation for topical application. AAPS PharmSciTech. 2011;12:496–506.

The original publication is available at www.springerlink.com. Link: http://www.springerlink.com/content/f615717040w105r6/

[101] Kavanagh GM, Ross-Murphy SB. Rheological characterisation of polymer gels. Prog Polym Sci (Oxford). 1998;23:533–562.

[102] Tosh SM, Marangoni AG. Determination of the maximum gelation temperature in gelatin gels. Appl Phys Lett. 2004;84:4242–4244.

[103] McNaught AD, Wilkinson A (eds.). IUPAC. Compendium of Chemical Terminology, 2nd ed. (the "Gold Book"). Ettre, L. S. (1993), "Nomenclature for chromatography (IUPAC Recommendations 1993)" (3.8.04: retardation factor, RF in planar chromatography; p. 845). Blackwell Scientific Publications, Oxford; 1997. ISBN 0-9678550-9-8.

[104] Kligman AM, Christophers E. Preparation of isolated sheets of human stratum corneum. Arch Dermatol. 1963;88:702–705.

[105] Mitriaikina S, Müller-Goymann CC. Comparative permeation studies of nondiluted and diluted betamethasone-17-valerate semisolid formulations through isolated human stratum corneum and artificial skin construct. Skin Pharmacol Physiol. 2009;22:142–150.

[106] Brinkmann I, Müller-Goymann CC. Role of isopropyl myristate, isopropyl alcohol and a combination of both in hydrocortisone permeation across the human stratum corneum. Skin Pharmacol Appl Skin Physiol. 2003;16:393–404.

[107] Akomeah FK, Martin GP, Brown MB. Variability in human skin permeability in vitro: Comparing penetrants with different physicochemical properties. J Pharm Sci. 2007;96:824–834.

[108] Fokuhl J, Müller-Goymann CC. Untersuchung der Unversehrtheit von humanem exzidiertem Stratum corneum mittels TEER-Messungen. In: Poster for DPhG Jahrestagung, Erlangen; 2007. Available from:

http://www.pharmtech.tu-bs.de/files/muegoy/JFokuErlangen0709.pdf

[109] Lebo D, Lee C, Lee J, Cupo F, Ryoo J. Development of skin permeation study method for terbinafine HCl; AAPS J. 2005;7:261.

[110] Özcan I, Abacı, Uztan AH, Aksu B, Boyacıoğlu H, Güneri T, Özer Ö. Enhanced topical delivery of terbinafine hydrochloride with chitosan hydrogels. AAPS PharmSciTech. 2009;10:1024–1031.

[111] Zatz JL (ed.), Skin Permeation Fundamentals and Application. Wheaton, Illinois, US: Allured Publishing Corp.; 1993. ISBN 931710-28-6.

[112] Cardoso SG, Schapoval EES. High-performance liquid chromatographic assay of terbinafine hydrochloride in tablets and creams. J Pharm Biomed Anal. 1999;19:809–812.

[113] ICH Expert Working Group. Validation of Analytical Procedures: Text and Methodology Q2 (R1); 2005. p. 11–13.

[114] Lusiana, Reichl S, Müller-Goymann CC. Keratin film made of human hair as a nail plate model for studying drug permeation. Eur J Pharm Biopharm. 2011;78:432–440.

Available from:
http://www.sciencedirect.com/science/article/pii/S0939641111000488
http://dx.doi.org/10.1016/j.ejpb.2011.01.022

[115] Bradford MM. A rapid and sensitive method for the quantitation of microgram quantities of protein utilizing the principle of protein dye binding. Anal Biochem. 1976;72:248–254.

[116] Laemmli UK. Cleavage of structural proteins during the assembly of the head of bacteriophage T4. Nature. 1970;227:680–685.

[117] Hasegawa T, Kim S, Tsuchida M, Issiki Y, Kondo S, Sugibayashi K. Decrease in skin permeation and antibacterial effect of parabens by a polymeric additive, poly(2-methacryloyloxyethyl phosphorylcholine-co- butylmetacrylate). Chem Pharm Bull. 2005;53:271–276.

[118] Sakai M, Imai T, Ohtake H, Azuma H, Otagiri M. Effects of absorption enhancers on the transport of model compounds in Caco-2 cell monolayers: Assessment by confocal laser scanning microscopy. J Pharm Sci. 1997;86:779–785.

[119] Franz TJ. Percutaneous absorption on the relevance of in vitro data. J Invest Dermatol. 1975;64:190–195.

[120] Kobayashi Y, Miyamoto M, Sugibayashi K, Morimoto Y. Enhancing effect of N-acetyl-L-cysteine or 2-mercaptoethanol on the in vitro permeation of 5-fluorouracil or tolnaftate through the human nail plate. Chem Pharm Bull. 1998;46:1797–1802.

[121] Olsen EA. Methods of hair removal. J Am Acad Dermatol. 1999;40:143–155.

[122] Mohorčič• M, Torkar A, Friedrich J, Kristl J, Murdan S. An investigation into keratinolytic enzymes to enhance ungual drug delivery. Int J Pharm. 2007;332:196–201.

[123] Quintanar-Guerrero D, Ganem-Quintanar A, Tapia-Olguín P, Kalia YN, Buri P. The effect of keratolytic agents on the permeability of three imidazole antimycotic drugs through the human nail. Drug Dev Ind Pharm. 1998;24:685–690.

[124] Cabana A, Aït-Kadib A, Juhász J. Study of the gelation process of polyethylene oxide(a)-polypropylene oxide(b)-polyethylene oxide, copolymer (poloxamer 407) aqueous solutions. J Colloid Interface Sci. 1997;190:307–312.

[125] Montalvo G, Valiente M, Rodenas E. Rheological properties of the L phase and the hexagonal, lamellar, and cubic liquid crystals of the CTAB/benzyl alcohol/water system. Langmuir. 1996;12:5202–5208.

[126] Valenta C, Schultz K. Influence of carrageenan on the rheology and skin permeation of microemulsion formulations. J Control Release. 2004;95:257–265.

[127] Choi HG, Lee MK, Kim MH, Kim CK. Effect of additives on the physicochemical properties of liquid suppository bases. Int J Pharm. 1999;190:13–19.

[128] Yong CS, Choi JS, Quan QZ, Rhee JD, Kim CK, Lim SJ, Kim KM, Oh PS, Choi HG. Effect of sodium chloride on the gelation temperature, gel strength and bioadhesive force of poloxamer gels containing diclofenac sodium. Int J Pharm. 2001;226:195–205.

[129] Rhee YS, Shin YH, Park CW, Chi SC, Park ES. Effect of flavors on the viscosity and gelling point of aqueous poloxamer solution. Arch Pharm Res. 2006;29:1171–1178.

[130] Pandit NK, Kisaka J. Loss of gelation ability of Pluronic® F127 in the presence of some salts. Int J Pharm. 1996;145:129–136.

[131] Anderson BC, Cox SM, Ambardekar AV, Mallapragada SK. The effect of salts on the micellization temperature of aqueous poly(ethylene oxide)-b-poly(propylene oxide)b-poly(ethylene oxide) solutions and the dissolution rate and water diffusion coefficient in their corresponding gels. J Pharm Sci. 2002;91:180–188.

[132] Ganguly R, Aswal VK. Improved micellar hydration and gelation characteristics of PEO-PPO-PEO triblock copolymer solutions in the presence of LiCl. J Phys Chem B. 2008;112:7726–7731.

[133] Liu T, Chu B. Formation of homogeneous gel-like phases by mixed triblock copolymer micelles in aqueous solution: FCC to BCC phase transition. J Appl Crystallogr. 2000;33:727–730.

[134] Artzner F, Geiger S, Olivier A, Allais C, Finet S, Agnely F. Interactions between poloxamers in aqueous solutions: Micellization and gelation studied by differential scanning calorimetry, small angle X-ray scattering, and rheology. Langmuir. 2007;23:5085–5092.

[135] Egle H. Schnelles und zuverlässiges therapeutisches Drug-Monitoring mit HPLC-UV und LC/LC-MS/MS aus komplexen Matrizes. PhD Thesis. Fakultät für Chemie, Pharmazie und Geowissenschaften der Albert-Ludwigs-Universität zu Freiburg; 2005.

[136] McGaughey, G B M Gagné, Rappé AK. π-Stacking interactions. Alive and well in proteins. J Biol Chem. 1998;273:15458–15463.

[137] Peters T. Vergleich verschiedener Analysenmethoden zur Estradiolbestimmung in wäßrigen Lösungen im Hinblick auf Sättigungslöslichkeit, Adsorption und Stabilität. Diplomarbeit. Martin-Luther-Universität Halle-Wittenberg; 2000.

[138] Gendy AME, Jun HW, Kassem AA. In vitro release studies of flurbiprofen from different topical formulations. Drug Dev Ind Pharm. 2002;28:823–831.

[139] Gilbert JC, Hadgraft J, Bye A, Brookes LG. Drug release from Pluronic F-127 gels. Int J Pharm. 1986;32:223–228.

[140] Shin SC, Cho CW, Choi HK. Permeation of piroxicam from the poloxamer gels. Drug Dev Ind Pharm. 1999;25:273–278.

[141] Wu HLS, Miller SC. In vitro release of nicotinic acid alkyl esters from poloxamer vehicles. Int J Pharm. 1990;66:213–221.

[142] Jeong B, Kim SW, Bae YH. Thermosensitive sol-gel reversible hydrogels. Adv Drug Deliv Rev. 2002;54:37–51.

[143] Gianni C. Update on antifungal therapy with Terbinafine. G Ital Dermatol Venereol. 2010;145:415–424.

[144] Gunt HB, Kasting GB. Effect of hydration on the permeation of ketoconazole through human nail plate in vitro. Eur J Pharm Sci. 2007;32:254–260.

[145] Hui X, Wester RC, Barbadillo S, Lee C, Patel B, Wortzmman M, Gans EH, Maibach HI. Ciclopirox delivery into the human nail plate. J Pharm Sci. 2004;93:2545–2548.

[146] Glombitza B, Müller-Goymann CC. Influence of different ceramides on the structure of in vitro model lipid systems of the stratum corneum lipid matrix. Chem Phys Lipids. 2002;117:29–44.

[147] Cappel MJ, Kreuter J. Effect of nonionic surfactants on transdermal drug delivery: II. Poloxamer and poloxamine surfactants. Int J Pharm. 1991;69:155–167.

[148] Otto A, Wiechers JW, Kelly CL, Hadgraft J, Du Plessis J. Effect of penetration modifiers on the dermal and transdermal delivery of drugs and cosmetic active ingredients. Skin Pharmacol Physiol. 2008;21:326–334.

[149] Lin HM, Nash RA. An experimental method for determining the Hildebrand solubility parameter of organic nonelectrolytes. J Pharm Sci. 1993;82:1018–1026.

[150] Zia H, Ma JKH, O'Donnell JP, Luzzi LA. Cosolvency of dimethyl isosorbide for steroid solubility. Pharm Res. 1991;8:502–504.

[151] Twist JN, Zatz JL. The effect of solvents on solute penetration through fuzzy rat skin in vitro. J Soc Cosmet Chem. 1989;40:231–242.

[152] Funke AP, Schiller R, Motzkus HW, Ginther C, Miller RH, Lipp R. Transdermal delivery of highly lipophilic drugs: In vitro fluxes of antiestrogens, permeation enhancers, and solvents from liquid formulations. Pharm Res. 2002;19:661–668.

[153] Rossi P, Wiechers JW, Kelly C. Improved delivery and efficacy with dimethyl isosorbide. Cosmet Toil. 2005;120:107–111.

[154] Squillante E, Needham T, Maniar A, Kislalioglu S, Zia H. Codiffusion of propylene glycol and dimethyl isosorbide in hairless mouse skin. Eur J Pharm Biopharm. 1998;46:265–271.

[155] Morimoto Y, Wada Y, Seki T, Sugibayashi K. In vitro skin permeation of morphine hydrochloride during the finite application of penetration-enhancing system containing water, ethanol and l-menthol. Biol Pharm Bull. 2002;25:134–136.

[156] Trommer H, Neubert RHH. Overcoming the stratum corneum: The modulation of skin penetration. Skin Pharmacol Physiol. 2006;19:106–121.

[157] Aungst BJ, Blake JA, Hussain MA. Contributions of drug solubilization, partitioning, barrier disruption, and solvent permeation to the enhancement of skin permeation of various compounds with fatty acids and amines. Pharm Res. 1990;7:712–718.

[158] Baden HP, Kubilus J. Fibrous proteins of bovine hoof. J Invest Dermatol. 1983;81:220–224.

[159] Donnan FG. The theory of membrane equilibria. Chem Rev. 1924;1:73–90.

[160] DeLauder SF, Kidwell DA. The incorporation of dyes into hair as a model for drug binding. Forensic Sci Int. 2000;107:93–104.

[161] Abdel-Rahman SM, Nahata MC. Stability of terbinafine hydrochloride in an extemporaneously prepared oral suspension at 25 and 4 °C. Am J Health-Syst Pharm. 1999;56:243–245.

[162] Barreiro-Iglesias R, Bromberg L, Temchenko M, Hatton TA, Concheiro A, Alvarez-Lorenzo C. Solubilization and stabilization of camptothecin in micellar solutions of pluronic-g-poly(acrylic acid) copolymers. J Control Release. 2004;97:537–549.

[163] Dimitrova E, Bogdanova S, Mitcheva M, Tanev I, Minkov E. Development of model aqueous ophthalmic solution of indomethacin. Drug Dev Ind Pharm. 2000;26:1297–1301.

[164] Jaime GL, Isabel SM, Angel C, Carmen AL. Poloxamines and poloxamers as polymeric micellar carriers for simvastatin: Interactions at the air-water interface and in bulk solution. J Phys Chem C. 2010;114:1181–1189.

[165] Eichner R, Kahn M. Differential extraction of keratin subunits and filaments from normal human epidermis. J Cell Biol. 1990;110:1149–1158.

[166] Cooper D, Sun TT. Monoclonal antibody analysis of bovine epithelial keratins. Specific pairs as defined by coexpression. J Biol Chem. 1986;261:4646–4654.

[167] Kvedar JC, Kubilus J, Baden HP. Cytokeratins of the bovine hoof: Classification and studies on expression. Biochim Biophys Acta. 1986;884:462–473.

[168] Cannell DW. Permanent waving and hair straightening. Clin Dermatol. 1988;6:71–82.

[169] Bolduc C, Shapiro J. Hair care products: Waving, straightening, conditioning, and coloring. Clin Dermatol. 2001;19:431–436.

[170] Khengar RH, Brown MB, Turner RB, Traynor MJ, Holt KB, Jones SA. Free radical facilitated damage of ungual keratin. Free Radic Biol Med. 2010;49:865–871.

[171] Holbrook KA, Odland GF. Regional differences in the thickness (cell layers) of the human stratum corneum: An ultrastructural analysis. J Invest Dermatol. 1974;62:415–422.

[172] Fernández-Torres B, Pereiro M, Guarro J. Comparison of two methods for antifungal susceptibility testing of Trichophyton rubrum. Eur J Clin Microbiol. 2002;21:70–71.

[173] Barros MEDS, Santos DDA, Hamdan JS. Evaluation of susceptibility of Trichophyton mentagrophytes and Trichophyton rubrum clinical isolates to antifungal drugs using a modified CLSI microdilution method (M38-A). J Med Microbiol. 2007;56:514–518.

[174] Moore CB, Walls CM, Denning DW. In vitro activities of terbinafine against Aspergillus species in comparison with those of itraconazole and amphotericin B. Antimicrob Agents Chemother. 2001;45:1882–1885.

[175] Meletiadis J, Meis JFGM, De Hoogp GS, Verweij PE. In vitro susceptibilities of 11 clinical isolates of Exophiala species to six antifungal drugs. Mycoses. 2000;43:309–312.

[176] Coelho LM, Aquino-Ferreira R, Maffei CML, Martinez-Rossi NM. In vitro antifungal drug susceptibilities of dermatophytes microconidia and arthroconidia. J Antimicrob Chemother. 2008;62:758–761.

[177] Osborne CS, Leitner I, Favre B, Ryder NS. Antifungal drug response in an in vitro model of dermatophyte nail infection. Med Mycol. 2004;42:159–163.

[178] Nowrozi H, Nazeri G, Adimi P, Bashashati M, Emami M. Comparison of the activities of four antifungal agents in an in vitro model of dermatophyte nail infection. Indian J Dermatol. 2008;53:125–128.